AD-A171 288 NOWCASTING THERMODYNAMIC PROFILES USING A TRIANGLE OF WIND PROFILERS IN AN ADVECTION MODEL(U) AIR FORCE INST OF TECH WRIGHT-PATTERSON AFB OH R A SKOV 1986 1/2

UNCLASSIFIED AFIT/CI/NR-86-121T F/G 4/2 NL

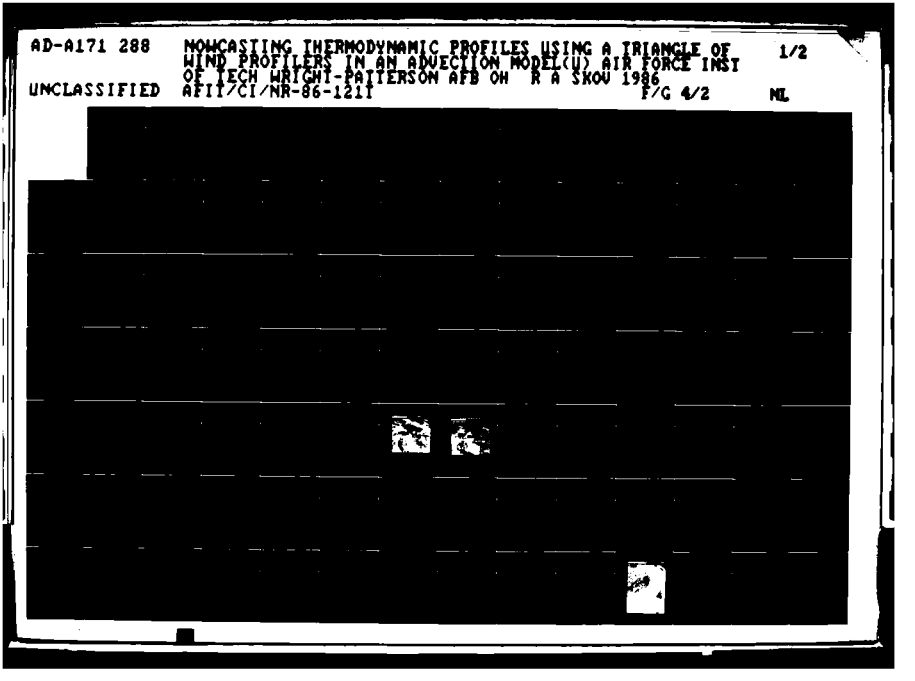

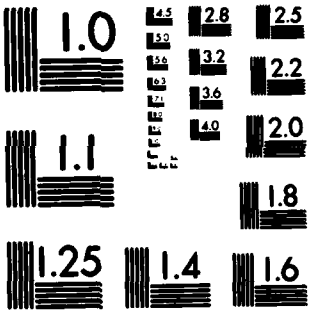

CROCOPY RESOLUTION TEST CHART
NATIONAL BUREAU OF STANDARDS-1963-A

AD-A171 288

(1)

SECURITY CLASSIFICATION OF THIS PAGE (When Data Entered)

REPORT DOCUMENTATION PAGE		READ INSTRUCTIONS BEFORE COMPLETING FORM
1. REPORT NUMBER AFIT/CI/NR 86-121T	2. GOVT ACCESSION NO.	3. RECIPIENT'S CATALOG NUMBER
4. TITLE (and Subtitle) Nowcasting Thermodynamic Profiles Using A Triangle Of Wind Profilers In An Advection Model		5. TYPE OF REPORT & PERIOD COVERED THESIS/DISSERTATION 6. PERFORMING ORG. REPORT NUMBER
7. AUTHOR(s) Randall Alan Skov		8. CONTRACT OR GRANT NUMBER(s)
9. PERFORMING ORGANIZATION NAME AND ADDRESS AFIT STUDENT AT: University of Oklahoma		10. PROGRAM ELEMENT, PROJECT, TASK AREA & WORK UNIT NUMBERS
11. CONTROLLING OFFICE NAME AND ADDRESS AFIT/NR WPAFB OH 45433-6583		12. REPORT DATE 1986 13. NUMBER OF PAGES 107
14. MONITORING AGENCY NAME & ADDRESS(if different from Controlling Office)		15. SECURITY CLASS. (of this report) UNCLAS 15a. DECLASSIFICATION/DOWNGRADING SCHEDULE
16. DISTRIBUTION STATEMENT (of this Report) APPROVED FOR PUBLIC RELEASE; DISTRIBUTION UNLIMITED		
17. DISTRIBUTION STATEMENT (of the abstract entered in Block 20, if different from Report)		
18. SUPPLEMENTARY NOTES APPROVED FOR PUBLIC RELEASE: IAW AFR 190-1		
19. KEY WORDS (Continue on reverse side if necessary and identify by block number)		
20. ABSTRACT (Continue on reverse side if necessary and identify by block number) ATTACHED.		

LYNN E. WOLAVER
Dean for Research and
Professional Development
AFIT/NR

DD FORM 1 JAN 73 1473 EDITION OF 1 NOV 65 IS OBSOLETE

SECURITY CLASSIFICATION OF THIS PAGE (When Data Entered)

ABSTRACT

During the 1985 PRE-STORM project, a set of three 50 MHz wind profilers was installed and operated in Kansas and Oklahoma. An experiment has been devised which tests the utility of these profiler data as a complement to the twice-daily rawinsonde observation network. The goal of this research was to determine if, by use of the profiler data in an advection model, we can "predict" the thermodynamic sounding during the twelve-hour period between standard rawinsonde observations. A Cressman-type objective analysis scheme is used to obtain initial fields of u, v, θ, q and z on a fifteen level, 1530 km square grid around the profiler triangle. Using the thermodynamic, moisture and continuity equations, local tendencies of θ and q are obtained at each gridpoint. Each hour, the u and v fields are reanalyzed using the new profiler winds. Thermodynamic and wind "soundings" extracted from the gridded data are verified against the supplemental soundings taken during PRE-STORM. Results indicate that despite being limited by the availability of profiler winds, the simple advection model design and the effects of deep convection, the model-produced soundings are an improvement over both persistence and initial soundings modified with surface data. Many enhancements are identified which can upgrade the quality and quantity of the profiler data as well as the advection model results.

THE UNIVERSITY OF OKLAHOMA

GRADUATE COLLEGE

NOWCASTING THERMODYNAMIC PROFILES USING A TRIANGLE OF WIND PROFILERS IN AN ADVECTION MODEL

A THESIS

SUBMITTED TO THE GRADUATE FACULTY

in partial fulfillment of the requirements for the

degree of

MASTER OF SCIENCE IN METEOROLOGY

By

RANDALL ALAN SKOV

Norman, Oklahoma

1986

NOWCASTING THERMODYNAMIC PROFILES USING A TRIANGLE OF WIND PROFILERS IN AN ADVECTION MODEL

A THESIS

APPROVED FOR THE SCHOOL OF METEOROLOGY

By Frederick H. Carr
James F. Kimpel
D. Lesins

ACKNOWLEDGEMENTS

I sincerely thank Dr. Frederick Carr, the chairman of my committee, for sharing his time, wisdom and invaluable experience in guiding me through this undertaking. I would also like to thank Dr. Glen Lesins and Dr. James Kimpel, my committee members, for their timely suggestions and enthusiasm regarding my research.

I especially thank my wife, Jinda. In addition to typing the manuscript, she made numerous suggestions that contributed to the unity of the thesis. I could not have completed this research without her support, understanding, encouragement and guidance.

My appreciation is extended to Les Showell of NSSL and John Augustine of WRP, ERL for providing me with the PRE-STORM rawinsonde and profiler data. I am grateful to Brian Jewett, Kevin Thomas, Leslie Schlecht and Wes Roberts for their assistance in processing the data. I would also like to thank Kathy Kanak for drafting the figure titles.

I greatly appreciate the Air Force Institute of Technology for providing me the opportunity and support to further my academic knowledge.

Finally, and above all, I praise my Lord and Savior, Jesus Christ for his eternal grace, guidance and companionship. He has kept me on the right path.

TABLE OF CONTENTS

LIST OF TABLES

LIST OF FIGURES

ABSTRACT

During the 1985 PRE-STORM project, a set of three 50 MHz wind profilers was installed and operated in Kansas and Oklahoma. An experiment has been devised which tests the utility of these profiler data as a complement to the twice-daily rawinsonde observation network. The goal of this research was to determine if, by use of the profiler data in an advection model, we can "predict" the thermodynamic sounding during the twelve-hour period between standard rawinsonde observations. A Cressman-type objective analysis scheme is used to obtain initial fields of u, v, θ, q and z on a fifteen level, 1530 km square grid around the profiler triangle. Using the thermodynamic, moisture and continuity equations, local tendencies of θ and q are obtained at each gridpoint. Each hour, the u and v fields are reanalyzed using the new profiler winds. Thermodynamic and wind "soundings" extracted from the gridded data are verified against the supplemental soundings taken during PRE-STORM. Results indicate that despite being limited by the availability of profiler winds, the simple advection model design and the effects of deep convection, the model-produced soundings are an improvement over both persistence and initial soundings modified with surface data. Many enhancements are identified which can upgrade the quality and quantity of the profiler data as well as the advection model results.

NOWCASTING THERMODYNAMIC PROFILES USING A TRIANGLE OF WIND PROFILERS IN AN ADVECTION MODEL

CHAPTER I

INTRODUCTION

The present operational upper-air network is not designed to sample the atmosphere with the necessary time and space resolution required for mesoscale modeling. Ecklund et al. (1979) indicate that much of the variability in the wind field is missed by the twice daily synoptic soundings. Similarly, the thermodynamic variables in a sounding may change significantly between the standard rawinsonde observations. For example, a shift in the wind may allow the return of low-level moisture and create a potentially unstable air mass. Or possibly, a subsiding air mass in the mid-levels moves over and effectively caps a region where the 1200 GMT sounding indicated a strong potential for severe convection. Whatever the case, having reliable soundings between standard observing times would greatly benefit forecasters during periods when rapid changes in the wind, temperature and moisture fields are occurring.

As part of the Preliminary Regional Experiment for STORM-Central (PRE-STORM) program in May-June 1985, a triangle of three 50 MHz wind

profilers was assembled and operated in Oklahoma and Kansas. With the availability of hourly wind data from these profilers, we can assess the value of more frequent upper-air data and test, for the first time, the utility of a network of wind profilers in the Central Plains. Given an initial state of wind, temperature and moisture provided by the standard rawinsonde network, one approach to obtain thermodynamic profiles between standard rawinsonde observations is to use the hourly wind data from the three PRE-STORM profilers and a simple advection model to compute changes in the temperature and moisture fields. This method produces gridded nowcasts of the wind and thermodynamic variables for essentially any desired time between the standard rawinsonde launch times. From this grid, soundings can be reconstructed for locations of interest and compared to actual soundings which were launched from fourteen sites in Kansas and Oklahoma during PRE-STORM (Fig. 1.1) (Topeka, KS did not participate). The model-produced soundings can also be compared with persistence or modified soundings (i.e., using the original sounding for the next twelve hours or modifying the original sounding with new surface data). The goal of this research, therefore, is to determine if, through using profiler winds in an advection model, we can improve our knowledge of the thermodynamic sounding during the twelve-hour period between standard rawinsonde observations.

Gage and Balsley (1978) provide an excellent history of clear-air radar technology. Beginning with the investigation of over-the-horizon radio propagation in the early 1940's, radar technology advanced into the Doppler era by the 1960's with the introduction of new radar techniques and subsequent understanding of the causes of clear-air

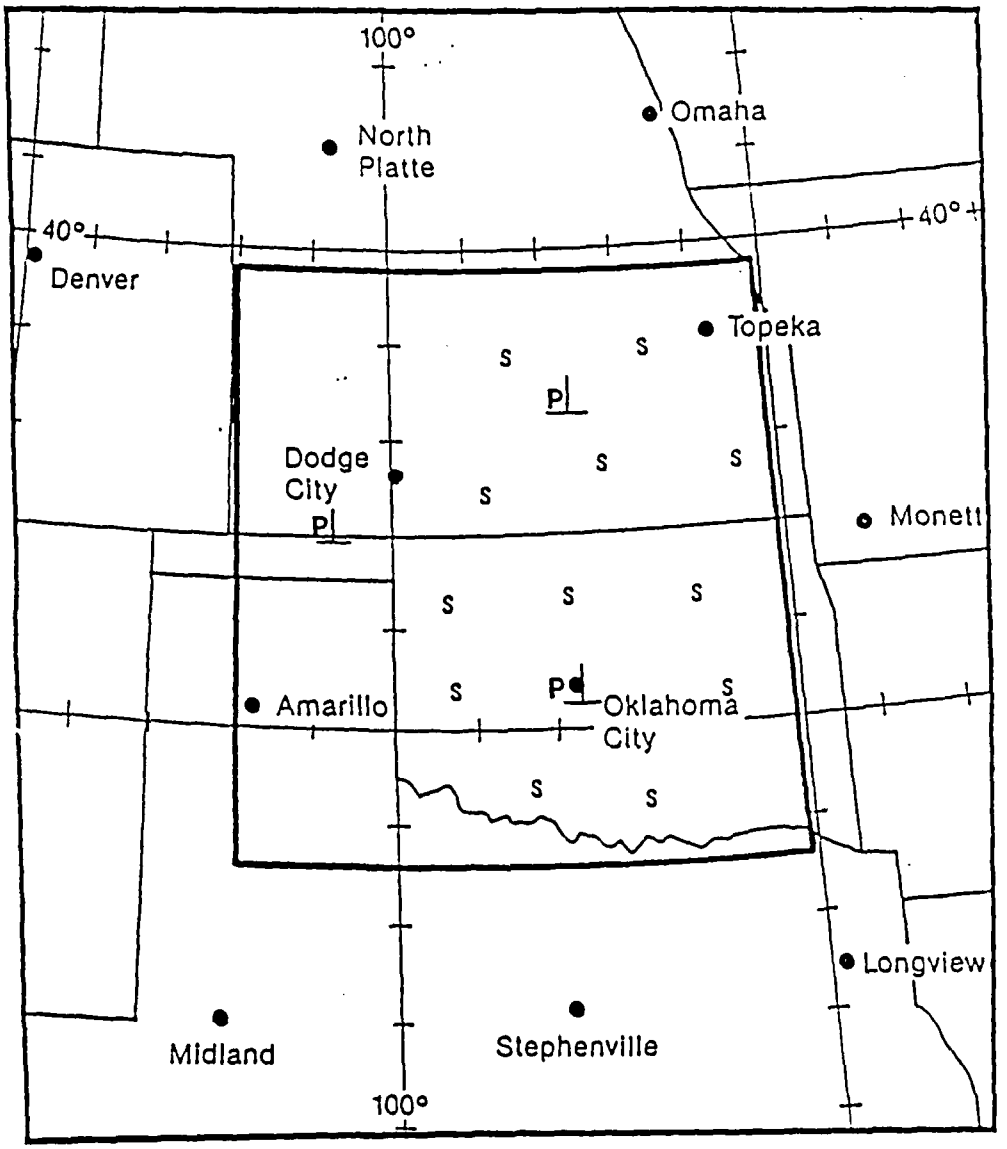

Figure 1.1. Locations of the PRE-STORM wind profiler sites ("I") and the supplemental sounding sites ("s") (Cunning, 1985).

echoes. The early Doppler radars operated at microwave frequencies; however, within the last decade, several VHF systems have been constructed. These radars, because of their longer wavelengths, are capable of observing tropospheric and low to mid-stratospheric winds using current doppler radar techniques.

Of interest in this study are the performance and characteristics of VHF radars similar to those used in the PRE-STORM program. Typically, a 50 MHz wind profiler uses a large (100 x 100 m), but low cost array of phased antennas. The horizontal wind components are measured using two fixed antenna beams which point 15° from vertical, usually to the north and east. Often, a third, fixed, zenith-pointing antenna is added to measure the vertical velocities and tropopause height. Without this third antenna, data averaging periods of sufficient length, usually an hour, are required to minimize the effects of vertical air motion on the horizontal wind measurements (Strauch et al., 1984). The height resolution of the radar, typically 300 meters, is dependent upon the range resolution and the antenna beam width (Hogg et al., 1983). The minimum attainable height is often large (1 to 2 km AGL) because of bandwidth limitations imposed by frequency authorizations (Strauch, Decker and Hogg, 1983). Chapter III provides more detail on the performance characteristics of the three PRE-STORM wind profilers.

Recent studies indicate that although some discrepancies between winds from 50 MHz wind profilers and comparison rawinsondes can be attributed to identifiable causes, other variations cannot be completely explained. In a study during August and September 1985, Kessler, Eilts

and Thomas (1985) compare data from one of the PRE-STORM wind profilers with rawinsonde data from the Oklahoma City Weather Service Forecast Office (WSFO), 46 km north of the profiler site. They found that the average profiler winds were approximately 2 ms^{-1} less than the mean rawinsonde winds. Also, most comparisons yielded at least one layer with large deviations in either the wind speed or direction. In another study of 50 MHz wind profiler accuracy, Ecklund, et al. (1979) show differences between sounding and profiler winds to be generally less than 5 ms^{-1} but had one discrepancy of over 20 ms^{-1}. Earlier, Ecklund et al. (1977) found agreement to within 2 ms^{-1} but wind speeds were light (1-14 ms^{-1}).

Research into the operational use of wind profilers has increased in the past five years. Strauch, et al. (1983) describe the five wind profilers which compose the Colorado wind-profiling network. These profilers were developed by the Wave Propagration Laboratory (WPL) and provide wind data automatically and continuously with unattended operation. Data from this network are being used for real-time testing of improved forecast methods and for mesoscale research. The Denver WSFO uses the wind profilers to track short waves, determine the strength of mountaintop winds and the potential for lee waves (Schlatter, 1985). Gage and Nastrom (1985) demonstrate positive correlation between vertical velocities obtained directly from the Platteville, Colorado wind profiler and the rainfall rate during an intense Colorado spring upslope storm. Zamora and Shapiro (1984) show the advantages of the high temporal resolution that wind profilers provide in a comparison of vorticity and divergence calculations with

those using conventional rawinsonde data.

On a broader scale, there is a great deal of interest in using profiler data to improve the initialization of numerical weather prediction models (Browning, 1982). In addition, they would be ideal for updating a model during a four dimensional data assimulation period. To accomplish either would require a national or at least regional network of profilers. In late August 1985, authorization for the procurement of such a network was granted by the National Oceanic and Atmospheric Administration (NOAA) (Profiler Forum, Sep, 1985). The network of thirty wind profilers across the central United States should be completed in 1989. Until then, much can be done with existing wind profiler data to investigate many of its potential applications. This thesis is a consideration of one of these applications.

CHAPTER II

METHODS

It is important to understand that the models and methods for data processing used in this research could not be developed in a complete operational or real-time sense. Ideally, the advection model would be run in hourly increments as new profiler data becomes available. However, as will be dicussed in Chapter III, much of the profiler data is incomplete and could not be handled on an hour-by-hour basis. As a result, the procedures developed here are quite modular. The concept of reading outputted data from previously executed programs into another program, processing, and writing the newly processed data to another output file is used extensively in this research.

Chapter II describes the series of procedures used in this modular approach. The following is a general overview. First, a 1530 km square, pressure coordinate grid is developed using fifteen equally spaced (50 mb) layers from 900 mb to 200 mb. Next, an objective analysis program is used to put the potential temperature, specific humidity, geopotential height and horizontal wind information from the initial rawinsonde and profiler data into gridded arrays. The initial vertical velocity fields are then computed from the gridded horizontal wind data. In a separate computer program, the hourly-updated wind fields are calculated using a combination of gridded wind data and new

profiler data in another objective analysis scheme. Finally, an additional program is formulated to update the potential temperature and specific humidity fields using a simple advection model.

Developing the Grid

The cornerstone of the grid is the selected verification site, hereafter referred to as the station of interest (SOI). Here, the SOI is either one of the twelve PRE-STORM supplemental rawinsonde sites or one of the NWS rawinsonde stations which participated in PRE-STORM by launching additional soundings. Preferably, the SOI is located near or within the triangle of wind profilers. This limits the possible Oklahoma verification sites to Oklahoma City, Woodward and Enid, and possible Kansas sites to Pratt, Dodge City and McConnell AFB. However, the model could be set up to produce a sounding for any desired location. The selection of the SOI is based upon the availability of sounding data for verification and the synoptic and mesoscale weather events. Once the SOI is selected, the general wind pattern is evaluated to determine the upstream direction and how far the grid should be skewed upstream to minimize the boundary effects on the nowcast soundings. For example, in northwest flow, the grid might be offset such that the distance between the SOI and the grids' northern and western borders is nearly 1000 km, leaving approximately 500 km from the SOI to the grid's eastern and southern borders. The grid is placed on a polar stereographic projection and is true at the SOI latitude. This minimizes the distortion of the projection. In order to have several

gridpoints within the profiler triangle, a grid spacing of 90 km (approximately one-fourth the distance between any two profilers) is used. This mesoscale spatial resolution is allowable despite using synoptic scale rawinsonde data because the wind profiler data is available every hour.

Objective Analysis of the Initial Data

Cressman (1959) introduced a method of objective analysis which uses reported data to make successive corrections to an initial guess field. The technique uses bilinear interpolation from the gridded first guess field to obtain an estimate of the value at each observation site. The difference between the estimate and the actual observation is calculated for each station, then a new value is computed for each gridpoint using the following distance-weighted correction formula.

$$S = S_{est} + \frac{\sum_{k=1}^{N} W_k (S_k - S_{est})}{\sum_{k=1}^{N} W_k} \qquad (2.1)$$

where S is the new gridpoint value

S_{est} is the station estimate from guess field

S_k is the station observation value

N is the number of stations within influence radius R

W_k is the weight applied to the difference between S_{est} and S_k

$$W_k = \frac{R^2 - d^2}{R^2 + d^2} \qquad (2.2)$$

where R is the radius of influence and d is the distance from the gridpoint to the station. The influence radius is decreased with each successive scan to allow the analysis of data over a spectrum of horizontal scales.

A four-pass Cressman analysis scheme is used to obtain the initial analysis of potential temperature (θ) and specific humidity (q) for the advection model. An approximate mean value for each parameter is used as the first guess field on each constant pressure surface. Potential temperature ranges linearly from 295 K at 900 mb to 332.5 K at 200 mb, and specific humidity decreases from 13 gkg^{-1} at 900 mb to 0.175 gkg^{-1} at 200 mb. The same Cressman scheme is used on the geopotential heights (z) which are derived from the temperature data using the hypsometric equation. First guess values of z range from 1 km at 900 mb to almost 12.2 km at 200 mb. A 1200 km influence radius is used for the first scan to incorporate all temperature and moisture data that may be advected into the profiler triangle during the model run. For each subsequent scan, R is decreased by 300 km to a minimum R of 300 km for the fourth scan. The fact that many of the rawinsonde stations in the western half of the domain are located at altitudes above the lowest model levels induces a large region with very little low-level data. To accommodate this and missing data from a few other stations, an adjustable R is used to ensure that at least two reporting stations influence each gridpoint for each scan. This is done by temporarily increasing R until more than one reporting station is reached. The result, after four passes of the analysis scheme, is initial fields of θ, q and z which are ready for use in the advection model.

The purpose for obtaining geopotential height values at each gridpoint is to allow the use of profiler data into the model. Since the advection model is run on pressure levels and profiler winds are archived on height levels, there is a need to know the height (in km) of each pressure level over each profiler site. Bilinear interpolation is used to obtain these heights from the four gridpoints around each profiler. It is assumed that $\partial z / \partial t = 0$ during the twelve-hour model run. This assumption is acceptable because a typical change in the geopotential height of a constant pressure surface during a twelve-hour model run ($\lesssim 100$ m) is small compared to the height resolution of profiler data ($\gtrsim 300$ m). With this height data, the profiler winds are interpolated to the model pressure surfaces and are ready for use in the initial wind analysis and the wind-updating model. The four-pass Cressman analysis scheme descibed above is used to obtain the u and v wind fields on the grid. However, the wind fields are composed using both the data from the 51 rawinsonde stations and the initial hour winds from the three profilers. The first guess field for u and v is zero. The supplemental rawinsonde data from PRE-STORM were not used in the analyses because these data would not normally be available for real-time operations.

Obtaining Vertical Velocities

After completing the objective analysis, the initial vertical velocity field (ω) is computed kinematically from the u and v fields using the mass continuity equation in pressure coordinates.

$$-\frac{\partial \omega}{\partial p} = \frac{\partial u}{\partial x} + \frac{\partial v}{\partial y} = \text{Div} \tag{2.3}$$

By integrating 2.5 from p to p + Δp and applying the trapezoidal rule to the right-hand side yields

$$\omega_k = \omega_{k-1} + \frac{\Delta p}{2} (\text{Div}_{k-1} + \text{Div}_k), \quad k = 2,3,\ldots,N \tag{2.4}$$

where N is the number of model levels. Ideally, the model should incorporate surface and boundary layer wind data so that the model extends down to the surface, or say, 1000 mb. In this ideal model, ω is assumed to be zero at the lowest level, or if terrain is included, ω at the bottom level is proportional to $\vec{V} \cdot \vec{\nabla} h$, where h is topography. Therefore, applying 2.4 successively yields the vertical velocity at each level for a particular location (gridpoint).

A significant problem with the kinematic technique is that it is very sensitive to errors in the horizontal wind field. A 10% error in wind measurement can result in a 100% error in the divergence. These errors accumulate in the vertical integration and become quite evident in the lower stratosphere where ω should be small, but the computed values are usually large. By adjusting the divergence such that $\omega_{top} = 0$, the effect of these errors is reduced (O'Brien, 1970). From the original data

$$\int_{p_o}^{p_{top}} \text{Div}\ dp = \omega_{top} = \text{Residual}$$

To correct each level by the same amount, a correction factor (CF) is subtracted from the divergence at each level to obtain an adjusted

divergence (Div').

$$Div_k' = Div_k - CF \tag{2.5}$$

$$\text{where } CF = \frac{\text{Residual}}{p_o - p_{top}}$$

The vertical velocities to be used in the model are obtained by applying 2.5 in 2.4 and vertically integrating. Note that the original u and v fields are no longer consistent with the adjusted divergence. This inconsistency can be removed by techniques such as presented by Sasaki (1979). Since Rusk (1985) shows that the root mean square vector error between the observed and the adjusted winds is only 1-2 ms-1, a corrective procedure was not applied. In addition, because divergence is not computed on the boundaries, it is assumed that the vertical velocity on a border point is equal to the vertical velocity at one gridpoint toward the interior of the grid.

For this research, however, data constraints which are discussed in Chapter III led to developing the model without a boundary layer. This produces a significant problem since forcing ω at 900 mb to zero reduces the magnitude of ω throughout the model, particularly in the lower levels. To improve the estimates of ω, it is assumed that the wind field, and therefore the divergence field, is constant between 900 mb and 950 mb. This allows the computation of ω at the lowest level of the model, (i.e., 900 mb), through the assumption that ω at 950 mb is zero.

Wind-Updating Model

The wind-updating model is a key link to achieving successful results from the advection model. Because the PRE-STORM profiler triangle covers only a small portion of the grid, a single-pass Cressman objective analysis is used. This analysis scheme employs a combination of the hour's new profiler winds and the preceeding hour's gridded u and v fields to obtain the new "updated" gridded wind fields. Since, after initialization, the only new information in the model is the profiler data, the goal is to maximize the effect of the profiler winds within the triangle and allow the winds away from the triangle to gradually be modified by the profilers. This is accomplished by conducting two consecutive objective analyses at each gridpoint using a 400 km radius of influence (R) for the profiler data and a 100 km R for the gridpoint data. First, all gridpoints within 100 km of the evaluated gridpoint are considered as data in an analysis using the first term in both the numerator and the denominator on the right-hand side of equation 2.6.

$$S'_{i,j} = \frac{\sum_{l=i-1}^{i+1} \sum_{m=j-1}^{j+1} W_{l,m} S_{l,m} + \sum_{k=1}^{N} W_k a_k}{\sum_{l=i-1}^{i+1} \sum_{m=j-1}^{j+1} W_{l,m} + \sum_{k=1}^{N} W_k} \qquad (2.6)$$

where $S'_{i,j}$ is the new value of u and v at the gridpoint being evaluated

$S_{l,m}$ is the previous hour's gridpoint value of u and v, and

$W_{l,m}$ is the weight applied to the gridpoint data using equation 2.2 with R being 100 km and d the distance from the gridpoint to a neighboring gridpoint. Second, the remaining two terms on the right-

hand side of 2.6 are computed where

N is the number of profilers within influence radius R

a_k is the u or v profiler observation, and

W_k is the weight applied to the profiler data using equation 2.2 with R being 400 km and d the distance between the i,j gridpoint and the profiler. This combination of analysis schemes allows the profiler data to dominate the new wind value of a gridpoint near the profiler triangle. Concurrently, the gridpoint data analysis functions as a mild smoother, particularly at gridpoints which are just within the 400 km influence radius of the profiler data. After the updated u and v wind fields are computed for each level, the new vertical wind fields are computed kinematically as discussed earlier.

Advection Model

Due to the introductory nature of this investigation, the advection model was designed using a simple format. During the model development, it was hoped that the value of the profiler winds could be determined using an uncomplicated approach before attempting more complex techniques. For input data, the advection model requires the new wind fields from the wind-updating model along with the thermodynamic and wind information from the objective analysis of the initial rawinsonde and profiler data. The advection model runs for a twelve-hour period using twenty minute time steps. Each hour, a newly-updated wind field is introduced to the model to advect temperature and moisture for the next three time intervals. Upstream differencing is used because it is natural to look upstream when forecasting temperature and moisture

changes by advection. In addition, upstream differencing will not produce negative values of moisture. The predicted variables in the model are potential temperature, θ, given by the First Law of Thermodynamics in the form

$$\frac{\partial \theta}{\partial t} = -\vec{V}_h \cdot \vec{\nabla}_h \theta - \omega \frac{\partial \theta}{\partial p} + \frac{\theta}{C_p T} \dot{H} \qquad (2.7)$$

and specific humidity, q, given by

$$\frac{\partial q}{\partial t} = -\vec{V}_h \cdot \vec{\nabla}_h q - \omega \frac{\partial q}{\partial p} + E - P \qquad (2.8)$$

where $\dot{H}$ is the diabatic heating rate, E evaporation, P precipitation and the other variables have their standard meteorological meanings. In principle, $\dot{H}$ would be the sum of all diabatic effects, but it is used here to represent only the latent heat of condensation. Correspondingly, E is just the evaporation of falling rain.

For each i,j location on the grid, the new values of θ and q are calculated starting at the top of the model and continuing downward to the lowest level. First, the advection terms in 2.7 and 2.8 are computed for a twenty minute time step (Δt) and are added to the previous values of θ and q, respectively. Then, the gridpoint is checked for supersaturation by determining the saturation specific humidity (q_s) through the use of Poisson's equation and a polynomial approximation for computing the saturation vapor pressure (Lowe, 1977). If q_s is less than the updated value of q, then the difference (Δq) is assumed to be condensed, added to any precipitation falling into the

gridpoint from above and precipitated out of the level. Thus, P in 2.8 is now known. The third term on the right-hand side of 2.7 can be written as

$$\frac{\theta}{C_p T}\left[-L\,\frac{\Delta q}{\Delta t}\right] = \frac{-L}{C_p}\,\frac{\Delta q}{\Delta t}\left[\frac{1000}{p}\right]^{R/C_p} \qquad (2.9)$$

where L is the latent heat of condensation (2.5×10^6 Jkg^{-1}) and Δq is negative for condensation. The total change in potential temperature on the level due to latent heat ($\Delta\theta$) during the time step is then

$$\Delta\theta = -L\,\frac{\Delta q}{C_p}\left[\frac{1000}{p}\right]^{R/C_p} \qquad (2.10)$$

The updated values of θ and q for the time step at the gridpoint are obtained by adding Δq and $\Delta\theta$ to the q and θ values computed from the advection terms. The amount of moisture condensed is stored for use in the levels below.

If the gridpoint is not saturated and there is precipitation falling into the level, then evaporative cooling is assumed to occur. The extent of evaporation into the unsaturated level is based upon the assumption that "the big drops get through". To simulate this, a limit on the amount of moisture which can be evaporated into the layer is set. The new gridpoint value of relative humidity (rhnew) is limited to approximately the current relative humidity (rh) plus 25 percent of the difference between saturation (rh = 1.0) and rh before evaporative cooling. For example, given rh = 0.60,

rhnew = 0.60 + 0.25(1.00 - 0.60) = 0.70

The new value of q for the gridpoint (q_{new}) would then be increased according to

$$q_{new} = 0.70 q_s$$

and $\Delta\theta$ is cooled in accordance with 2.10, where Δq is positive. Any excess precipitation after applying this evaporation technique is precipitated to the level below. Of course, if originally there is only a little precipitation (not enough to raise rh to rhnew), then all the precipitation is absorbed by the gridpoint and none falls through to the level below. All precipitation falling below 900 mb is accumulated as rainfall.

CHAPTER III

DATA PREPARATION

As discussed in Chapter II, the advection model uses two sets of data as input. The initial fields of potential temperature (θ), specific humidity (q), geopotential height (z), and horizontal wind (u and v) are comprised from thermodynamic and wind data from 51 standard rawinsonde stations in the central and western United States and northern Mexico. In addition, the wind data from the three PRE-STORM profilers are used in computing the initial fields of u and v. The subsequent wind profiler data are the backbone of this research; providing hourly information on the changing wind fields, it is the only data inputted into the advection model after initializing the model run. This chapter discusses how these data are prepared for use in the model from the raw rawinsonde and profiler data collected during two PRE-STORM cases.

Case Studies

Since the goal of this research is to determine the usefulness of hourly profiler winds in an advection model, there are several preferred synoptic conditions within the profiler triangle when selecting a case to study. Having a significant change in wind direction and/or speed at

several of the model levels is of primary importance. If the wind field is relatively constant in time, the advection model would not have the opportunity to test the usefulness of the profiler data. A change in temperature and/or dewpoint temperature at one or more model pressure levels over a twelve-hour period will provide a case in which the advection model can improve upon the current method of updating a sounding using only surface observations. A third preferred condition is to use a daytime case because additional soundings are often desired prior to afternoon convection. A daytime case will also provide an excellent opportunity to compare soundings produced from the model with soundings produced using the common technique of modifying the lowest levels of the 1200 GMT sounding with new surface data. Finally, although precipitation physics are included in the model, thunderstorm updrafts and downdrafts and, therefore, their effects on temperature and moisture profiles are very difficult to simulate without making the model much more complex. For this reason, it is best if the thunderstorms develop late in the twelve-hour period.

The first case study is the twelve-hour period from 0000 GMT to 1200 GMT on June 11th, 1985. Figure 3.1 indicates a 500 mb short wave trough extending from the central Dakotas to southeastern Colorado at the start of the period. The associated 850 mb cold front extends from a low pressure center in south central Nebraska across northwestern Kansas into southern Colorado (Fig. 3.2). During the afternoon of the 10th, a large area of thunderstorms developed ahead of both the cold front and the upper level trough. By 0300 GMT on the 11th, the thunderstorm complex developed into a mesoscale convective system (MCS)

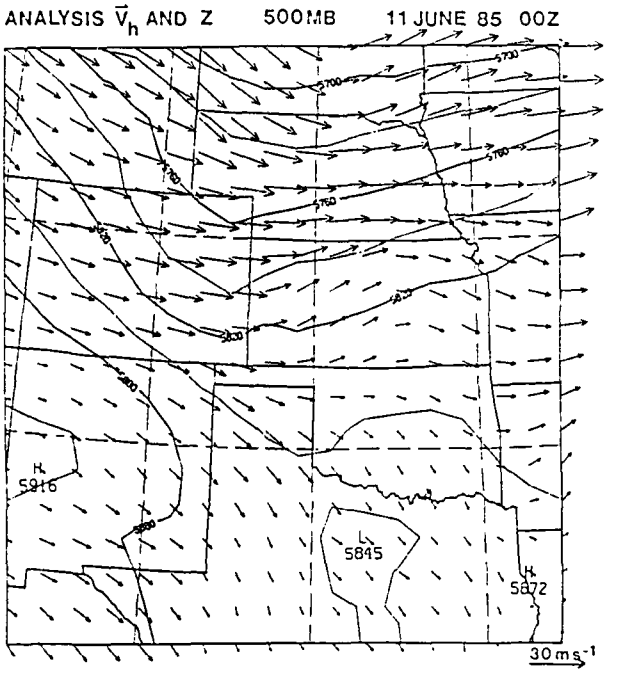

Figure 3.1. 500 mb analysis of horizontal wind and geopotential height for 0000 GMT 11 June 1985. Contour interval is 30 m.

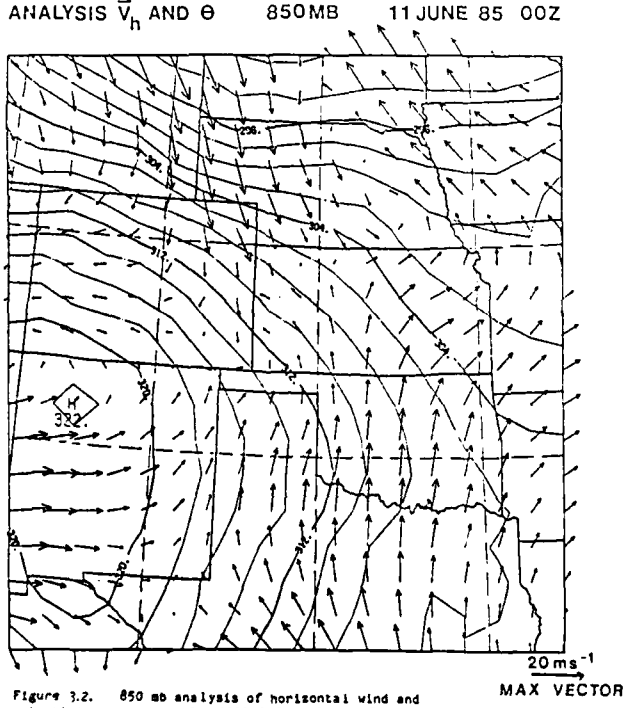

Figure 3.2. 850 mb analysis of horizontal wind and potential temperature for 0000 GMT 11 June 1985. Contour interval is 2 K.

covering the western one-half of Kansas and northwestern and north central Oklahoma. During the next four hours, the MCS weakened and the resultant squall line moved rapidly southeastward through Oklahoma with the passage of the short wave. This case was selected for study primarily because it was the first available set of PRE-STORM profiler data. The case also features frontal/trough passage at all levels and strong horizontal gradients of temperature and moisture. The primary disadvantages are that it is a nighttime case, and the MCS moved into the profiler triangle only an hour after model initialization.

The second case study is from 1200 GMT on May 12th, 1985 to 0000 GMT on May 13th, 1985. This case was selected because it is a daytime event in which thunderstorms developed nine to twelve hours after model initialization. Figures 3.3 and 3.4 indicate the moisture return ahead of a developing 900 mb low over the Texas panhandle during the twelve-hour period. The abundant low-level moisture combined with daytime heating to initiate deep convection over north central Texas. The activity developed northward into southwestern Oklahoma where a warm front extending northeastward into southeastern Kansas triggered rapid thunderstorm development and intensification from Wichita Falls, Texas to Oklahoma City. The principal disadvantage with this case is that there is little change in the wind field above 600 mb during the twelve-hour period.

Rawinsondes

Two sources of rawinsonde data are used in this research. The first is the standard rawinsonde stations which launch soundings twice

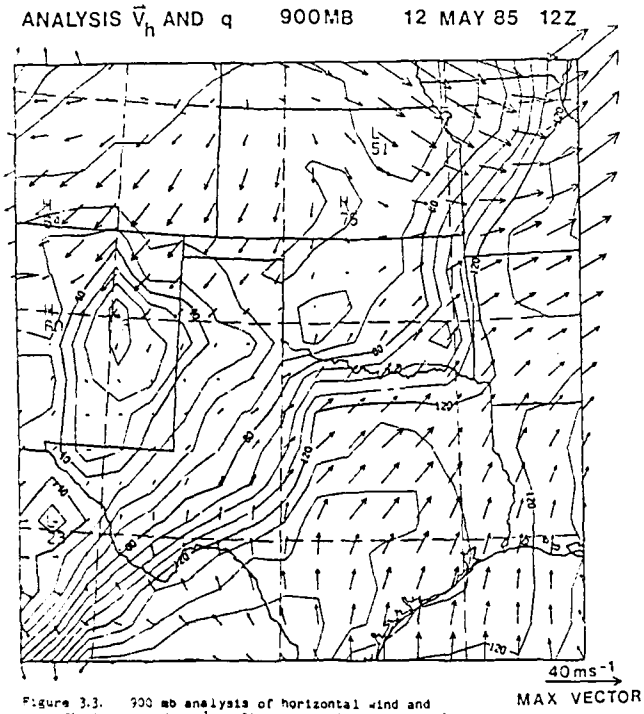

Figure 3.3. 900 mb analysis of horizontal wind and specific humidity (gkg^{-1} x 10) for 1200 GMT 12 May 1985. Contour interval is 1 gkg^{-1}.

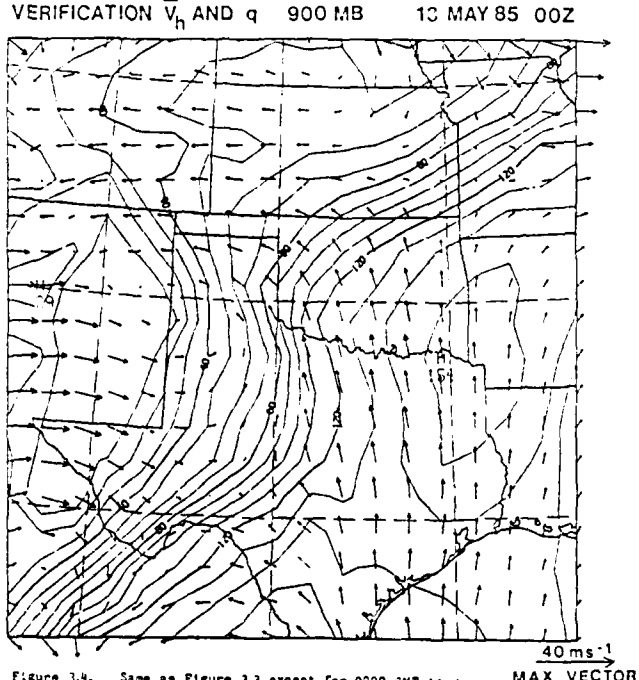

Figure 3.4. Same as Figure 3.3 except for 0000 GMT 13 May 1985.

daily. The second, which is discussed in detail later in this chapter, is additional soundings launched as part of the PRE-STORM program. The standard rawinsonde data is used to initialize the gridded arrays of θ, q, z, u and v. The 51 standard rawinsonde stations are selected because they provide upper-air data over an area which extends approximately 500 km beyond the grid domain in each direction. This ensures that the objective analysis near the grid borders uses data from both outside and inside the grid domain.

For each rawinsonde launch site, the TTBB significant level data and the PPBB wind data are used to obtain the thermodynamic and wind data at each pressure level of the model. If available, standard level data (TTAA) are used to supplement missing or incomplete TTBB or PPBB data. Temperature and dewpoint depression are converted to potential temperature and specific humidity using Poisson's equation and a polynomial approximation for computing saturation vapor pressure (Lowe, 1977). Since the data are already on pressure surfaces, they are interpolated logarithmically to the model pressure levels. As this is done, the virtual temperature (T_v) at each model pressure level is calculated from the temperature (T) and specific humidity (q) at the same level using

$$T_v = T(1.0 + 0.6078q).$$

Since the rawinsonde wind data is provided in thousands of feet MSL, the geopotential height (z) of the model pressure levels is determined using the hypsometric equation. The wind data are then converted into u and v components and linearly interpolated to the model pressure levels. When

interpolation to a model pressure level is not possible because of missing data or high terrain, unrealistic values are put into the corresponding level of the thermodynamic and/or wind arrays for flagging during the objective analysis.

Wind Profilers

As introduced in Chapter I, the PRE-STORM wind profilers provide an opportunity to assess the value of more frequent wind data. However, one of the major obstacles during this research was processing the profiler data into the form required for the wind-updating model discussed in Chapter II. This, although not difficult, is quite cumbersome because the format for the wind data is different for each of the three profilers.

The profiler-unique data formats are a result of each profiler being designed and operated by a different organization. The National Severe Storms Laboratory (NSSL), in conjunction with the University of Oklahoma, operated a WPL wind profiler near Norman, Oklahoma. Because of its two-beam design, wind data are only available on an hourly basis and are derived from a composite of up to twelve data samples through the use of a sliding consensus window (Fischler and Bolles, 1981), (Chadwich, Frisch and Strauch, 1984). At each height, the largest set of measurements within 4 ms^{-1} of each other is used to calculate the average wind (Hogg et al., 1983). If the largest "grouping" contains less than four samples, the wind value for that particular altitude and time is recorded as missing. Because the radar operates in a dual pulse-width mode, the vertical resolution of the wind data varies with

height. The 3.7 μs pulse provides 24 levels of data from 1.97 km MSL to 8.61 MSL with a height interval of 290 meters. Eighteen levels of data with an 870 meter vertical interval, from 2.98 km MSL to 17.71 km MSL, are attainable using the 9.7 μs pulse mode. The data from the Norman profiler is formatted in two sections, one for the 3.7 μs pulse data and one for the 9.7 μs pulse data, and therefore has a data overlap of nearly 6 km.

The second profiler was operated near Liberal, Kansas by the Aeronomy Laboratory. This radar is a three-beam system and thus can provide wind data every thirty minutes. Like the Norman profiler, the Liberal system operates in a dual-pulse mode and uses a consensus window to derive the wind data. However, the data are provided in only one section (i.e., no vertical overlap). From 2.3 km MSL to 10.4 km MSL the vertical resolution is 290 meters and from 10.4 km MSL to 17.9 km MSL the vertical resolution is 580 meters.

The Radian Corporation installed and operated the third wind profiler near McPherson, Kansas. Using Yagi-type antennas, this West German-made prototype SOUSY 50 MHz system has an average power on the order of ten times greater than the Norman profiler. Its greater power allows coverage from 2.6 km MSL to 13.9 km MSL with 150 meter vertical resolution. As with the Liberal profiler, the three-beam design of the McPherson profiler allows for a new wind composite every thirty minutes. Unlike the other profilers, however, the McPherson profiler requires an attendant and therefore could not operate continuously during PRE-STORM (Kaimal, Dec., 1985).

The following procedures are used to obtain hourly wind data on the model pressure levels from the raw wind profiler data. Although the approach is generally the same, the data processing techniques used for each profiler are described separately. Before continuing, however, the first step in processing the raw data from all three profilers is to convert the wind data from direction and speed to u and v components. If a data point is missing, it is awarded u and v values which are flagged for future identification.

For the two cases studied here, the McPherson, KS profiler data are the most cumbersome to process, primarily because the data sets are not continuous in time. Figure 3.5 shows how the McPherson data in the June 11th case contains several gaps in time when observations were not collected. Since the half-hourly data are averaged to hourly data anyway (explained below), the missing data at 0130 GMT, 0200 GMT, 0630 GMT and 0700 GMT are replaced by extrapolating the data with which they would have been averaged (i.e., 0100 GMT, 0230 GMT, 0600 GMT and 0730 GMT respectively). The lack of data during the last three hours is remedied by assuming the wind field is constant from 0900 GMT to 1200 GMT. In addition to the extrapolation, 43 egregiously bad observations are discarded from the McPherson data set. Figure 3.6 demonstrates the result of this scheme. Linear interpolation in the vertical is then used to obtain winds at each reporting level (Fig. 3.7). Where necessary, the observation from the highest level of reported data is extrapolated upward to replace missing data at the top level or levels of the wind profile. Because the Norman profiler data is only available on an hourly basis, the next step is to average the half-hourly

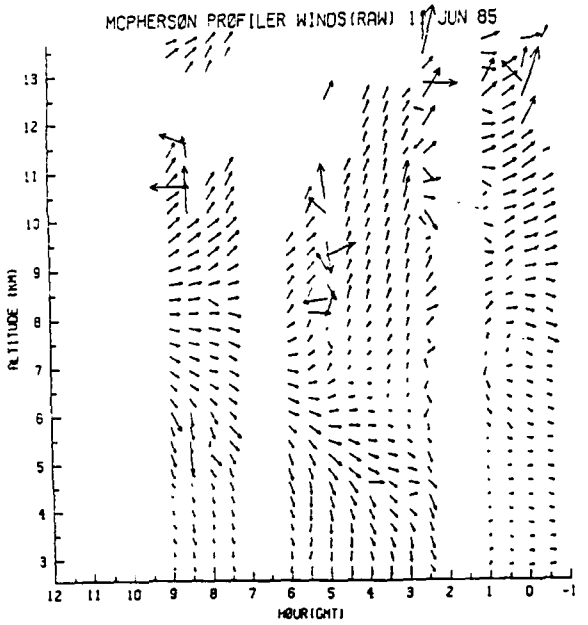

Figure 3.5. Raw profiler winds (ms^{-1}) from 2330 GMT 10 June to 1130 GMT 11 June 1985 for McPherson, KS. Times represent the beginning of the 30 minute averaging period. Altitudes are MSL.

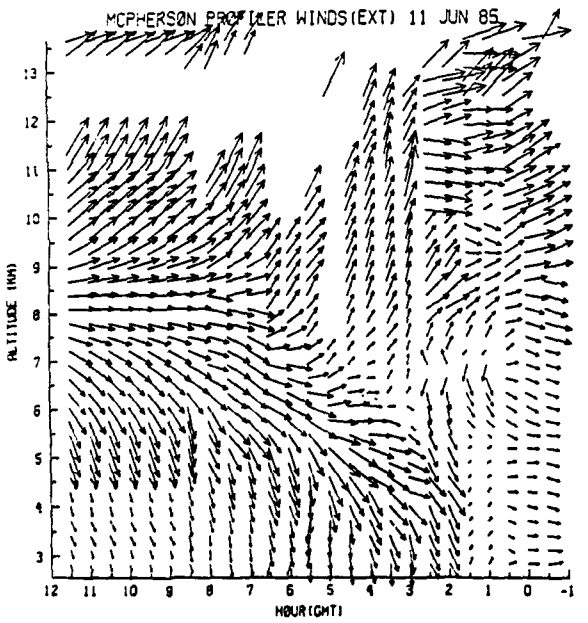

Figure 3.6. Profiler winds from 2330 GMT 10 June to 1130 GMT 11 June 1985 for McPherson, KS after extrapolation in time. Altitudes are MSL.

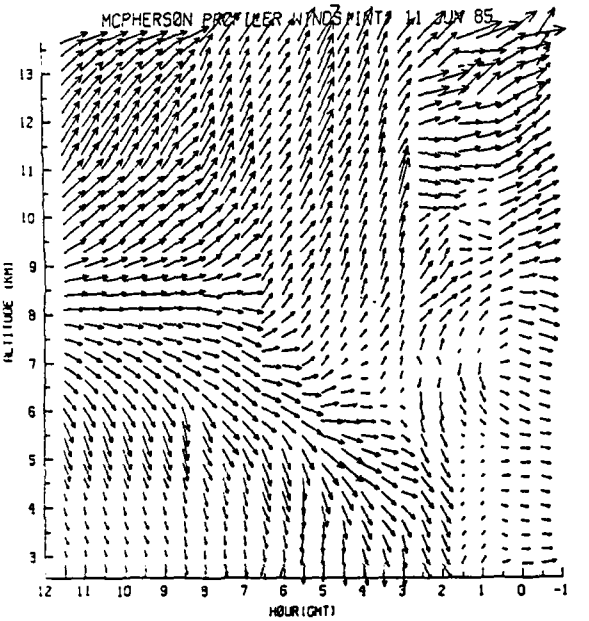

Figure 3.7. Same as in Figure 3.6 except after vertical interpolation/extrapolation.

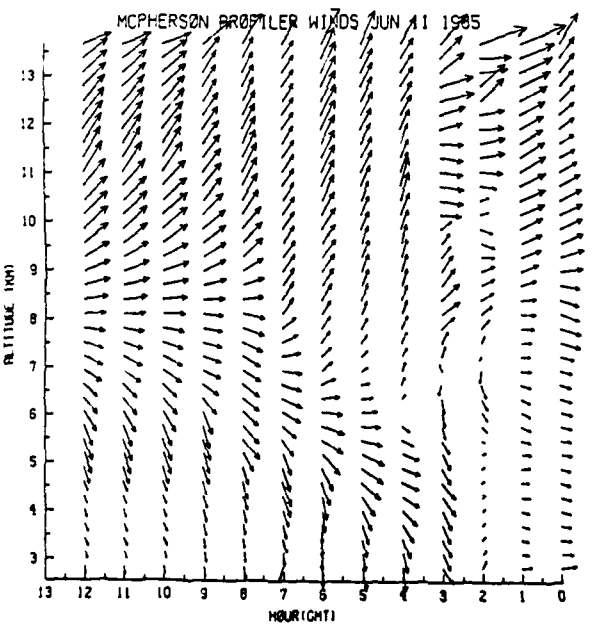

Figure 3.8. Same as in Figure 3.7 except winds are one-hour averages.

McPherson data into hourly data (Fig. 3.8). The final step in preparing the profiler winds is to linearly interpolate the data from the reported heights (km MSL) to the model levels using the model pressure level heights (km MSL) obtained from the rawinsonde data as described in Chapter II (Fig. 3.9). Here it is assumed that the height field is constant during the twelve-hour model period because a typical twelve-hour height tendency is much less than the vertical resolution of the profilers. However, before the interpolation can be completed, another problem inherent to the profiler data must be addressed. Since the lowest level of the model is 900 mb (approximately 1 km MSL) and the lowest reported profiler winds are generally 1-2 km AGL, a method to fill the data void must be developed. Because June 11th is a nighttime case, not enough surface data is available to deduce the surface wind field at the profiler sites. Therefore, the method used is simple extrapolation of the lowest reported profiler wind downward to the 900 mb level. Although crude, this is a reasonable alternative, particularly when a radiational inversion sets up. The constant wind with height from 900 to 800 mb in Figure 3.9 illustrates that the McPherson profiler does not sense the wind velocities below about 750 mb. With the completion of the interpolation to the model pressure levels, the profiler data is ready for use in both the initial Cressman analysis of the wind field and the wind-updating model as described in Chapter II.

The McPherson, KS data from the May 12-13 case required only slightly less effort to process. Since the McPherson profiler was not automated, profiler data was not collected between 0900 GMT and 2100 GMT

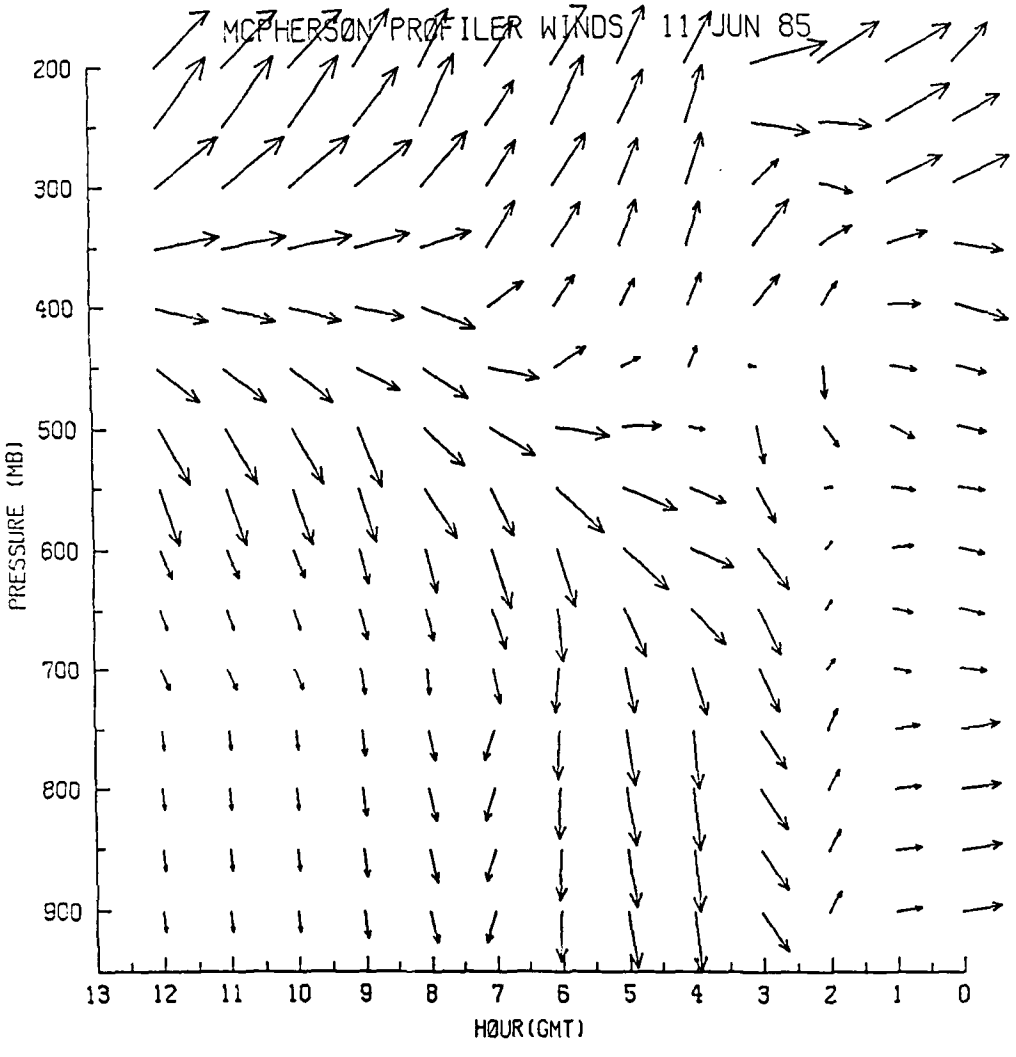

Figure 3.9. Model-level profiler winds from 0000 GMT to 1200 GMT 11 June 1985 for McPherson, KS. Times represent the beginning of the 60 minute period in which the winds are used in the model.

on 12 May 85 because the attendant was not available for duty. In addition, the quality of the data from 2100 GMT through 2300 GMT on 12 May 85 is very poor (not shown) and therefore, is not used (Fig. 3.10). As a result, wind data was manufactured for the 1200 GMT 12 May 85 to 0000 GMT 13 May 85 period by first vertically interpolating/extrapolating the 0900 GMT and 2330 GMT data as previously discussed and then interpolating in time between the two observations. This scheme provides reasonable results (Fig. 3.11) because surface and upper-air data indicate that the wind field did not change very much. As with the June case, before the profiler winds can be interpolated to the model pressure levels, the data void from 900 mb to approximately 750 mb must be filled. However, a different method than described earlier is used to accomplish this for the daytime case. The technique for May 12-13 uses surface wind observations to supplement the profiler winds and provide a lower bound for the vertical linear interpolation to the model pressure levels. The surface wind for the profiler sites is estimated using available information from nearby surface reporting stations (Table 3.1). Figure 3.12 shows the results of this procedure on the daytime case for McPherson.

Of the three PRE-STORM profilers, the one at Liberal, KS provided the most continuous and manageable data. Figure 3.13 shows the raw Liberal data for June 11th. In a few instances, interpolation was completed by hand to fill small gaps in the data. After averaging in time to obtain hourly data (Fig. 3.14), the data is vertically interpolated to the model pressure levels employing the same technique used on the McPherson data. The final result is depicted in Figure 3.15.

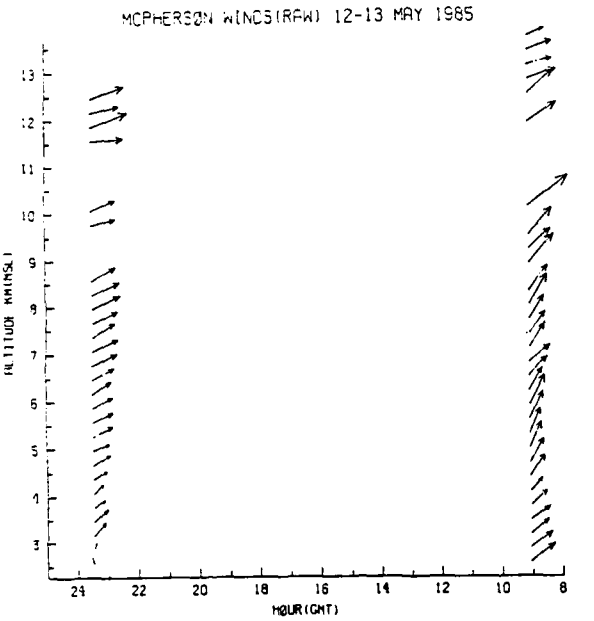

Figure 3.10. Raw profiler winds (ms^{-1}) from 0900 GMT 12 May to 0000 GMT 13 May 1985 for McPherson, KS. Times represent the beginning of the 30 minute averaging period.

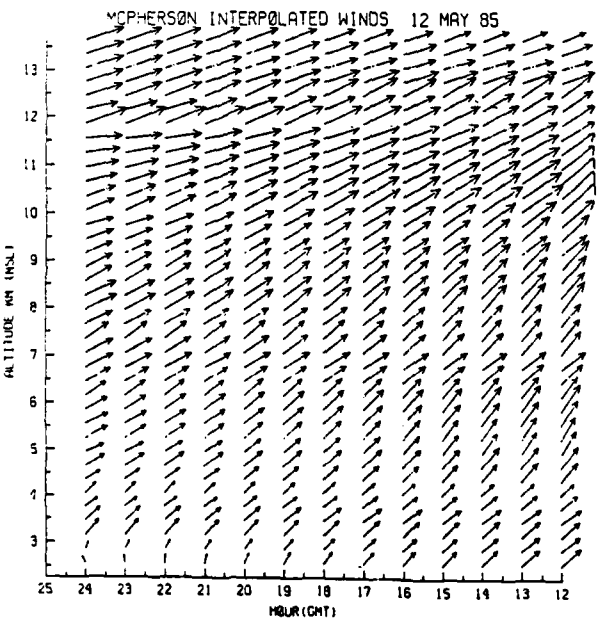

Figure 3.11. Profiler winds from 1200 GMT 12 May to 0000 GMT 13 May 1985 for McPherson, KS after interpolation in the vertical and in time.

Table 3.1

Estimated Surface Wind Observations 12-13 May 85

	McPherson, KS		Liberal, KS		Norman, OK*	
GMT	deg	kts	deg	kts	deg	ms^{-1}
1200	360	5	020	10	139	0.5
1300	010	5	070	5	126	0.7
1400	020	5	080	15	165	0.9
1500	020	5	110	10	094	0.7
1600	040	6	080	15	086	2.8
1700	360	6	090	15	083	3.4
1800	360	6	090	15	093	2.5
1900	040	12	120	15	128	2.9
2000	040	8	120	10	152	3.1
2100	070	12	120	15	161	4.2
2200	050	10	110	6	136	3.9
2300	100	10	110	15	130	4.9
0000	090	8	100	15	142	3.9

*data obtained from an automated observation site near Goldsby, OK.

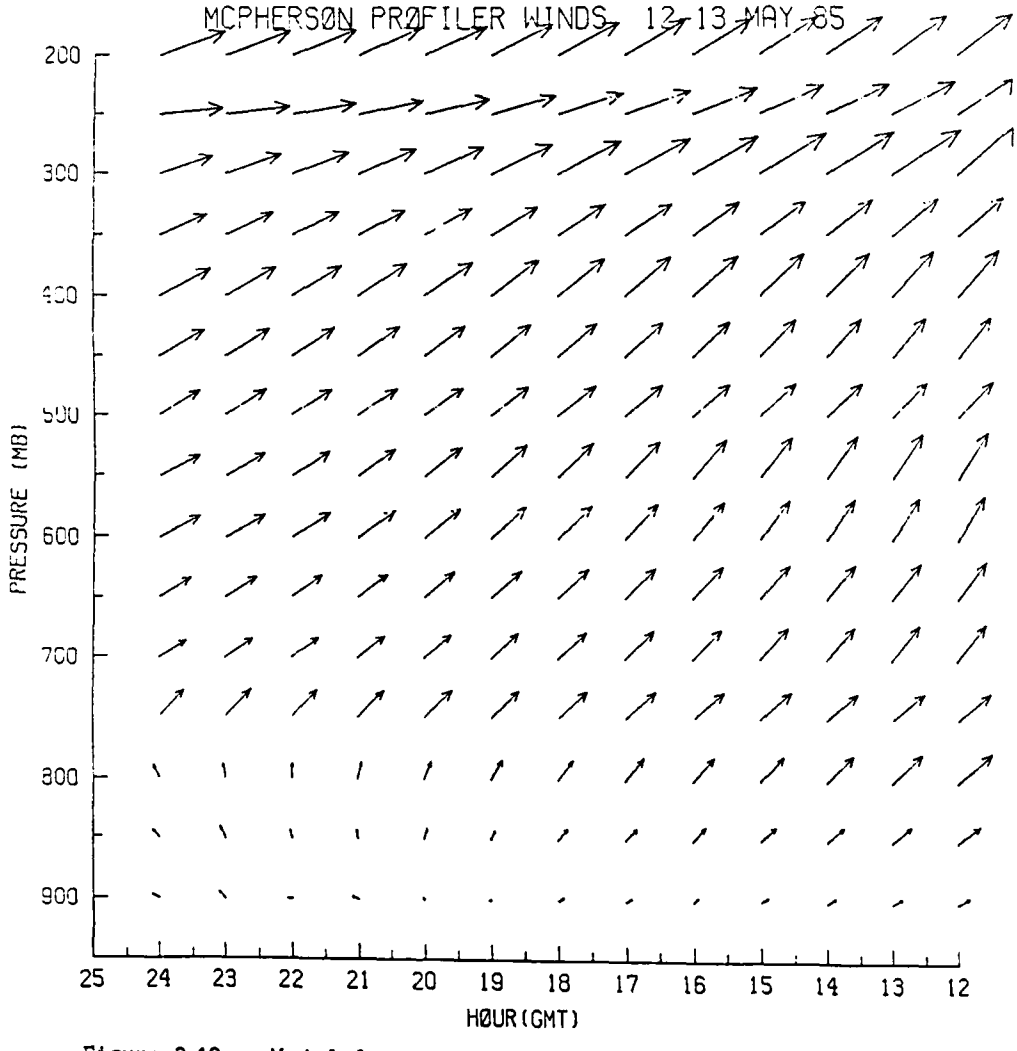

Figure 3.12. Model-level profiler winds from 1200 GMT 12 May to 0000 GMT 13 May 1985 for McPherson, KS. Times represent the beginning of the 60 minute period in which the winds are used in the model.

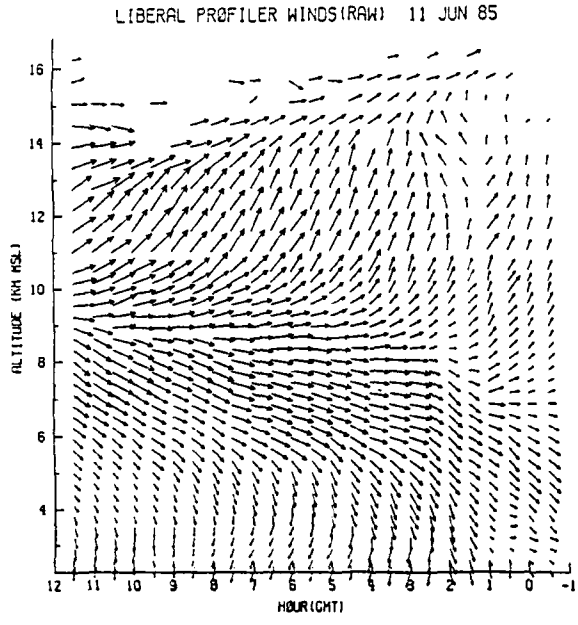

Figure 3.13. Same as in Figure 3.5 except for Liberal, KS.

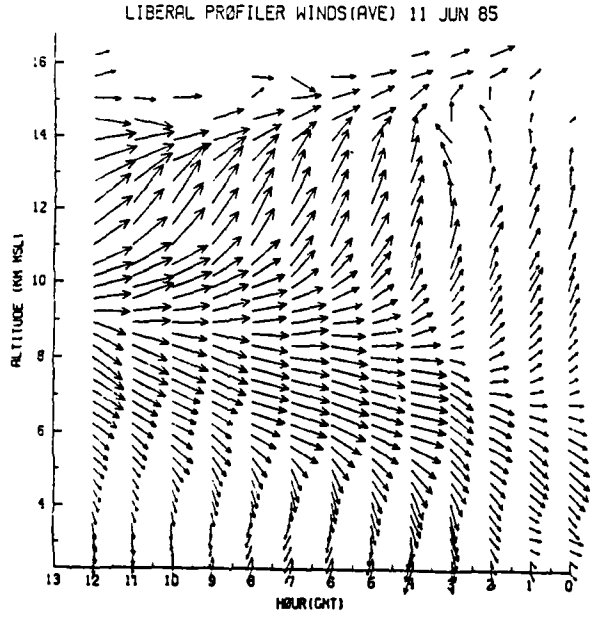

Figure 3.14. Same as in Figure 3.13 except winds are one-hour averages.

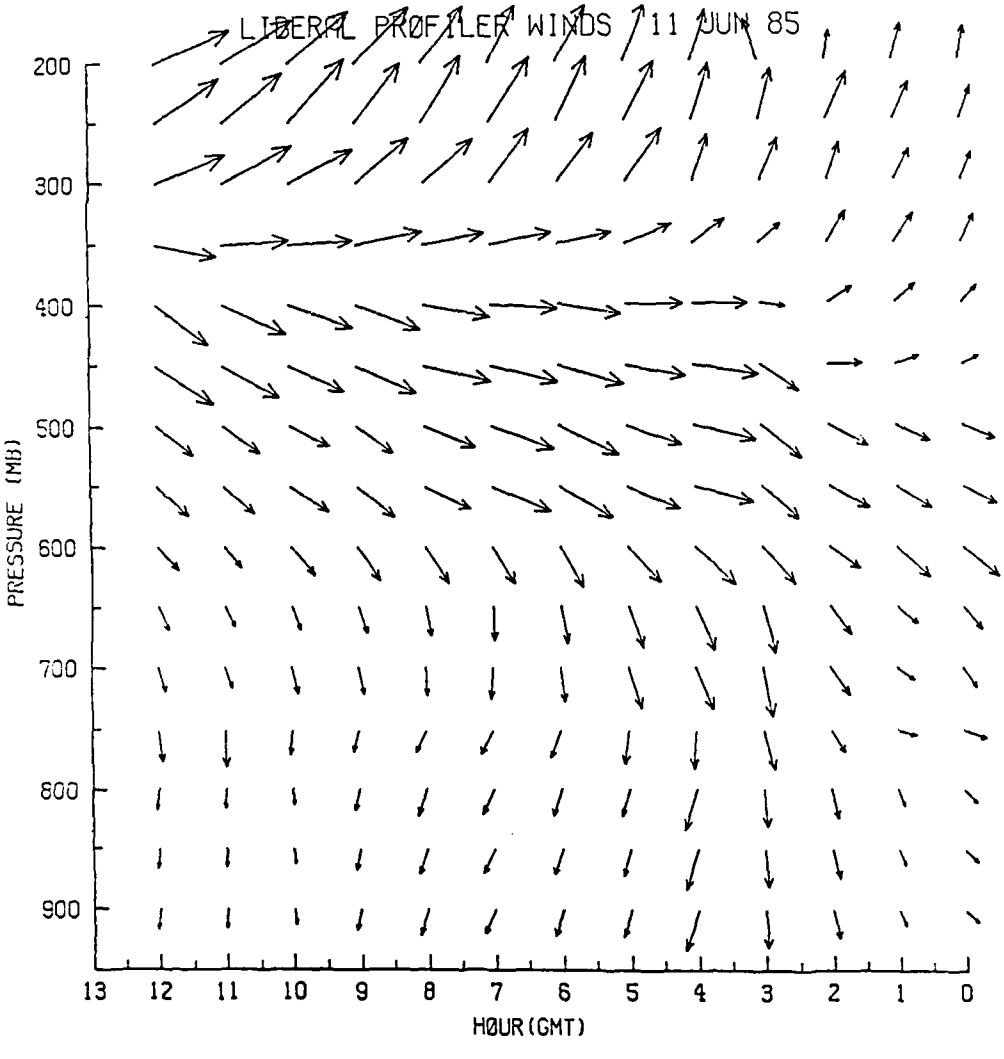

Figure 3.15. Model-level profiler winds from 0000 GMT to 1200 GMT 11 June 1985 for Liberal, KS. Times represent the beginning of the 60 minute period in which the winds are used in the model.

A very similar set of procedures is used to process the May 12-13 Liberal profiler data (Fig. 3.16). Interpolation in the vertical is first completed to fill the holes in the data then the winds are averaged to hourly intervals (not shown). Finally, the profiler winds are linearly interpolated to the model pressure levels (Fig. 3.17) using estimated surface wind observations and the procedure outlined for the McPherson daytime data.

The Norman profiling system differs from the McPherson and Liberal profilers. As discussed earlier, its two-beam design forces the hourly averaging of the winds. Also, both the short (3.7 μs) and the long (9.7 μs) pulse data are outputted for use. These differences alter some of the data processing procedures discussed above. In addition, before any Norman profiler data from PRE-STORM can be processed, a correction must be applied to the raw data which accounts for an error induced by sloping terrain at the antenna site. The Appendix details this problem and the method used to correct it. Figures 3.18 and 3.19 depict the corrected June 11th short and long pulse width profiler winds, respectively. Merging these two data sets is the next step to processing the Norman data (Fig. 3.20). Figure 3.21 shows the final results after the data are vertically interpolated to the model pressure levels in the same manner as the Liberal and McPherson June 11th profiler winds.

For the May 12-13 case, the Norman profiler data are first corrected for the antenna-beam pointing error according to the procedures outlined in the Appendix. As with the June 11th case, the short and long pulse width data (not shown) are merged into one data set

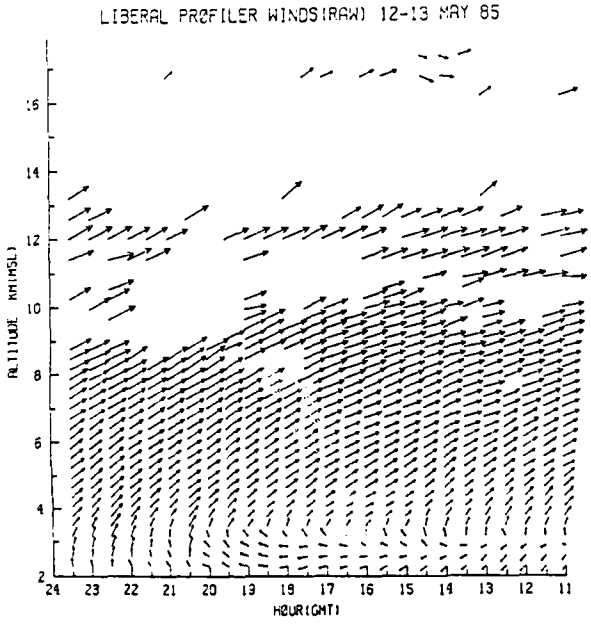

Figure 3.16. Same as in Figure 3.13 except from 1100 GMT to 2330 GMT 12 May 1985.

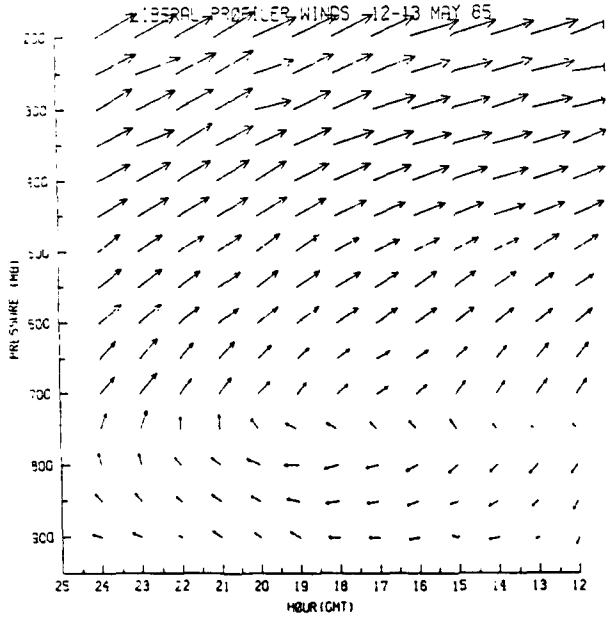

Figure 3.17. Same as in Figure 3.15 except from 1200 GMT 12 May to 0000 GMT 13 May 1985.

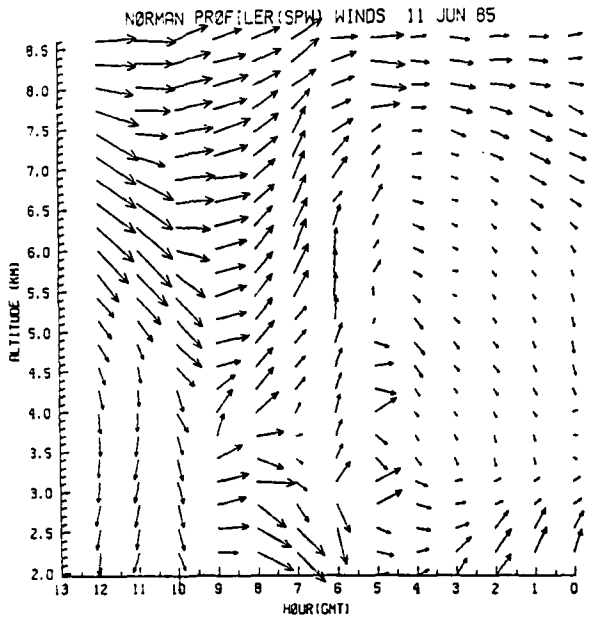

Figure 3.18. Raw short pulse width (3.7 μs) profiler winds (ms^{-1}) from 0000 GMT to 1200 GMT 11 June 1985 for Norman, OK. Times represent the beginning of the 60 minute averaging period. Altitudes are MSL.

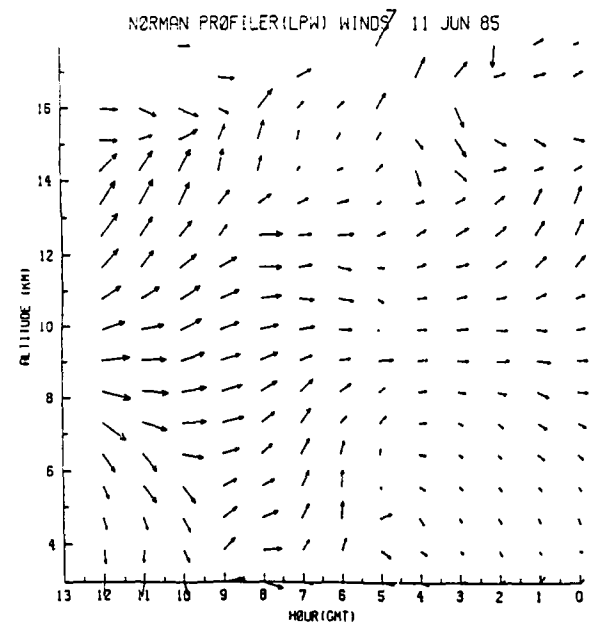

Figure 3.19. Same as in Figure 3.18 except for long pulse width (9.7 μs).

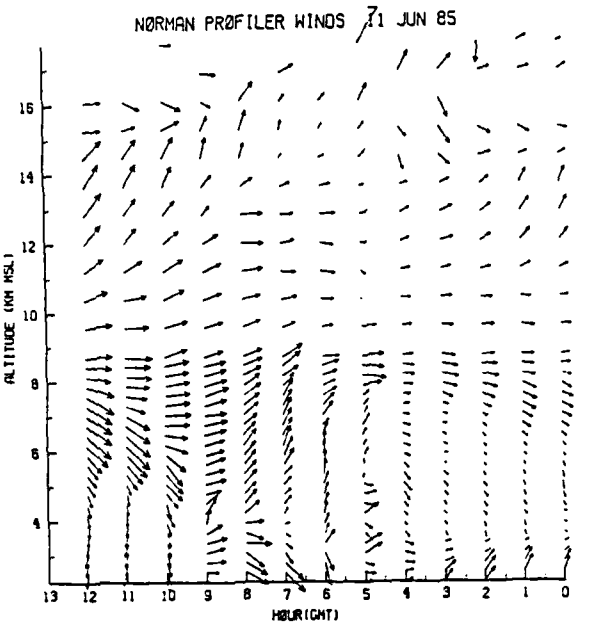

Figure 3.20. Same as in Figures 3.18 and 3.19 except for combined pulse widths.

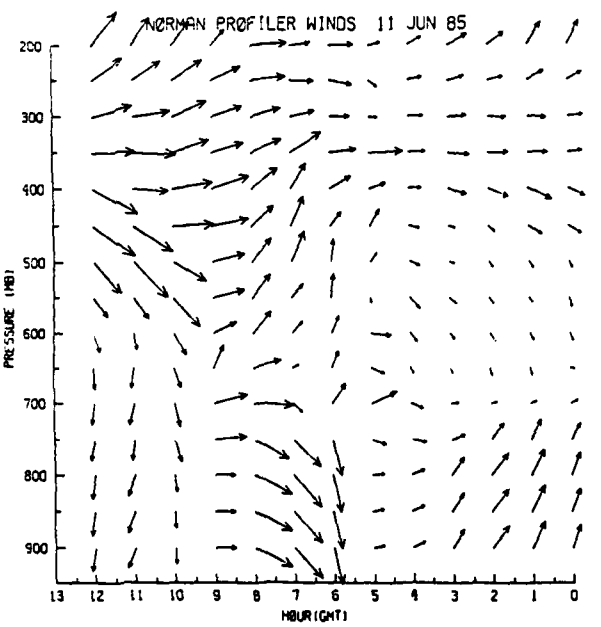

Figure 3.21. Model-level profiler winds from 0000 GMT to 1200 GMT 11 June 1985 for Norman, OK. Times represent the beginning of the 60 minute period in which the winds are used in the model.

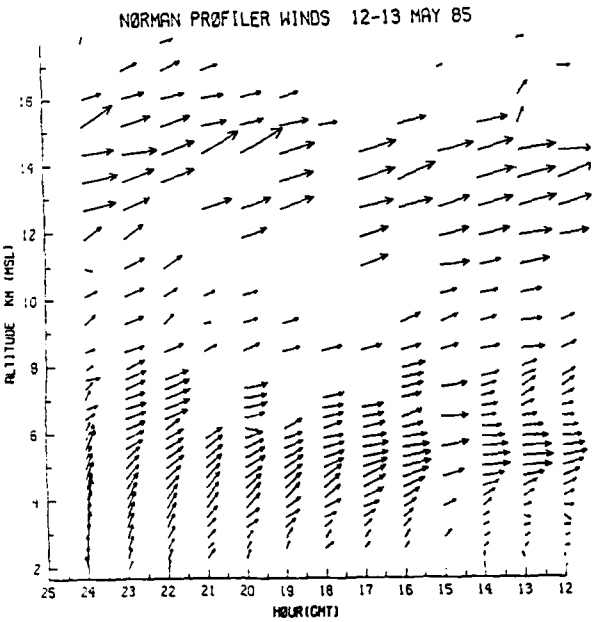

Figure 3.22. Same as in Figure 3.20 except from 1200 GMT 12 May to 0000 GMT 13 May 1985.

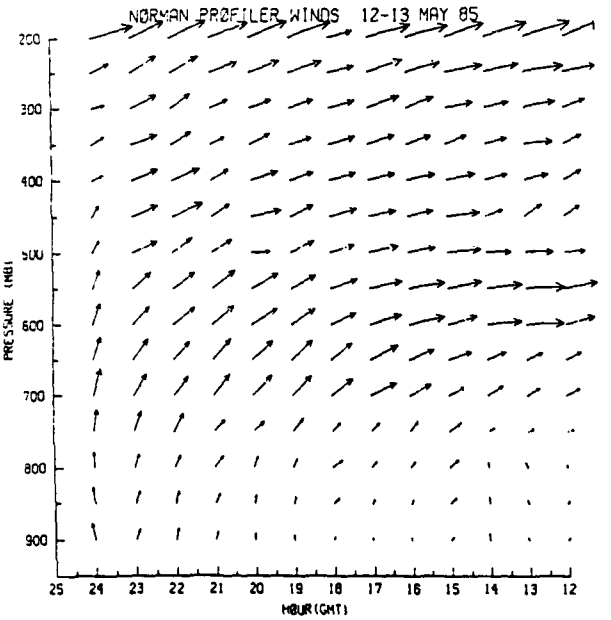

Figure 3.23. Same as in Figure 3.21 except from 1200 GMT 12 May to 0000 GMT 13 May 1985.

(Fig. 3.22). Note that only the long pulse width data are available at 1500 GMT on 12 May 85. Again, the final step in preparing the Norman profiler winds is to linearly interpolate the data to the model pressure levels (Fig. 3.23) using the estimated surface winds from Table 3.1 as a lower bound.

PRE-STORM Rawinsonde Data

The final source of data for this research is the PRE-STORM rawinsonde data. When requested by the PRE-STORM directors, all or part of a network of rawinsonde stations were activated and soundings were recorded. The network consisted of fourteen standard rawinsonde stations and twelve supplemental rawinsonde stations (Fig. 1.1). During periods of convective activity, soundings were frequently launched at 90-minute intervals. As with the McPherson, KS profiler, manpower restrictions prevented the rawinsonde network from operating on a 24 hour-per-day basis. Often, thunderstorm events were missed because the operators were not available for duty.

The PRE-STORM rawinsonde data is vital to this research because it is the verification data for the advection model soundings. However, the availability of the PRE-STORM soundings restricts which cases can be studied because of the operational limitations discussed above. In each of the two cases considered here, the verification point (or station of interest (SOI) as defined in Chapter II), are selected based upon the frequency of PRE-STORM rawinsonde data and the observed weather at the site. For the nighttime case, the supplemental rawinsonde station at Enid, OK is used because sounding data is available approximately every

90 minutes during the twelve-hour period in which a mesoscale convective system (MCS) traversed the site. Oklahoma City is the verification point for the daytime case because it is the only station which collected sounding data at both the start of the twelve-hour period (1200 GMT 12 May 85) and during the late afternoon on May 12th when the thunderstorms were developing. In both cases, the PRE-STORM rawinsonde data and the model-produced soundings are plotted on skew-T, log p diagrams for comparison.

CHAPTER IV

RESULTS AND DISCUSSION

Chapter IV presents results from the wind-updating and advection models. Using hourly profiler winds to update the wind analysis, changes are computed in the temperature and moisture fields. Recall that the goal of this research is to produce thermodynamic soundings which are more accurate than using the original sounding which has been modified at the lowest levels with surface data. To determine the degree of success of this research, the model results are presented from two perspectives. The first is to look at how well the models handled synoptic scale features such as frontal passages and gulf moisture return. The second is a direct comparison between model-produced soundings and rawinsonde data obtained from the PRE-STORM upper-air network. This chapter is divided into two main sections, one for each of the two cases studied.

Case I: 11 Jun 85 0000 GMT - 11 Jun 85 1200 GMT

As discussed in Chapter III, the June 11th case is noted for the large mesoscale convective system (MCS) which transited the profiler triangle (Figs. 4.1a and 4.1b). Although these thunderstorms dominated the region, the passage of a cold front and an upper-level short wave

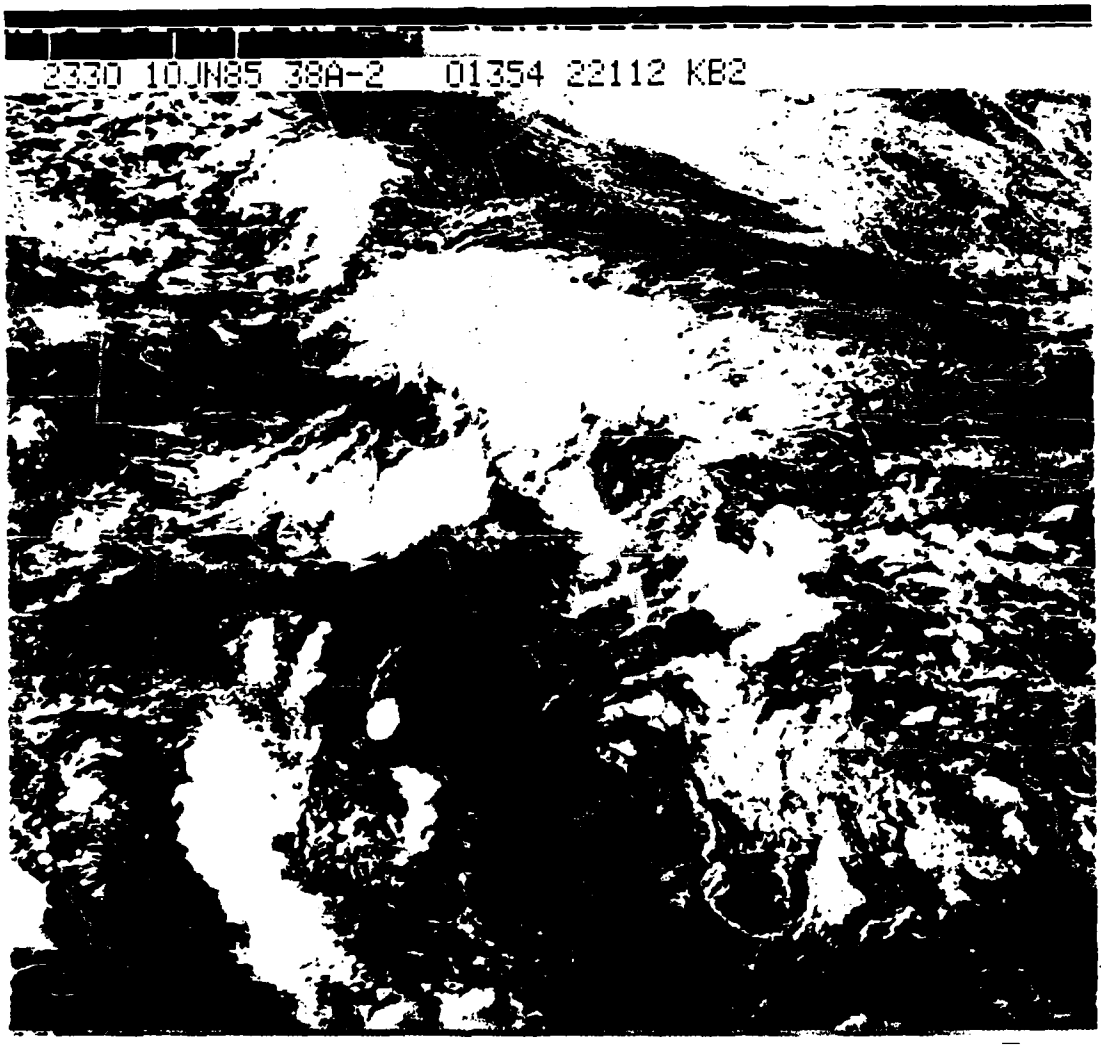

Figure 4.1a. Visible satellite picture for 2330 GMT 10 June 1985.

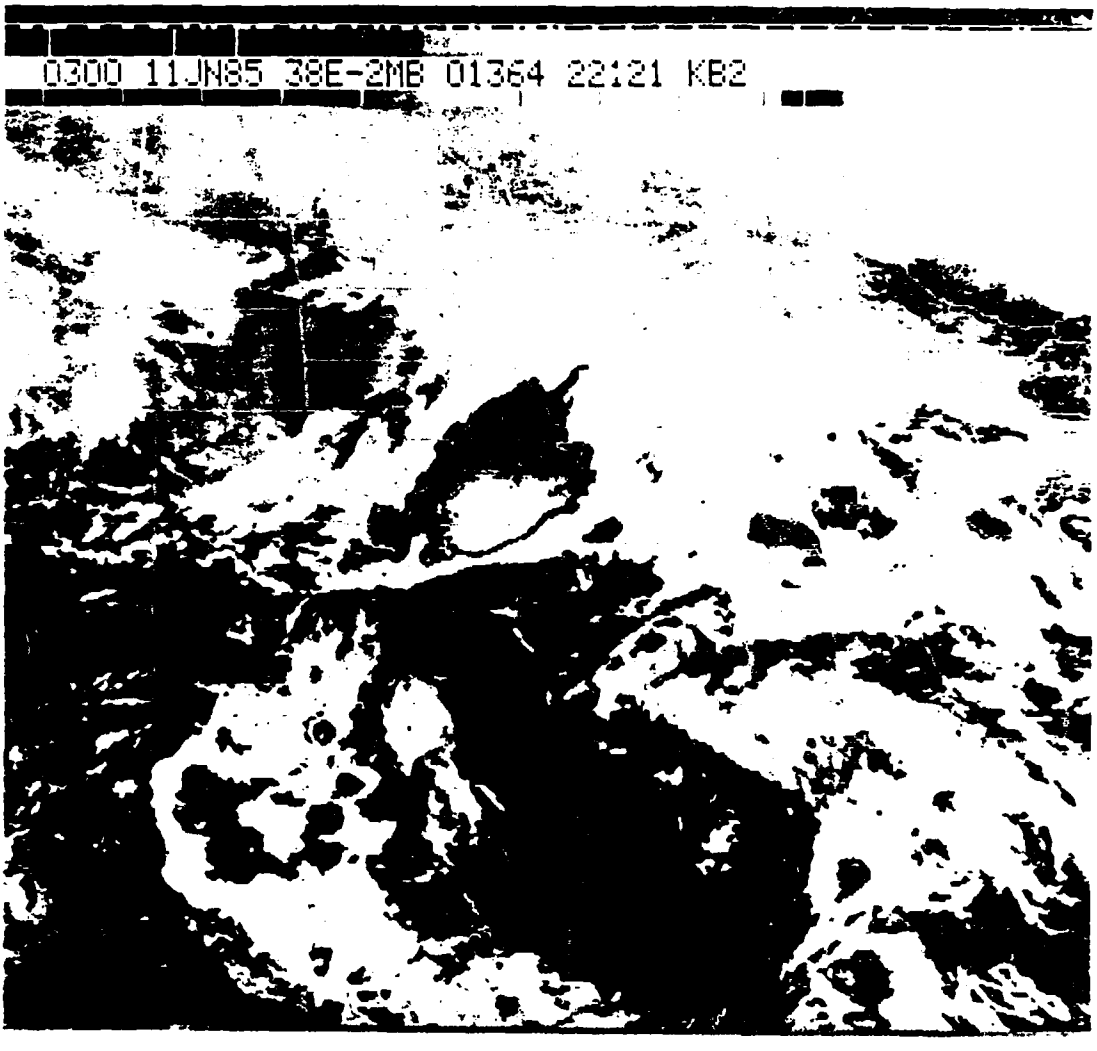

Figure 4.1b. Infrared satellite picture for 0300 GMT 11 June 1985.

through the triangle makes June 11th a very good case to test the wind-updating and advection models. The model-produced 500 mb and 850 mb horizontal and vertical wind fields and the 850 mb specific humidity fields are examined for continuity and compared to the verification analyses. In addition, the model-produced soundings for Enid, OK are contrasted with the Enid PRE-STORM soundings.

Wind-Updating Model Results

Recall how the wind-updating model works. A four-pass Cressman objective analysis scheme is used to obtain the initial fields of u and v from rawinsonde and profiler data. The updating of the wind field is performed every hour. The profiler data, after interpolation to model levels, is combined with the modeled gridpoint data via a one-pass Cressman scheme. The influence radius is 100 km for the gridpoint data and 400 km for the profiler information. This allows the profiler winds to have more weight near the triangle and prevent excessive smoothing due to the use of too many gridpoint values. It is important to remember that an upstream feature cannot be reflected in the updated wind fields until it reaches the profiler triangle.

Figure 4.2 shows the 0000 GMT analysis of the 500 mb short wave over western Kansas and the weak northwesterly flow over Oklahoma. By 0300 GMT (Fig. 4.3), the trough appears to have weakened as the winds across central and western Kansas have shifted to the northwest, but the southerly winds ahead of the trough are no longer visible. This apparent problem is in fact, an excellent example of the model's

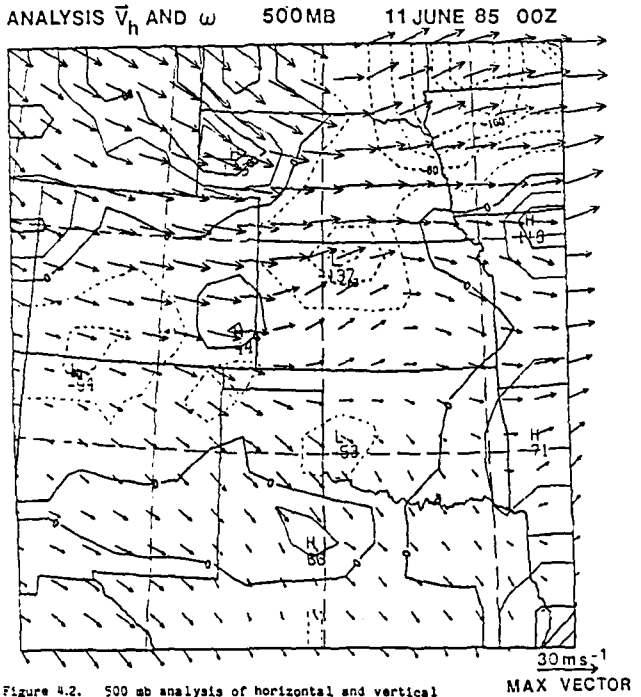

Figure 4.2. 500 mb analysis of horizontal and vertical wind (μbs^{-1} x 10) for 0000 GMT 11 Jun 1985. Contour interval is 4 μbs^{-1}. Dashed lines indicate rising motion, solid lines sinking motion.

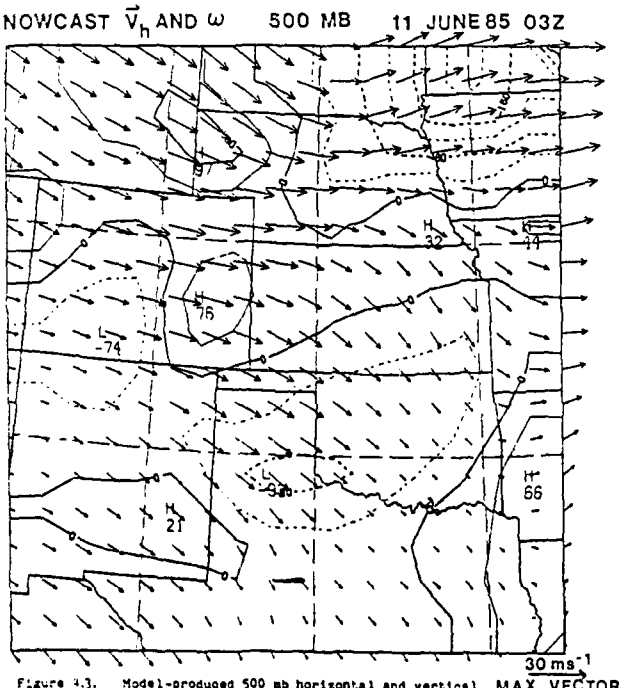

Figure 4.3. Model-produced 500 mb horizontal and vertical wind (μbs^{-1} x 10) for 0300 GMT 11 June 1985. Contour interval is 4 μbs^{-1}. Dashed lines indicate rising motion, solid lines sinking motion.

dependency upon the wind profiler observations. As Figures 3.7, 3.10 and 3.15 point out, by 0300 GMT, the 500 mb trough has passed the Liberal and McPherson profiler sites, but the Norman site is still experiencing weak northwesterly flow. This indicates that the short wave has a very small downstream horizontal scale, much smaller than the profiler triangle. By 0600 GMT, however, the 500 mb winds over Norman have backed and the short wave is once again apparent (Fig. 4.4). Although it is suspected that the modeled upward velocities in northern Oklahoma and southern Kansas are somewhat weak at 0300 GMT due to the absence of the short wave in the modeled wind field, the vertical motion field through the first six hours is reasonable. A large area of ascent has traversed southeastward with the frontal system, and the vertical velocities are typical for subsynoptic scale motions ($\sim$10 μbs^{-1}). However, they are 1-2 orders of magnitude smaller than the vertical velocities typically measured in thunderstorms (Peterson, 1984). This weakness in the vertical motion fields becomes more apparent in later discussions of the advection model results. Continuing to 0900 GMT and Figure 4.5, the base of the trough has moved into central Oklahoma with the area of subsidence dropping into western Oklahoma. The vigorous ascent over the Texas panhandle is due to the heightened convergence in the vicinity of the surface cold front. Finally, by 1200 GMT, the entire profiler region is under strong northwesterly flow at 500 mb (Fig. 4.6). This final nowcast compares extremely well with the 500 mb verification wind analysis at 1200 GMT (Fig. 4.7). The wind direction and speed in and around the profiler triangle are nearly the same in both figures.

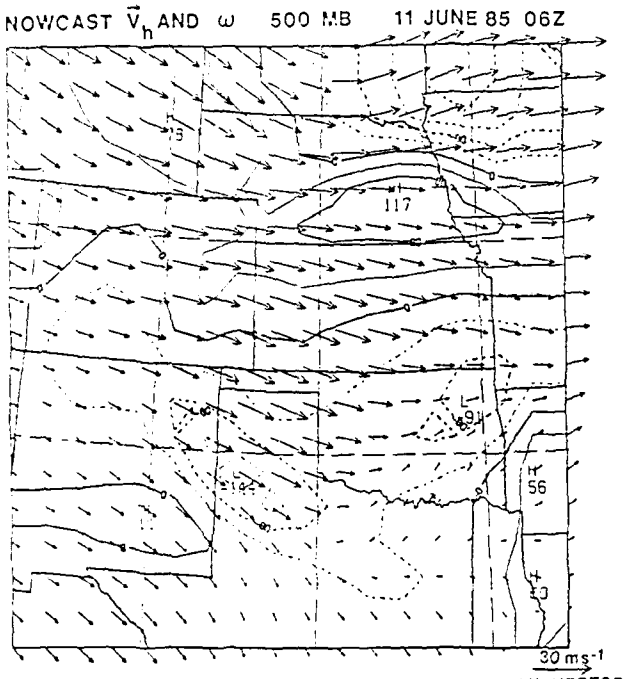

Figure 4.4. Same as in Figure 4.3 except for 0600 GMT 11 June 1985.

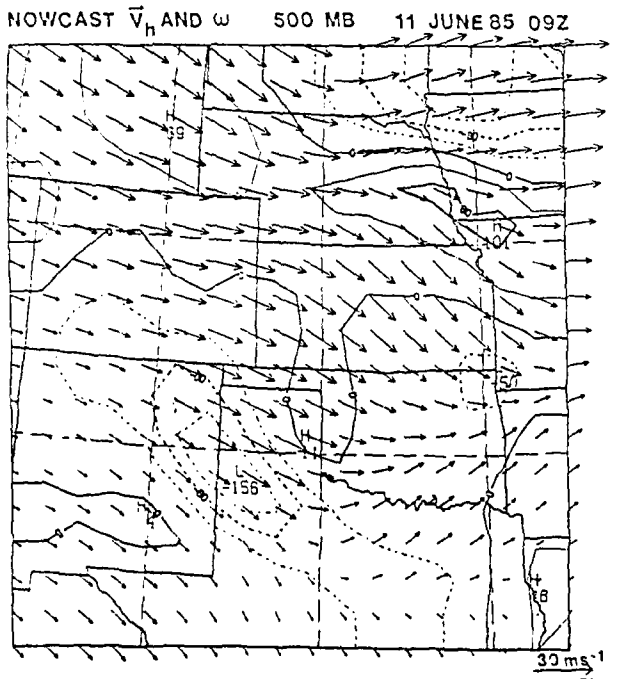

Figure 4.5. Same as in Figure 4.3 except for 0900 GMT 11 June 1985.

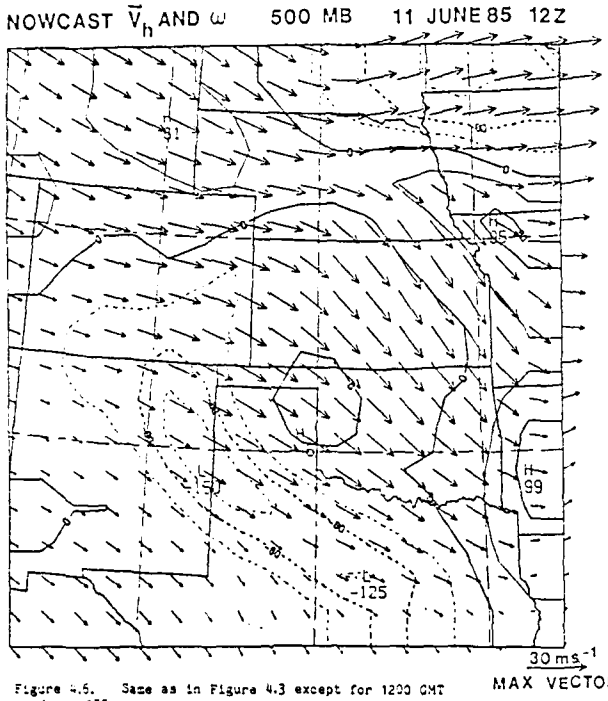

Figure 4.6. Same as in Figure 4.3 except for 1200 GMT 11 June 1985.

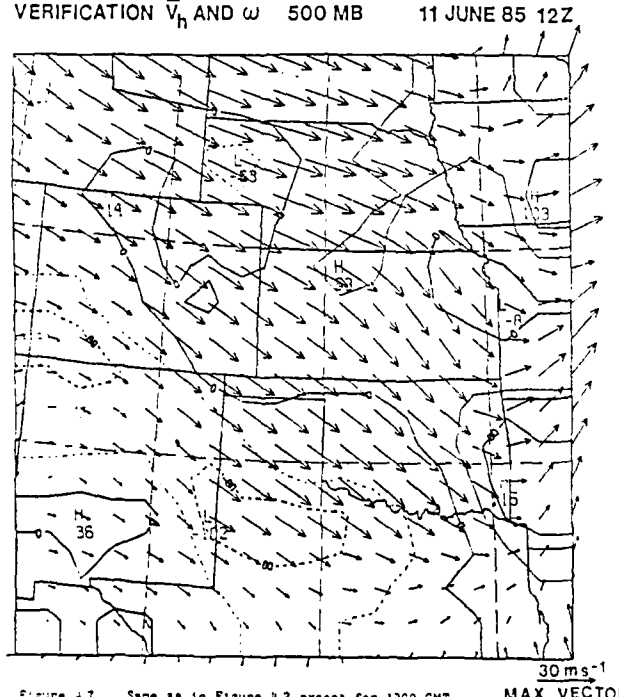

Figure 4.7. Same as in Figure 4.2 except for 1200 GMT 11 June 1985.

The wind-updating model indicates the complete reversal of the 850 mb wind field as the front passes through the profiler triangle during the twelve-hour period. Figure 4.8 shows the strong southerly winds over Kansas and Oklahoma and the frontal boundary over northwestern Kansas at 0000 GMT. Along with the analyzed regions of subsidence in central Kansas and the Nebraska panhandle, the areas of ascent in western Kansas, eastern Kansas and Nebraska agree with the satellite view of the respective areas of clear air and convective activity (Fig. 4.1a). After updating the wind field for three hours with new profiler winds, Figure 4.9 demonstrates how the winds across Kansas, northwestern Oklahoma and the Texas panhandle have reversed direction as the cold front, with help from the MCS outflow, has moved rapidly southeast. By 0600 GMT the wind at the Norman site has shifted to the northwest, and its influence on the gridpoints to the south is quite apparent as the model has moved the front into northern Texas (Fig. 4.10). This excessive frontal movement is the result of not having a profiler site to the south of Norman for use in the objective analysis. Note that the modeled position of the front is near the 400 km influence radius of the Norman and Liberal profilers. This is supported further by the fact that the modeled front has moved very little during the three-hour period leading to 0900 GMT (Fig. 4.11). Finally, the 1200 GMT nowcast wind direction (Fig. 4.12) within the profiler triangle compares very well with the 1200 GMT verification data (Fig. 4.13); however, the nowcast windspeeds are noticeably smaller than the verifying windspeeds. This discrepancy is due to the limitations of the wind profilers. As noted in Chapter III, the profilers could not measure the winds below

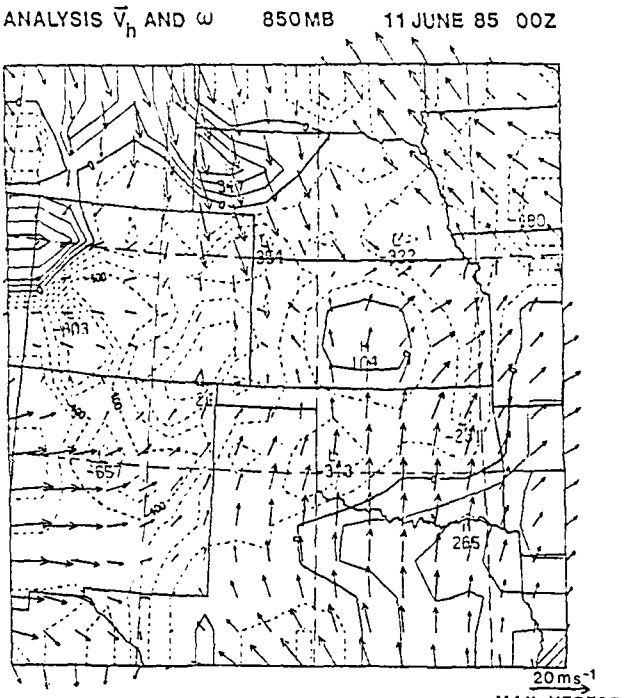

Figure 4.8. 850 mb analysis of horizontal and vertical wind (μbs^{-1} x 102) for 0000 GMT 11 June 1985. Contour interval is 1 μbs^{-1}. Dashed lines indicate rising motion, solid lines sinking motion.

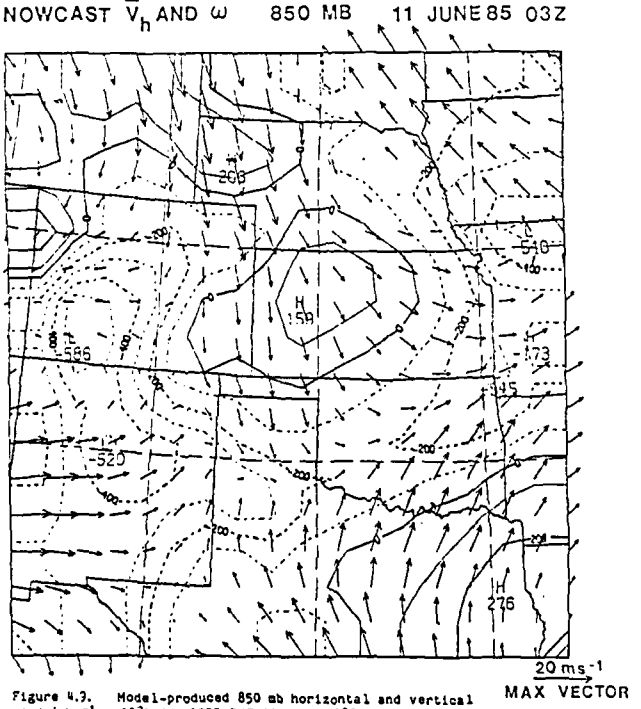

Figure 4.9. Model-produced 850 mb horizontal and vertical wind (μbs^{-1} x 102) for 0300 GMT 11 June 1985. Contour interval is 1 μbs^{-1}. Dashed lines indicate rising motion, solid lines sinking motion.

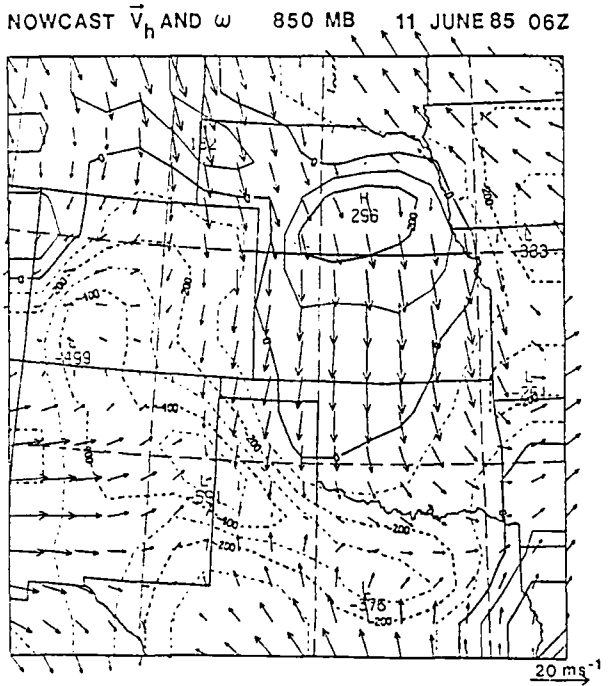

Figure 4.10. Same as in Figure 4.9 except for 0600 GMT 11 June 1985.

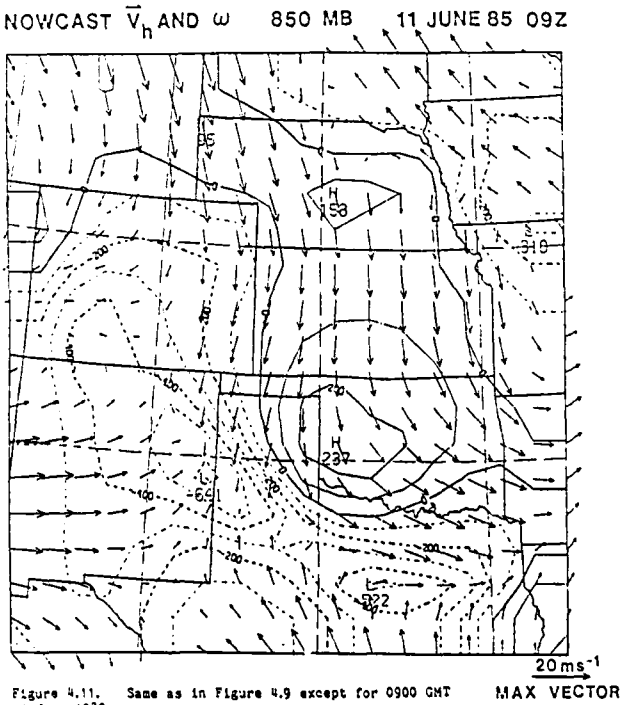

Figure 4.11. Same as in Figure 4.9 except for 0900 GMT 11 June 1985.

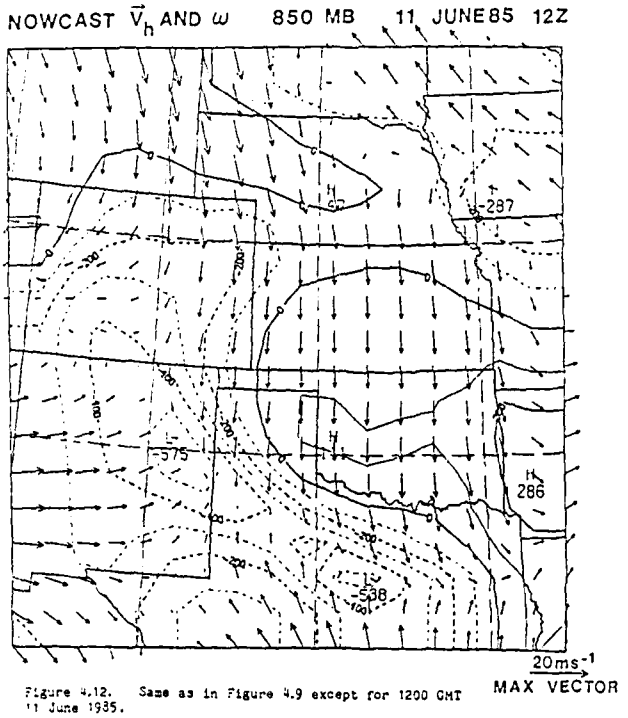

Figure 4.12. Same as in Figure 4.9 except for 1200 GMT 11 June 1985.

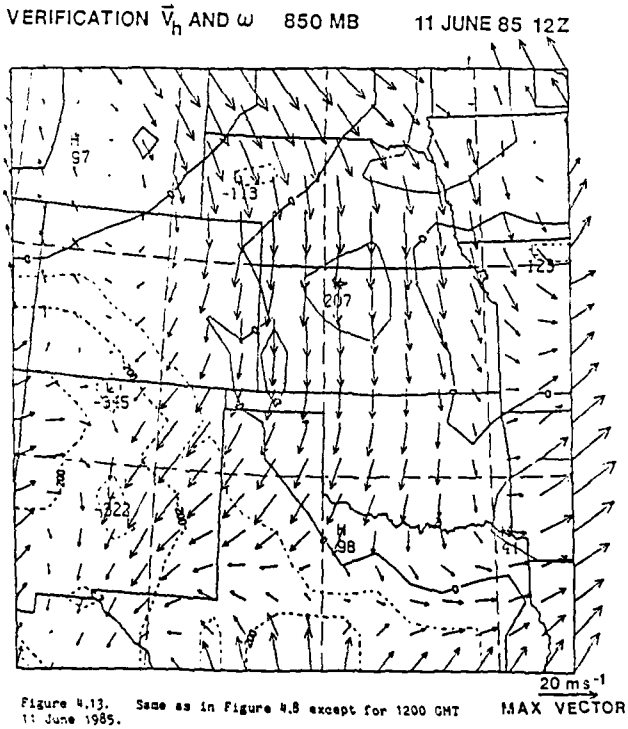

Figure 4.13. Same as in Figure 4.8 except for 1200 GMT 11 June 1985.

approximately 750 mb. In the June 11th case, the compensating technique is to extrapolate the lowest available wind data down to the 800, 850 and 900mb levels. The light 850 mb nowcast winds are due to the light, profiler-observed winds at 750 mb. The wind profilers were incapable of sensing the stronger northwesterly winds which are apparent between 800 mb and 900 mb over Enid, Oklahoma at 1200 GMT (Fig. 4.32). Figures 4.14 and 4.15 show how the nowcast and verification windspeeds at 750 mb are nearly identical.

The vertical motion profiles calculated from the updated wind fields are shown for every three hours in Figure 4.16 for Enid, Oklahoma. A verifying profile for Enid, computed from the complete analysis of 1200 GMT data is also shown. Despite the strong temporal changes in $\omega(p)$ during the period, the nowcast profile is nearly identical to the verifying one by 1200 GMT. This, of course, is due to the fact that the profiler winds are dominating the ω-calculation for Enid in both analyses, but it also indicates that the update procedure works very well, and that the profiles at the intermediate times should be equally as valid (to the extent that one believes in kinematic omegas). Figure 4.16 shows clearly that the increase in low-level ascent as the front passes is followed by strong subsidence in the lower troposphere, while ascent ahead of the upper-level short wave remains in the upper troposphere.

The success of the wind-updating model is limited by having only three profiler sites within a 1530 km square domain. The first limitation appears in Figure 4.9 in northwestern Kansas and southwestern Nebraska where there is a noticeable lull in the northwesterly winds.

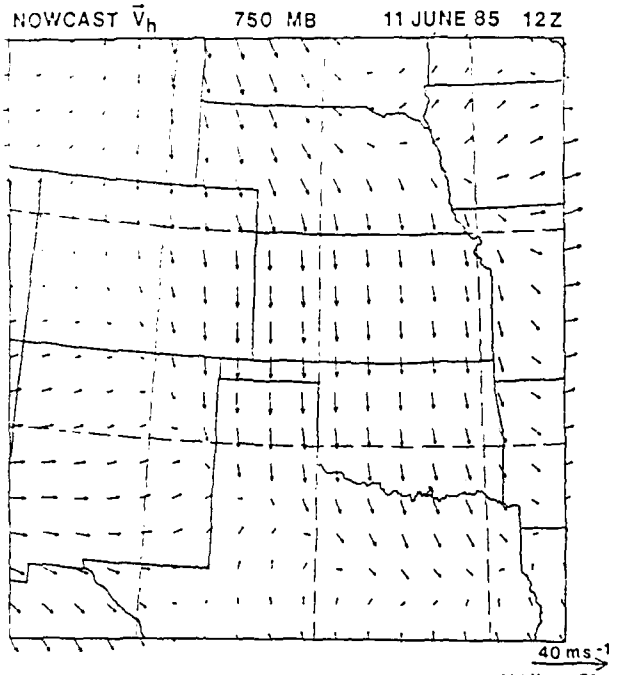

Figure 4.14. Model-produced 750 mb horizontal wind field for 1200 GMT 11 June 1985.

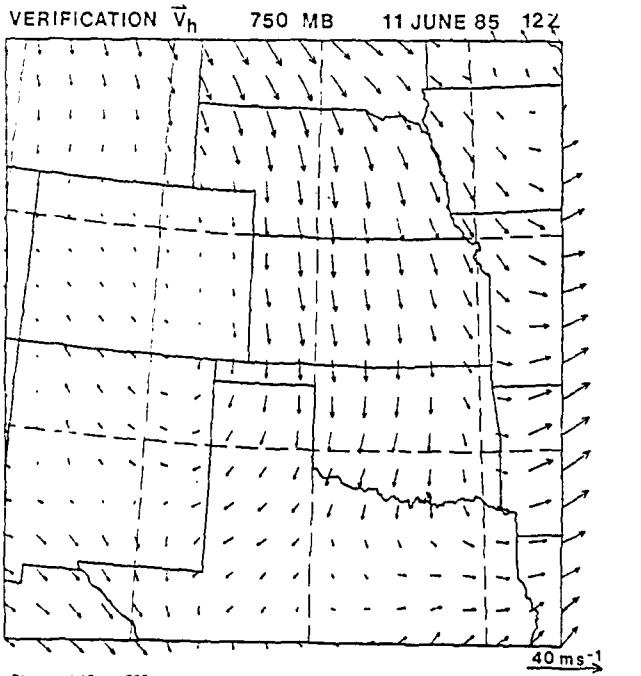

Figure 4.15. 750 mb analysis of horizontal wind for 1200 GMT 11 June 1985.

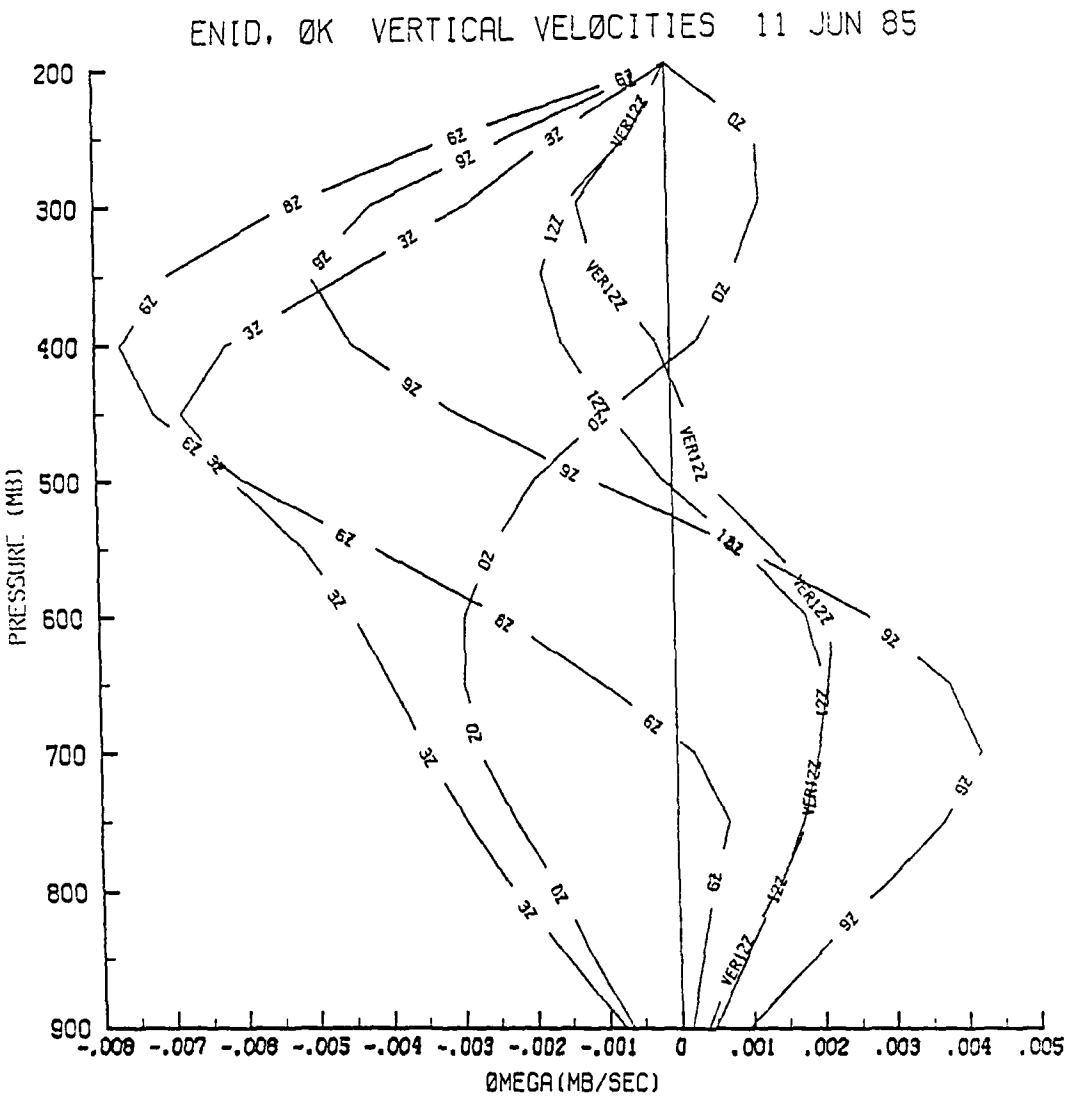

Figure 4.16. Vertical velocities (mbs^{-1}) for Enid, OK from 0000 GMT to 1200 GMT 11 June 1985. The 0Z and VER12Z curves are computed from observed data. The 3Z, 6Z, 9Z and 12Z curves are model-produced.

This is in the same location as the analyzed cold front in Figure 4.8 and is also just within the 400 km influence radius of the McPherson and Liberal profilers. By design of the wind-updating model described in Chapter II, the lighter windspeeds are due to the profilers having weak influence on the wind field at this range. The 400 km influence radius is used because it produces the best wind field results within the profiler triangle. A larger radius forces each profiler to have too great an influence on the grid point wind values nearest the other profilers, and would not necessarily resolve the type of problem found in Figure 4.9. In fact, if the front had initialized 200 km further northwest, it would take an influence radius of 600 km just to obtain the type of results seen in Figure 4.9 near the analyzed frontal zone. However, the larger influence radius would also degrade the accuracy of the wind field within the triangle.

Nevertheless, it is important to note that regardless of the influence radius, the model cannot move the front into the profiler triangle until the upstream profiler(s) sense(s) the frontal passage. Once this occurs, the modeled frontal position unrealistically jumps several hundred kilometers. In this case, the jump occurs when the McPherson profiler winds shift to the northwest at 0300 GMT (Fig. 3.9). Although in time, the modeled wind field adjusts to generally agree with the actual frontal position, the modeled post-frontal air mass is irreversibly lagged behind the actual post-frontal air mass. Evidence of this problem is discussed further with the advection model results.

Another caveat of having only three profilers is also caused by the influence radius of the profiler data. It is obvious from Figures 4.8

through 4.12 that the winds near the borders of the grid do not change. Again, although a larger influence radius for the profiler winds in the wind-updating model might alleviate some of the problem, the overall accuracy of the wind field would not necessarily improve. One solution to these problems is to have additional wind profilers located throughout the model domain. The result would be a much more accurate depiction of the hourly wind fields and would obviously improve the advection model output.

Advection Model Results

The advection model uses the hourly wind fields produced by the initial analysis and the wind-updating model to move the analyzed temperature and moisture fields around a 1530 km square region. As discussed in Chapter II, the advection model was designed with simplicity in mind. There are two methods by which the model potential temperature and specific humidity at a given grid point can change. The first is through horizontal or vertical advection, and the second is through condensation or evaporation. The results of the advection model are, therefore, highly dependent upon the accuracy of the modeled wind fields and ability of the model to handle precipitation.

Figures 4.17 through 4.21 depict the modeled moisture fields at 850 mb for June 11th. The analysis in Figure 4.17 shows a specific humidity maximum of nearly 14 gkg-1 in southwestern Kansas. It is easy to see in Figures 4.18 through 4.21 that as time lapses, the model advects drier air into the profiler region from the northwest. This general pattern of a dry air push from the northwest agrees with the 1200 GMT analysis

ANALYSIS $\vec{V}_h$ AND q 850MB 11 JUNE 85 00Z

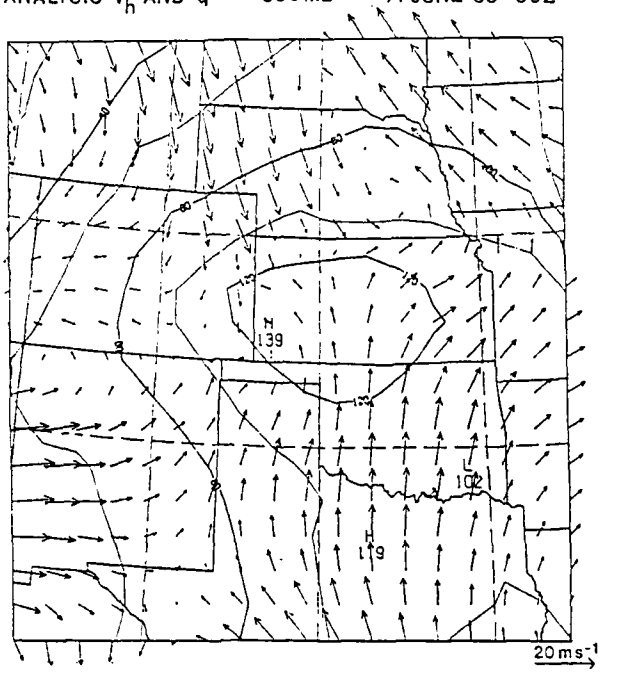

Figure 4.17. 850 mb analysis of horizontal wind and specific humidity (gkg^{-1} x 10) for 0000 GMT 11 June 1985. Contour interval is 2 gkg^{-1}.

NOWCAST $\vec{V}_h$ AND q 850 MB 11 JUNE 85 03Z

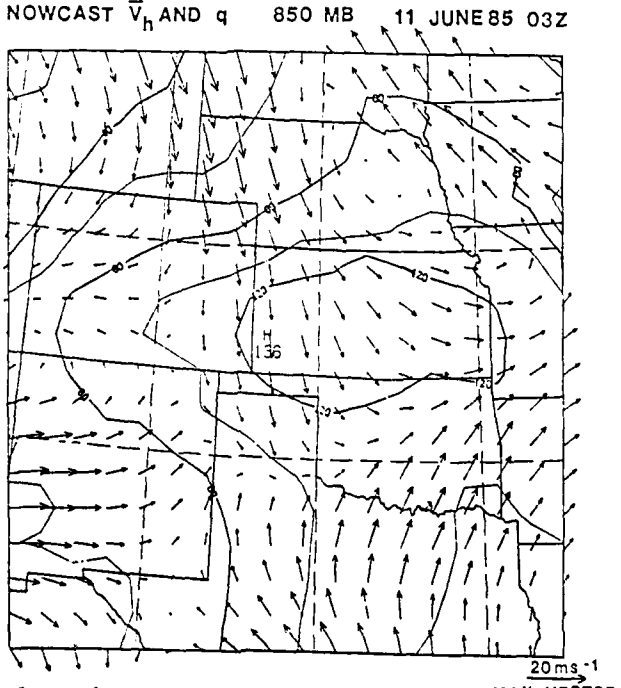

Figure 4.18. Model-produced 850 mb horizontal wind and specific humidity (gkg^{-1} x 10) for 0300 GMT 11 June 1985. Contour interval is 2 gkg^{-1}.

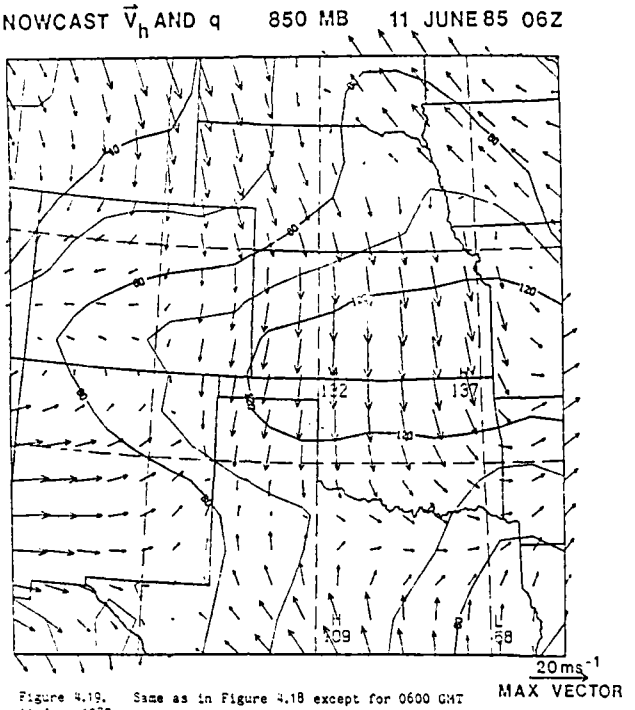

Figure 4.19. Same as in Figure 4.18 except for 0600 GMT 11 June 1985.

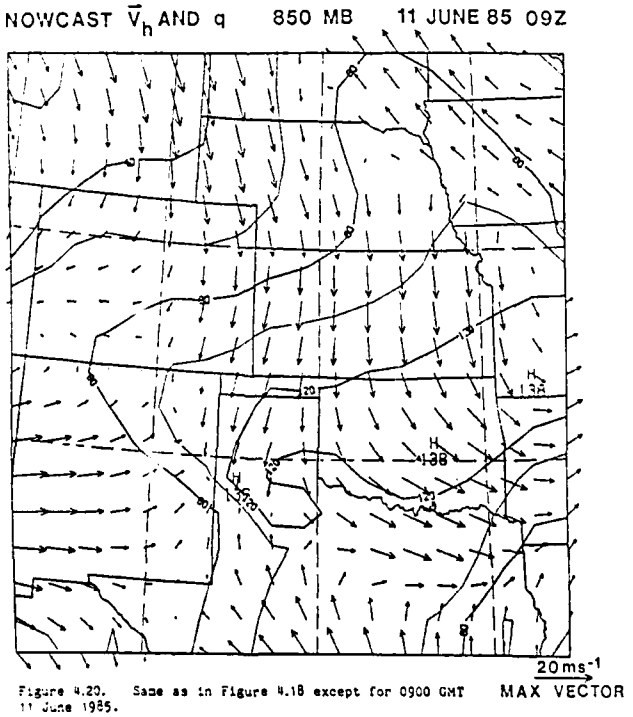

Figure 4.20. Same as in Figure 4.18 except for 0900 GMT 11 June 1985.

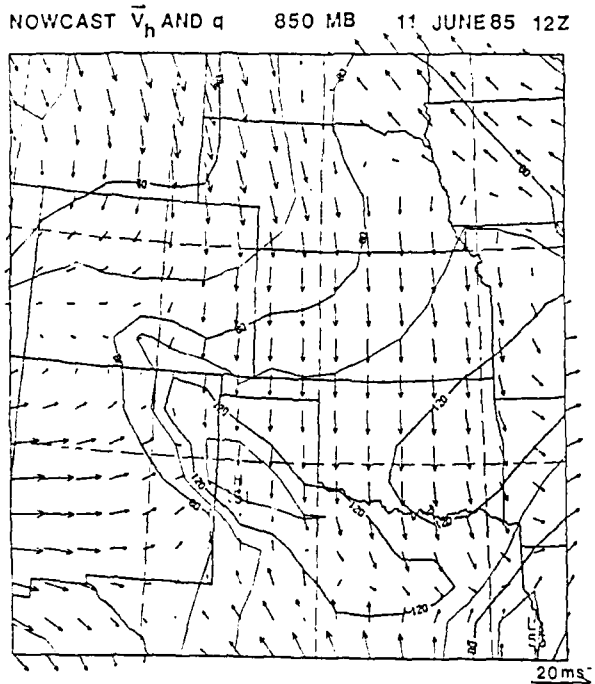

Figure 4.21. Same as in Figure 4.18 except for 1200 GMT 11 June 1985.

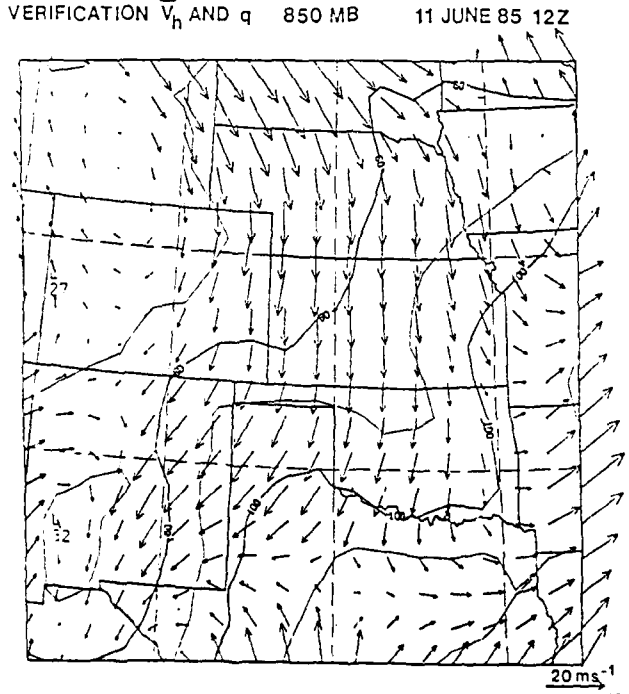

Figure 4.22. Same as in Figure 4.17 except for 1200 GMT 11 June 1985.

(Fig. 4.22). The agreement is particularly good in light of the fact that the modeled northwesterly winds and subsidence over Nebraska and Kansas (Fig. 4.12) are noticeably weaker than those in the 1200 GMT verification analyses (Fig. 4.13). This explains in part why the 1200 GMT nowcast (Fig. 4.21) values of specific humidity near the profilers are 2-4 gkg^{-1} too high.

It is likely, though, that this discrepancy is the result of the model's tendency to unrealistically jump the frontal position as it moves into and out of the profiler triangle. As discussed earlier, this forces an irreversible lag of the post-frontal air mass behind the actual post-frontal air mass. Note in Figure 4.17 that the front edge of the northwesterly flow in northwest Kansas at 0000 GMT correlates with the 12 gkg^{-1} contour of specific humidity. In the 1200 GMT analysis (Fig. 4.22), the leading edge of the front in northern Texas also correlates with the 12 gkg^{-1} contour. Yet, Figures 4.18 through 4.21 show that the modeled northwesterly winds pushed clear through the 12 gkg^{-1} contour, indicating that the position of the modeled post-frontal drier air is not consistent with the modeled frontal movement.

Another possible reason why the modeled specific humidities are too high is that the model can not simulate the vertical velocities of thunderstorms. Of course, this has a direct impact on the vertical transport of moisture and temperature changes due to adiabatic warming and cooling. The net result is that the advection model underestimates condensation, evaporation and precipitation in areas of deep convection. Figures 4.1b and 4.23 illustrate this point. The large thunderstorm complex completely dominated the profiler region for several hours,

producing average precipitation amounts of nearly one inch across Oklahoma and southern Kansas (Fig. 4.23). Conversely, the model shows no precipitation over much of Kansas and Oklahoma (Fig. 4.23). Note also how the areas where the model does produce precipitation are closely aligned with the high moisture bands in Figure 4.21. It is apparent from these figures that the modeled upward velocities over western Oklahoma and Kansas were never strong enough to support the rate of condensation which actually existed in the thunderstorms. The modeled condensation in these regions was quickly evaporated into the layers below and never reached the surface as precipitation. The slower condensation rate also caused temperatures in the mid and upper levels to be too cool (less latent heat release) and temperatures in the lower levels to be too warm (less evaporative cooling). This conclusion is supported by the fact that the modeled 850 mb potential temperature field at 1200 GMT (Fig. 4.24) in the vicinity of the profilers is 4-7 K warmer than the verification values (Fig. 4.25). The 850 mb modeled potential temperatures are too warm near the profilers because the model did not adequately evaporatively cool the air being advected into the region behind the front. Note how closely the 850 mb potential temperature maximum in southwest Oklahoma (Fig. 4.24) aligns with the modeled 850 mb subsidence maximum in Figures 4.11 and 4.12 and the modeled precipitation-free region in Figure 4.23. Also, note the agreement between the "cool" pocket of air in eastern Oklahoma in Figure 4.24 and the modeled precipitation band in Figure 4.23. It is clear that the vertical motions and subsequent precipitation from the thunderstorms induce large errors into the advection model output.

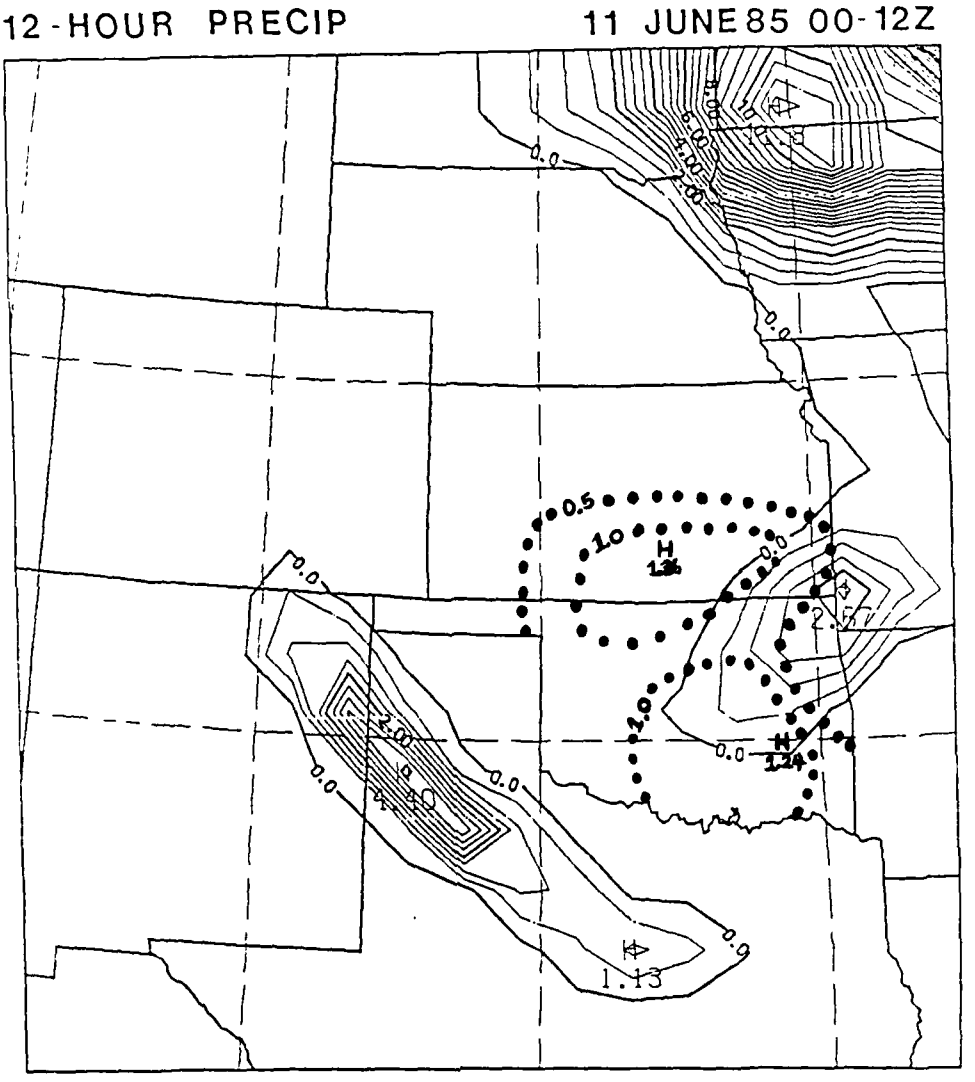

Figure 4.23. 12-hr precipitation accummulation from 0000 GMT to 1200 GMT 11 June 1985. Solid lines represent model-produced precipitation, dotted lines observed precipitation. Contour intervals are 0.5 inches. Observed data was obtained from 0600 GMT and 1200 GMT 11 June 1985 surface observations for Kansas and Oklahoma only.

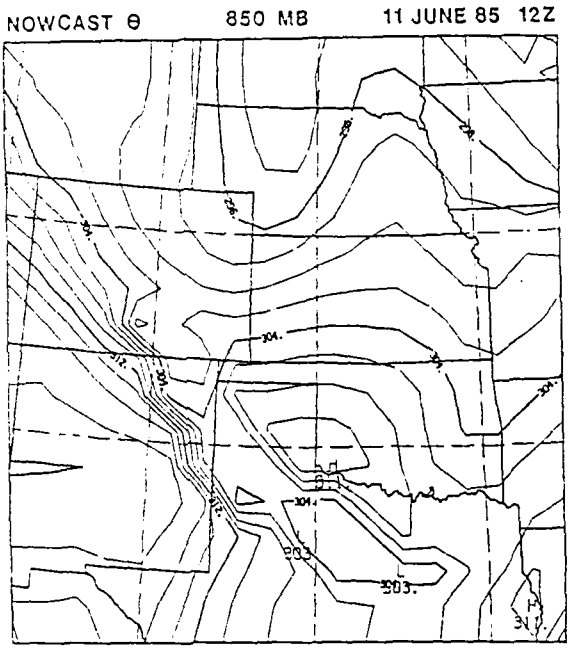

Figure 4.24. Model-produced 850 mb potential temperature field for 1200 GMT 11 June 1985. Contour interval is 2 K.

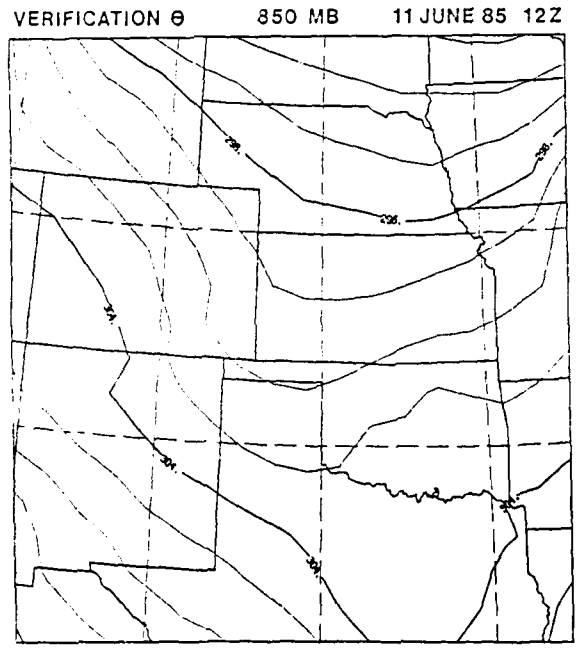

Figure 4.25. 850 mb analysis of potential temperature for 1200 GMT 11 June 1985. Contour interval is 2 K.

Sounding Comparisons

The actual skew-T, log p plots of the PRE-STORM soundings and the model-produced thermodynamic and wind profiles reveal several of the strengths and weaknesses of the wind-updating and advection models in addition to those discussed above. Two important observations concerning model limitations are obtained from the Enid, Oklahoma 11 Jun 85 0000 GMT sounding (Fig. 4.26) and the model analysis 0000 GMT nowcast for Enid. The first is a reminder that the lowest level of the model is 900 mb. It is obvious from Figure 4.27 that the analyzed fields of potential temperature, specific humidity and horizontal wind do not contain any information below 900 mb. This is of particular importance if a very shallow, low-level moist layer is present. The second point is that the model cannot initialize very sharp gradients of temperature or moisture because of the Cressman scheme and the distance between standard rawinsonde stations. This is most visible in the dewpoint temperature traces in Figures 4.26 and 4.27. The observed moist band between 900 and 800 mb is absent from the nowcast plot because the gridpoint over Enid, Oklahoma is influenced by much drier dewpoint temperatures from the Oklahoma City sounding. On the opposite end of the scale, the very dry layer from 500 mb to 400 mb is analyzed as being much more moist because the layer over Dodge City is nearly saturated.

The success of the model-produced thermodynamic profiles for the June 11th case is limited by the presence of the large thunderstorm complex, the associated small-scale short wave and the lag in the model's advection of the post-frontal air mass. Figure 4.28 shows the observed 0300 GMT sounding for Enid, Oklahoma as a thunderstorm was

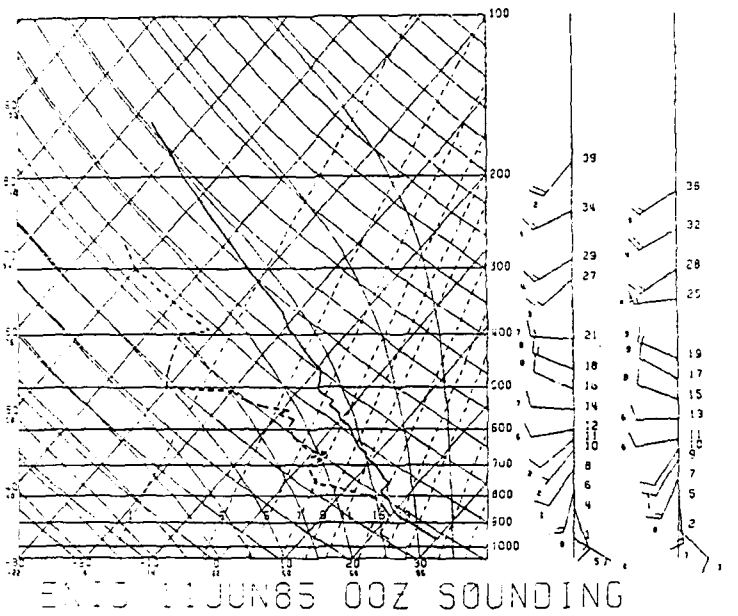

Figure 4.26. Skew T, log p diagram with 0000 GMT 11 June 1985 sounding data for Enid, OK. Full wind barb represents 10 ms^{-1}.

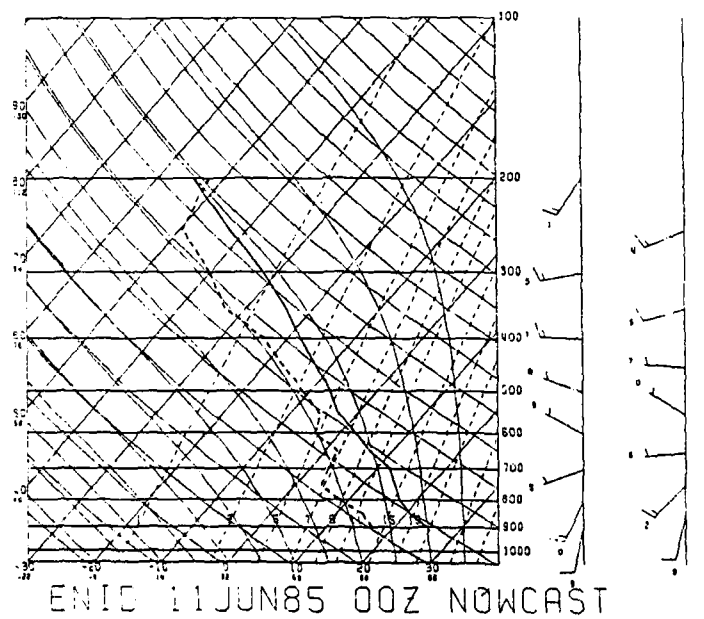

Figure 4.27. Skew T, log p diagram with 0000 GMT 11 June 1985 model-produced data for Enid, OK. Full wind barb represents 10 ms^{-1}.

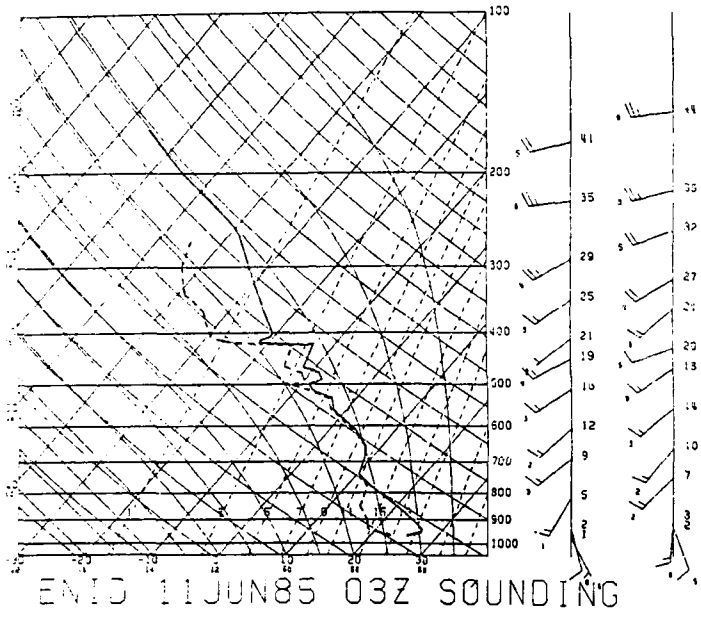

Figure 4.28. Same as in Figure 4.26 except for 0300 GMT 11 June 1985.

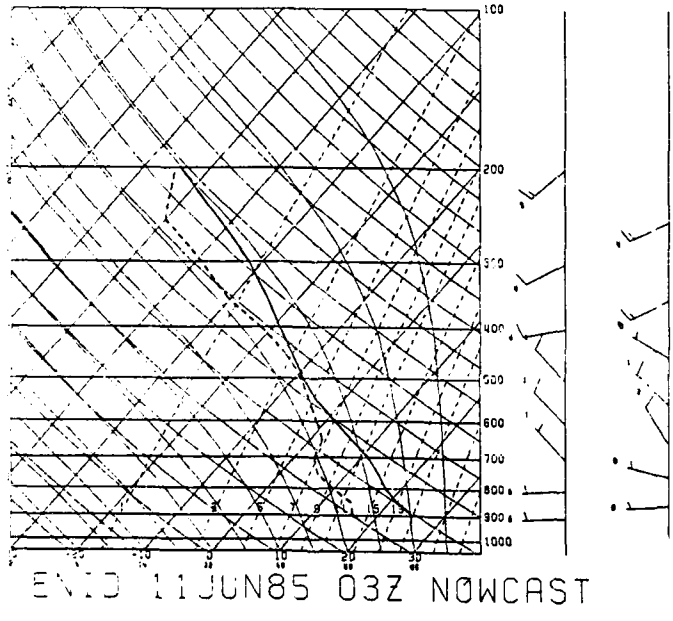

Figure 4.29. Same as in Figure 4.27 except for 0300 GMT 11 June 1985.

in progress. The most significant change since 0000 GMT is the large amount of moistening that occurred in the mid-troposphere. The nowcast sounding (Fig. 4.29) successfully shows significant moistening in the 600-400 mb layer while maintaining the drier layer near the surface. The most visible discrepancy in the 0300 GMT Enid nowcast is the warm layer from 850 mb to 650 mb. The mid-tropospheric winds strengthened and backed over Enid as the front and thunderstorms approached. This increased the convergence in the horizontal wind field, forcing stronger upward velocities and significant adiabatic cooling (5°C at 750 mb in three hours). The model is unable to portray these strong vertical velocities because, as discussed above in the wind-updating model results, the Norman profiler did not "sense" the approaching short wave until 0500-0600 GMT (Fig. 3.21). This can be seen in Figure 4.29 where the northwesterly winds below 400 mb are the result of the strong northwesterly winds at McPherson and Liberal behind the short wave, and the weak northwesterly flow still present over Norman. The actual southwesterly winds observed over Enid at 0300 GMT (Fig. 4.28) cannot be modeled because of the small horizontal scale of the southwesterly flow ahead of the short wave (Fig. 3.21).

By 0700 GMT, the thunderstorms had ended at Enid and the observed sounding (Fig. 4.30) indicates strong cold air advection and significant drying associated with the post-frontal air mass in the lower troposphere. However, the 0700 GMT nowcast sounding for Enid (Fig. 4.31) is saturated above 850 mb. As discussed above, there are two suspected reasons for this discrepancy. The first is that the modeled post-frontal air mass has not yet reached Enid. Note the similarities

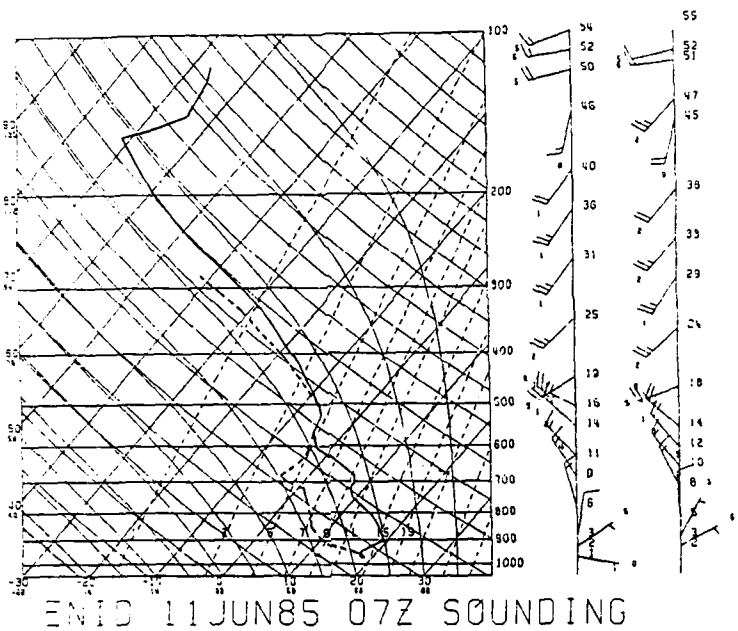

Figure 4.30. Same as in Figure 4.26 except for 0700 GMT 11 June 1985.

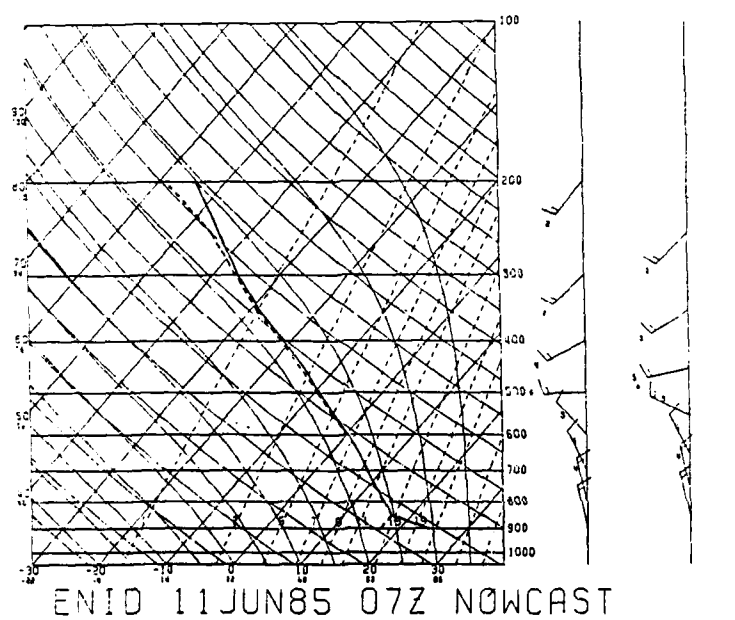

Figure 4.31. Same as in Figure 4.27 except for 0700 GMT 11 June 1985.

between the thermodynamic fields of the 1200 GMT nowcast sounding (Fig. 4.33) and the observed sounding at 0700 GMT (Fig. 4.30). It is apparent that the model required an additional five hours to advect the drier air mass into northern Oklahoma. The second possible reason for the saturated 0700 GMT nowcast sounding is that the model cannot simulate the strong vertical velocities in thunderstorms to allow the moisture to precipitate out of the column. This is supported by the 1.66" of precipitable water in the 0700 GMT nowcast compared with 1.10" of precipitable water above 900 mb in the observed sounding, and the 0.66" of rainfall measured on the ground for Enid. The inability of the model to produce heavy precipitation is also the driving force behind the small amount of evaporative cooling below 850 mb which resulted in a 900 mb temperature which is 5°C too warm. In addition, this model constraint led to the small amount of latent heat release above 550 mb, resulting in temperatures which are 2-3°C too cool. On a more positive note, although the windspeeds above 750 mb are 5-10 ms^{-1} too weak, the modeled wind directions in Figure 4.31 accurately depict the backing winds with height.

Finally, after modifying the wind field for twelve hours using only profiler winds, the 1200 GMT nowcast winds for Enid, Oklahoma (Fig. 4.33) compare exceptionally well with the observed 1200 GMT winds (Fig. 4.32). The only discrepancy is the wind direction below 600 mb. Figure 3.9 shows the constant-in-time north-northwest to north winds at 8-10 ms^{-1} below 600 mb for McPherson from 1000 to 1200 GMT. The 1200 GMT rawinsonde from Topeka, Kansas (approximately 110 km northeast of McPherson) recorded northwesterly winds at 10-15 ms^{-1} in the same layer.

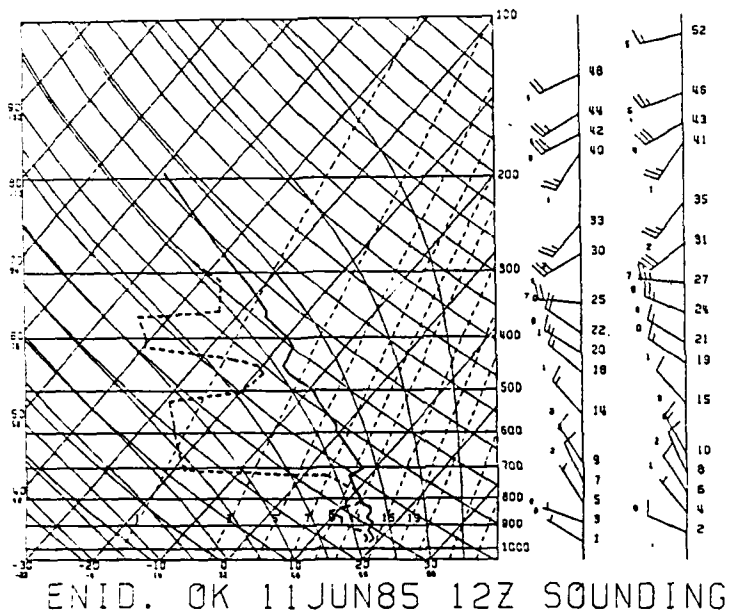

Figure 4.32. Same as in Figure 4.26 except for 1200 GMT 11 June 1985.

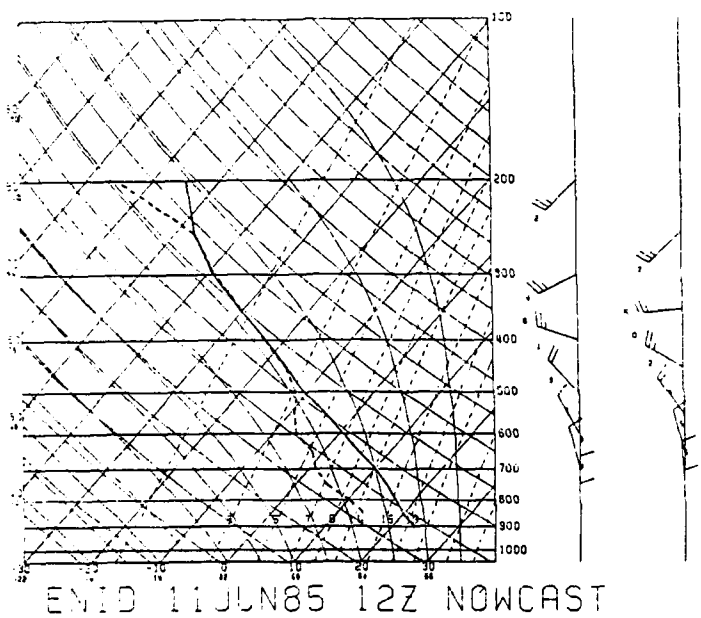

Figure 4.33. Same as in Figure 4.27 except for 1200 GMT 11 June 1985.

This indicates that the 900-600 mb winds over McPherson may have backed 15-30° after the last recorded profiler observation at 0930 GMT. Therefore, the discrepancy in the 1200 GMT nowcast wind field was likely caused by the lack of new wind data from the McPherson profiler after 0930 GMT and not by a deficiency in the wind-updating model. The nowcast thermodynamic profile at 1200 GMT for Enid disagrees extensively with the observed 1200 GMT sounding and is an indication that the model cannot recover from deep convective activity and the lag in advecting the post-frontal air mass as discussed above. However, the 1200 GMT nowcast does indicate that the temperature profile has cooled during the model run. This, at least, is an improvement over assuming that no changes occur during the twelve-hour period.

Case I Summary

The results from the June 11th case are encouraging. Using only the new data from the profilers, the wind-updating model depicts the complete reversal of the wind field as the surface front and upper-level short wave cross all three sites during the twelve-hour period. Many of the discrepancies in the modeled wind fields are the result of missing profiler data and/or having only three wind profilers. Some additional errors in the modeled wind fields are caused by motions on a smaller scale than the profiler triangle, particularly vertical motions in and around thunderstorms and the short wave which had a very small downstream horizontal scale. This case gave the advection model little opportunity for success because of the dominence of the large

thunderstorm complex and the lag in advecting the post-frontal air mass into the profiler triangle. The advection model is able to depict some of the influx of drier air from the northwest at low levels, but the thunderstorms have a detrimental effect on the temperature fields. This however, is not disheartening because the model is not designed to simulate a convective environment. Even so, the model generally portrays the overall cooling of the temperature profile during the twelve-hour period.

Case II: 12 May 85 1200 GMT - 13 May 85 0000 GMT

Many aspects of the May 12-13 case provide meaningful contrasts to the events of June 11th. First, the May case is a daytime event (1200 GMT to 0000 GMT) whereas the June case occurred at night. Second, the thunderstorms did not develop near the profilers until late in the afternoon on May 12th (Fig. 4.34) which allowed the model to run in the more ideal pre-convective environment. Unlike June 11th, the May case has very little change in the horizontal wind field above 600 mb during the twelve-hour modeling period. There is, however, significant turning in the low-level horizontal wind field as a warm front moves northward into Kansas.

Wind-Updating Model Results

As with the June 11th case, the wind-updating model has trouble handling the frontal position during the twelve-hour period. Figure 4.35 shows the 900 mb horizontal and vertical wind analyses at 1200 GMT

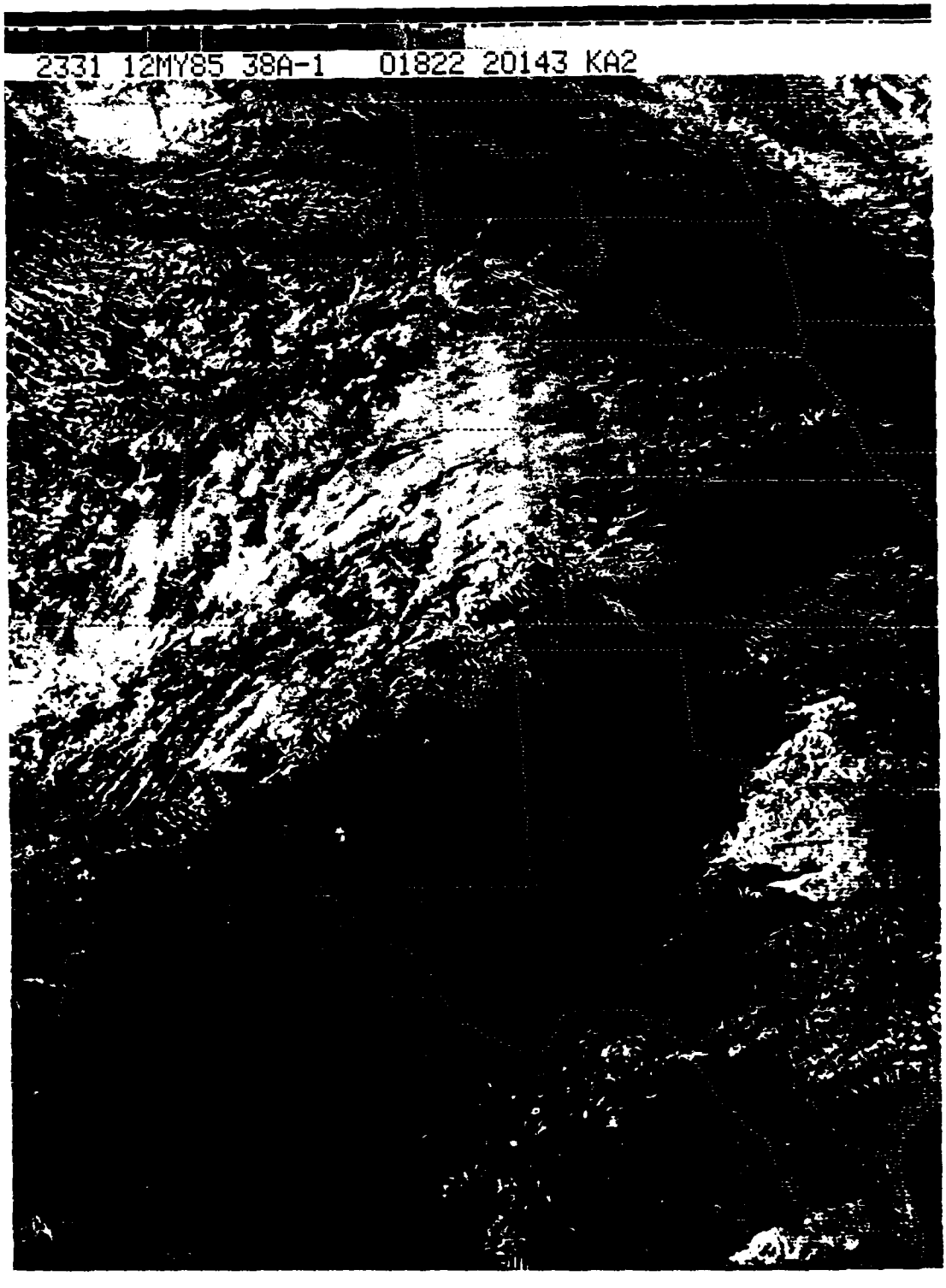

Figure 4.34. Visible satellite picture for 2331 GMT 12 May 1985.

on May 12th. A region of rising motion is centered along the convergence zone in north central Oklahoma while strong subsidence is present in northern Kansas. By 1800 GMT (Fig. 4.36), the modeled frontal boundary has pushed northward into central Kansas and the winds across central Oklahoma have backed slightly and weakened. It is believed that this frontal position is too far north and the 900 mb wind speeds are too weak across central Oklahoma. This is due to the inadequacy of the linear interpolation technique to depict the vertical wind structure of a frontal zone between the lowest available profiler data and the estimated surface observation. Although rawinsonde data for 1800 GMT is not available to verify the nowcast 900 mb winds across central Kansas and Oklahoma, surface observations and profiler data offer insight into the low-level wind structure. At McPherson, the linear interpolation between the southwest wind of 15 ms^{-1} near 2.5 km MSL (Fig. 3.11) and the north wind of 3 ms^{-1} at the surface (Table 3.1) resulted in southwest wind of only 4 ms^{-1} at 900 mb (Fig. 3.12). For Norman, the interpolation between the southwest wind of 10 ms^{-1} near 2.6 km MSL (Fig. 3.22) and the easterly 2 ms^{-1} surface wind (Table 3.1) yielded a 900 mb south-southwest wind of 3 ms^{-1} (Fig. 3.23). Since the surface wind at Norman veered 35° by 1900 GMT (Table 3.1), it can be assumed that the 1800 GMT frontal zone at Norman is very shallow and likely did not extend above 900 mb. Subsequently, the vertical profile below 2-3 km MSL is not linear and the 900 mb wind should contain a stronger southerly component. On the other hand, the McPherson surface winds remain from the north to northeast for several hours which indicated a deeper frontal zone and the likelihood of a more northerly

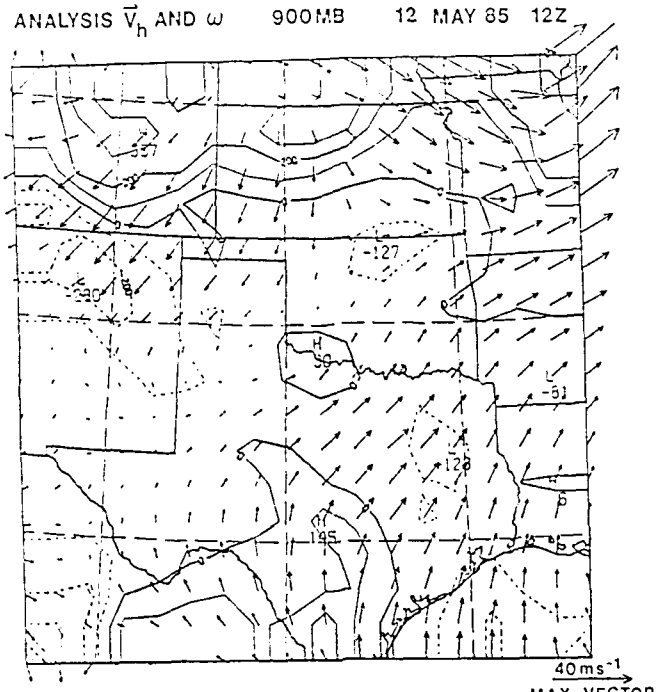

Figure 4.35. 900 mb analysis of horizontal and vertical wind ($\mu bs^{-1} \times 10^2$) for 1200 GMT 12 May 1985. Contour interval is 1 μbs^{-1}. Dashed lines indicate rising motion, solid lines sinking motion.

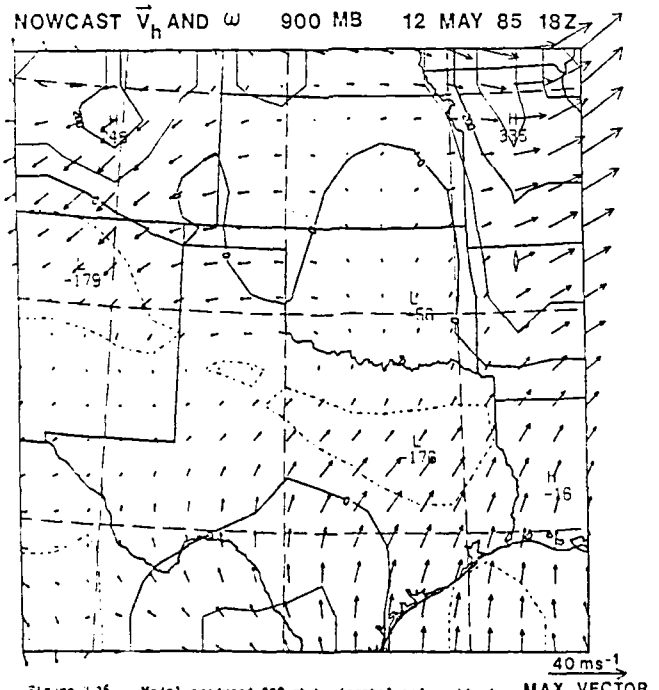

Figure 4.36. Model-produced 900 mb horizontal and vertical wind ($\mu bs^{-1} \times 10^2$) for 1800 GMT 12 May 1985. Contour interval is 1 μbs^{-1}. Dashed lines indicate rising motion, solid lines sinking motion.

component to the 900 mb winds over McPherson at 1800 GMT. The 900 mb wind fallacy does not invalidate the interpolation method, as it has merit later in the model run. However, this does point out that the data void in the lowest 1-2 km of a wind profile is significant, and the addition of surface data at the profiler sites is not always sufficient. Finally, by 0000 GMT, the nowcast windspeeds (Fig. 4.37) across Oklahoma and Kansas are stronger and much more representative of the actual 900 mb wind field in Figure 4.38. The agreement between the wind fields can be attributed to the northward progression of the front, leaving much more linear wind profiles at Norman and McPherson. Figure 4.39 depicts the kinematically computed vertical velocities over Oklahoma City for every three hours during the twelve-hour period. As with the June 11th case, the nowcast profile is very similar to the verifying one at 0000 GMT. The figure indicates weak ascent in the lower levels where there is convergence in the wind field while the upper atmosphere is undergoing weak subsidence.

Advection Model Results

The advection model successfully depicts the return of low-level moisture to central and eastern Oklahoma during the twelve-hour period of the May 12-13 case. Figure 4.40 shows the 900 mb band of moisture from eastern Texas to central Arkansas at 1200 GMT on May 12th. In addition, a tight moisture gradient exists from eastern and southern Oklahoma to a region of relatively dry air in the western half of Oklahoma and Kansas. As discussed earlier, the 900 mb winds across Oklahoma gradually back to a more southerly direction but are somewhat

AD-A171 288 NOWCASTING THERMODYNAMIC PROFILES USING A TRIANGLE OF WIND PROFILERS IN AN ADVECTION MODEL(U) AIR FORCE INST OF TECH WRIGHT-PATTERSON AFB OH R A SKOV 1986 2/2

UNCLASSIFIED AFIT/CI/NR-86-121T F/G 4/2 NL

END

DATE FILMED

10-86

DTIC

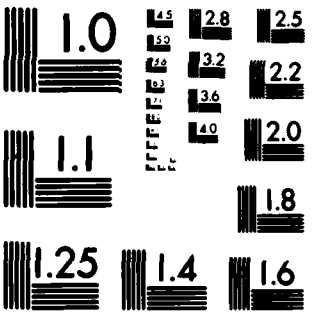

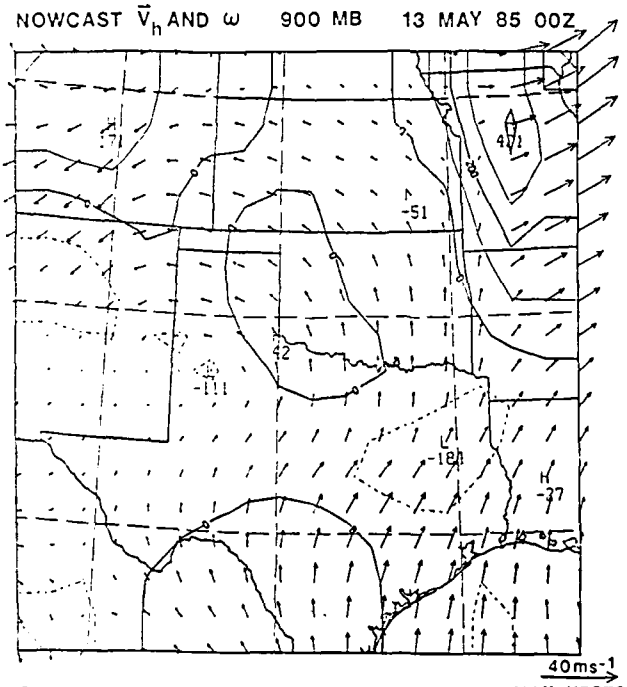

Figure 4.37. Same as in Figure 4.36 except for 0000 GMT 13 May 1985.

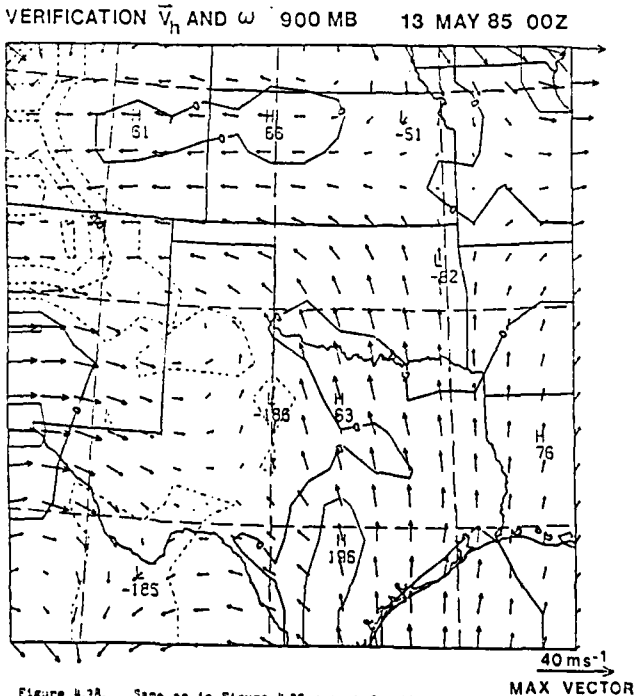

Figure 4.38. Same as in Figure 4.35 except for 0000 GMT 13 May 1985.

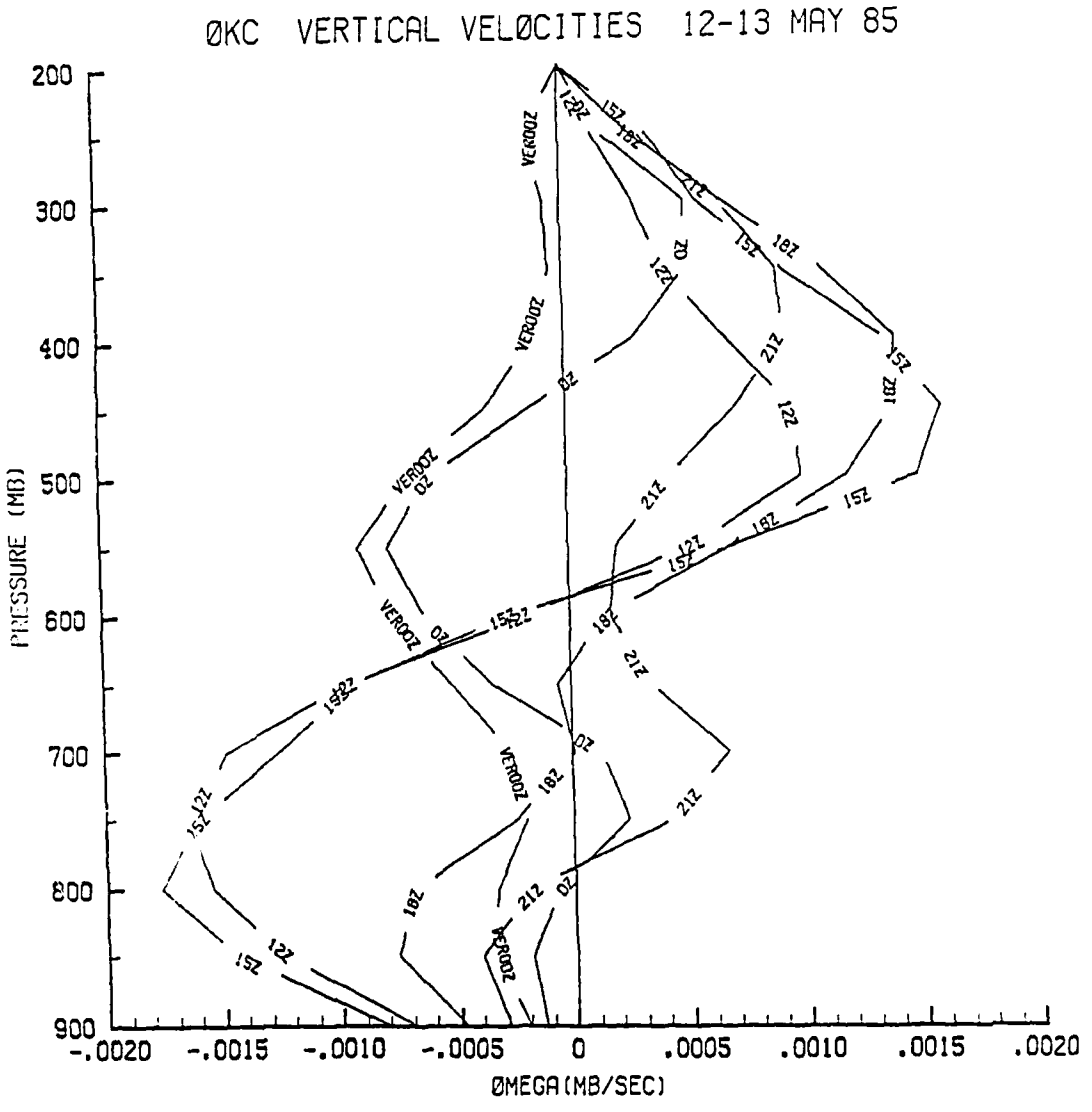

Figure 4.39. Vertical velocities (mbs^{-1}) for Oklahoma City, OK from 1200 GMT 12 May to 0000 GMT 13 May 1985. The 12Z and VER00Z curves are computed from observed data. The 15Z, 18Z, 21Z and 0Z curves are model-produced.

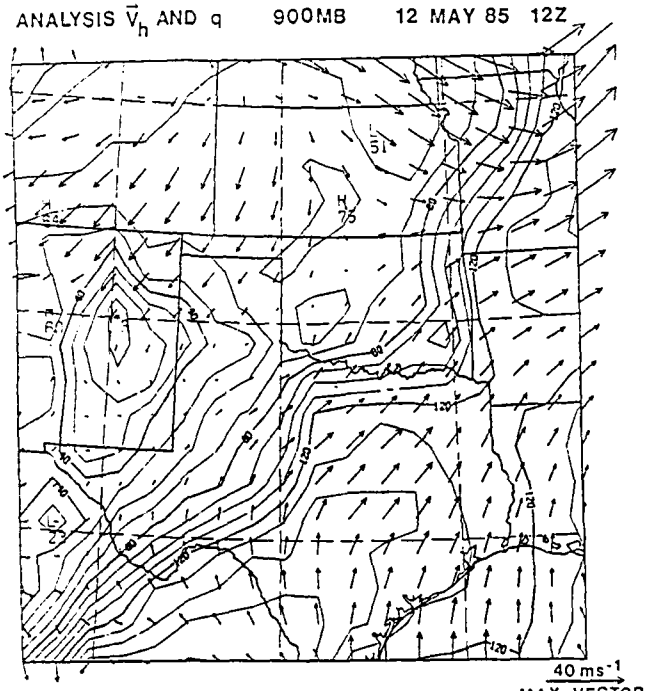

Figure 4.40. 900 mb analysis of horizontal wind and specific humidity (gkg^{-1} x 10) for 1200 GMT 12 May 1985. Contour interval is 1 gkg^{-1}.

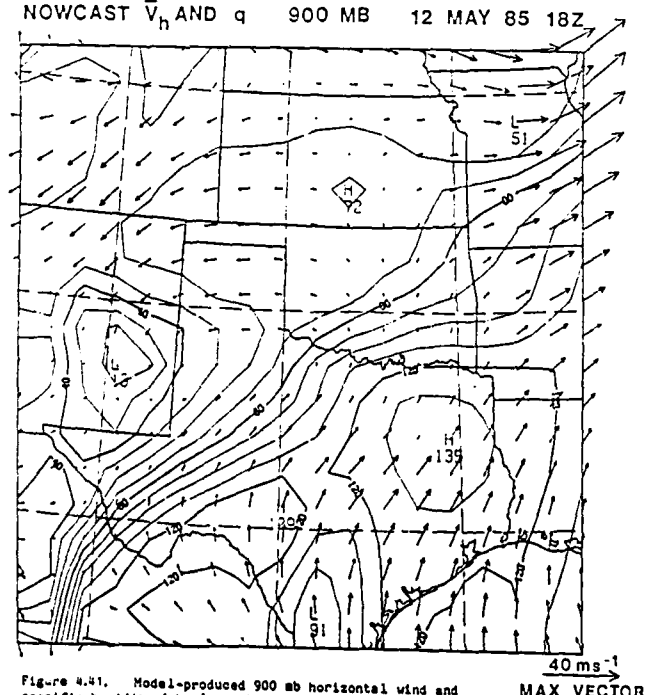

Figure 4.41. Model-produced 900 mb horizontal wind and specific humidity (gkg^{-1} x 10) for 1800 GMT 12 May 1985. Contour interval is 1 gkg^{-1}.

weak at 1800 GMT. Even so, the 1800 GMT 900 mb specific humidity field in Figure 4.41 indicates a northwesterly push of moisture into central Oklahoma. By 0000 GMT on May 13th, the 900 mb nowcast specific humidity across central Oklahoma has increased by 2-3 gkg^{-1} (Fig. 4.42). This pattern of low-level moisture influx agrees with the observed moisture field at 0000 GMT (Fig. 4.43) but the magnitude of the modeled specific humidity field is considerably smaller than the verification data. There are two prime reasons for this discrepancy. The first is the result of the weak southerly winds at 900 mb during the middle hours of the model run. As discussed earlier, these winds were very light because the linear interpolation technique used to obtain low-level winds does not work well in the presence of a shallow frontal zone. Therefore, the actual 900 mb winds were probably much stronger from the south. If the stronger winds had been modeled, more moisture would have been advected into central Oklahoma. The second cause for the discrepancy is the lack of moisture data below 900 mb in the model. The model assumes that the moisture at and below 900 mb is constant with pressure. This procedure, however, underestimates the vertical advection of moisture if the air below 900 mb has higher specific humidity. Figure 4.48 indicates a very shallow layer of moisture in the Oklahoma City sounding below 915 mb at 1200 GMT on May 12th. The model initialized using a 900 mb specific humidity value from the Oklahoma City 1200 GMT sounding which is considerably drier than the 960-915 mb layer. Figures 4.44-4.47 indicate the impact vertical advection of moisture can have on the specific humidity fields. Figure 4.44 shows an extremely dry layer of air and very weak horizontal moist air advection

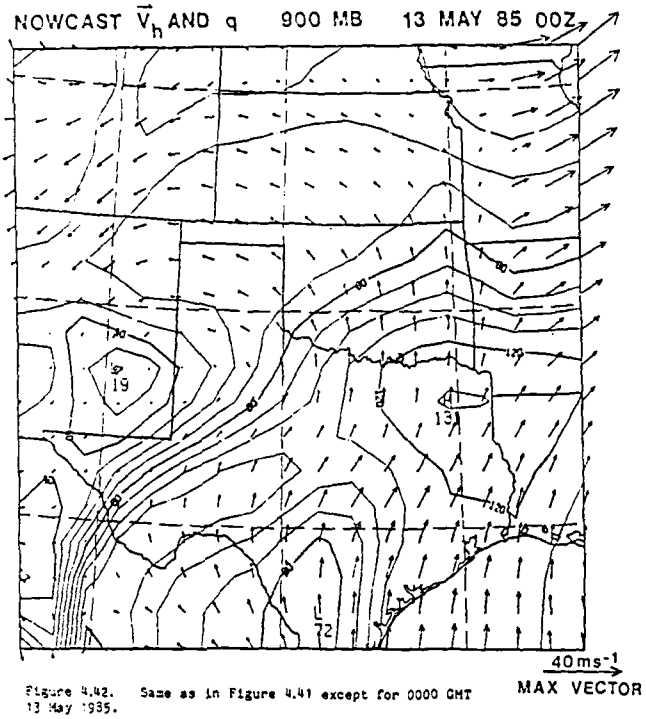

Figure 4.42. Same as in Figure 4.41 except for 0000 GMT 13 May 1985.

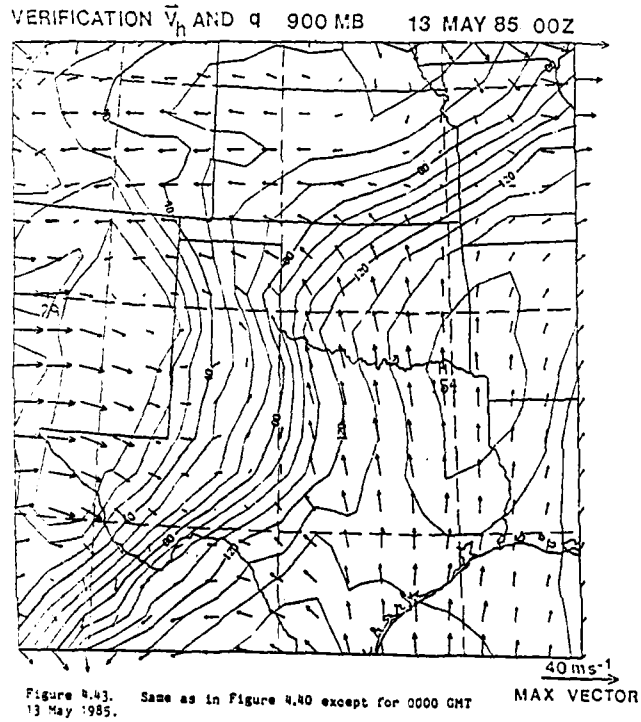

Figure 4.43. Same as in Figure 4.40 except for 0000 GMT 13 May 1985.

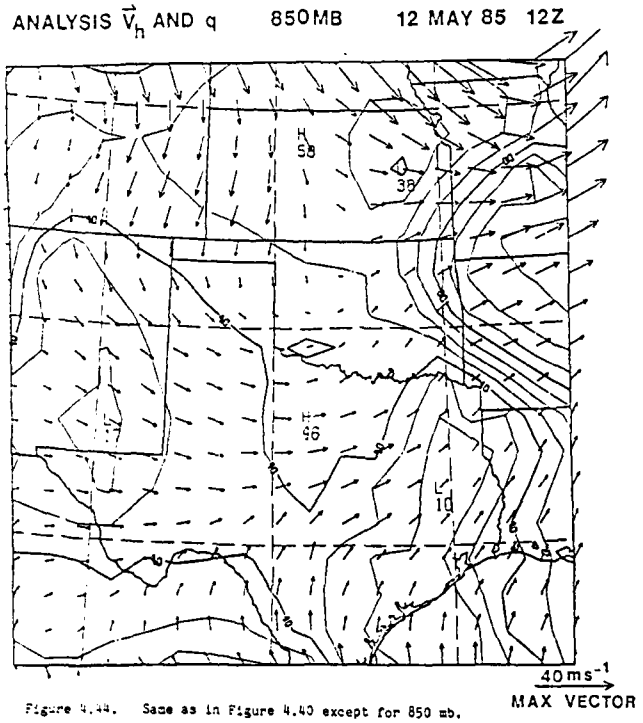

Figure 4.44. Same as in Figure 4.40 except for 850 mb.

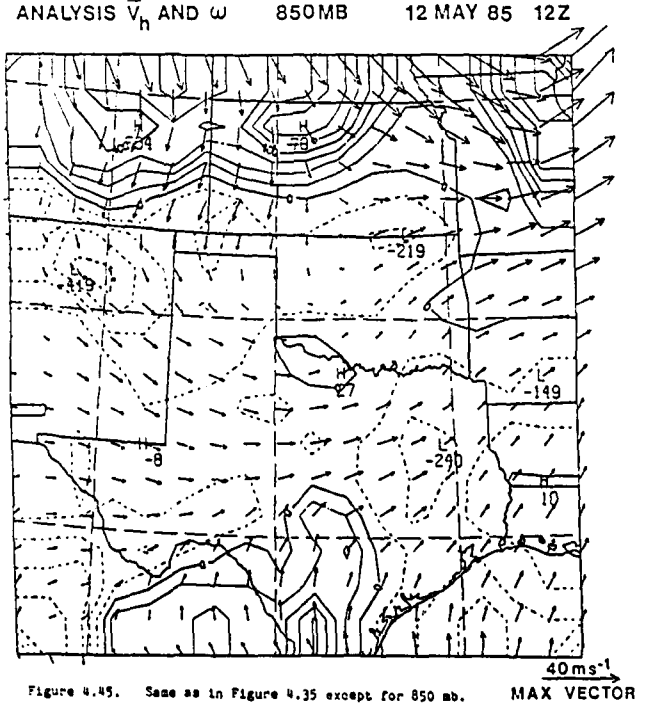

Figure 4.45. Same as in Figure 4.35 except for 850 mb.

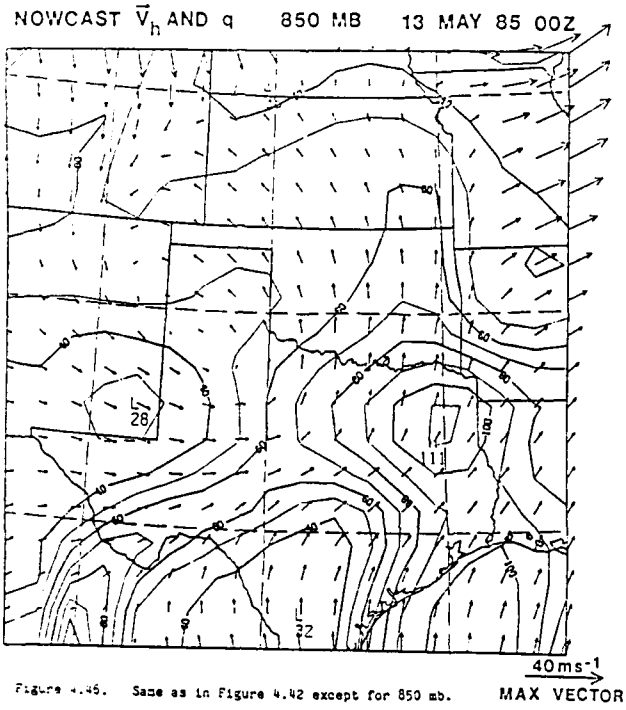

Figure 4.46. Same as in Figure 4.42 except for 850 mb.

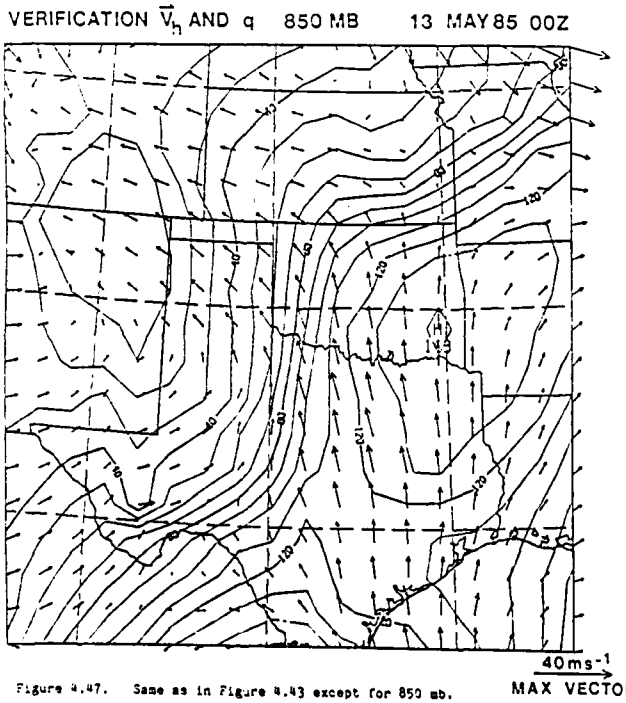

Figure 4.47. Same as in Figure 4.43 except for 850 mb.

at 850 mb over east Texas. This layer overlies the band of moisture at 900 mb (Fig. 4.40) and is generally rising at a rate near 7 mb hr^{-1} (Fig. 4.45). The model results in Figure 4.46 after twelve hours of ascent show a ten-fold increase in specific humidity in east Texas which compares very well with the 0000 GMT moisture analysis in Figure 4.47.

Sounding Comparisons

As with the June 11th case, many of the strengths and weaknesses of the wind-updating and advection models are made more visible by comparing the PRE-STORM soundings with the model-produced soundings. Also, since May 12-13 is a daytime case, it is interesting to contrast these soundings with the 1200 GMT rawinsonde which has been modified with new surface temperature and moisture data. The modifying technique assumes that there is no change in surface pressure from the time of the original sounding. In addition, it is assumed that the lapse rate is adiabatic and the mixing ratio is constant from the surface to the lowest level of the original sounding which has a potential temperature equal to or greater than that at the surface. To aid in the comparisons, the modifying technique is also applied to the model-produced sounding data. This effectively fills the void between 900 mb and the surface on the skew-T, log p diagrams and provides the most realistic thermodynamic profiles possible from the modeled data. However, it is important to note that the modifying technique does not alter the data within the advection model.

As discussed earlier, the 1200 GMT sounding for Oklahoma City is distinguished by a very shallow moist layer from 960 mb to 915 mb (Fig.

4.48). Except for this moist layer, which is below the lowest level of data entry into the model, the model-analysis 1200 GMT nowcast sounding for Oklahoma City (Fig. 4.49) closely resembles the observed profiles. Of course, this is due to the large influence of the Oklahoma City data on the gridpoint over Oklahoma City in the objective analysis. The next sounding from Oklahoma City was not launched until 2100 GMT. By then, the surface temperature had warmed 11°C and nine hours of ascent partially countered by warm-air advection and solar heating resulted in 3°C cooling at 850 mb (Fig. 4.50). Other noticible changes include moistening in the 850-815 mb and 600-550 mb layers, and approximately 2°C warming in the layer between 800 and 600 mb. Three degrees Centigrade of cooling near 550 mb was also present, along with 2°C of warming near 400 mb. Finally, the winds below 600 mb had strengthened and backed. Of course, only the increase in surface temperature and dewpoint temperature are depicted in the 1200 GMT sounding (Fig. 4.48) which has been modified with 2100 GMT surface data (Fig. 4.51). In comparison, however, the 2100 GMT nowcast (Fig. 4.52) shows not only the increase in surface temperatures, but also slight moistening near 850 and 600 mb. Approximately 1°C of warming was modeled between 800 and 600 mb, with 2°C of warming near 400 mb. The 2100 GMT nowcast also depicts the stronger, backing winds below 600 mb. Although the 2100 GMT nowcast does not portray all the changes, in particular the inversion below 800 mb, it is a slightly better depiction of the 2100 GMT sounding than the modified sounding. Figure 4.53 illustrates that by 0000 GMT on 13 May 85, continued surface heating and adiabatic cooling have broken the cap below 800 mb. In addition, dewpoint temperatures have increased

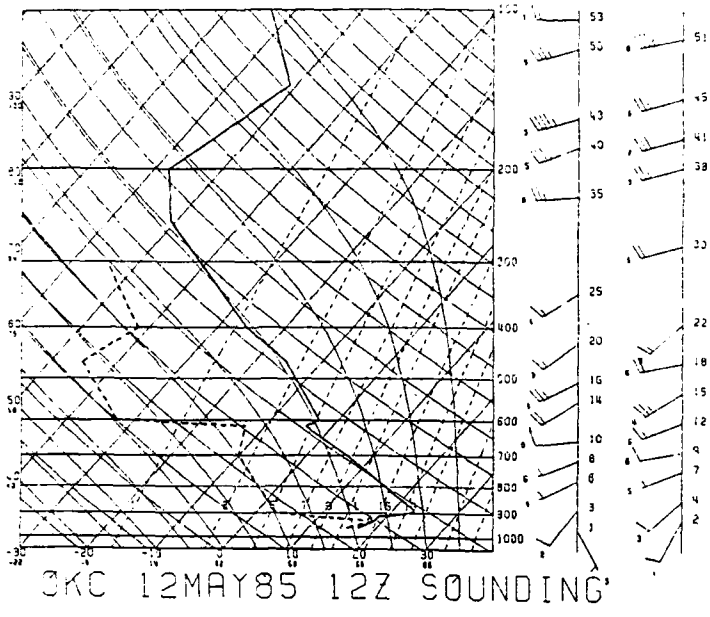

Figure 4.48. Skew T, log p diagram with 1200 GMT 12 May 1985 sounding data for Oklahoma City, OK. Full wind barb represents 10 ms^{-1}.

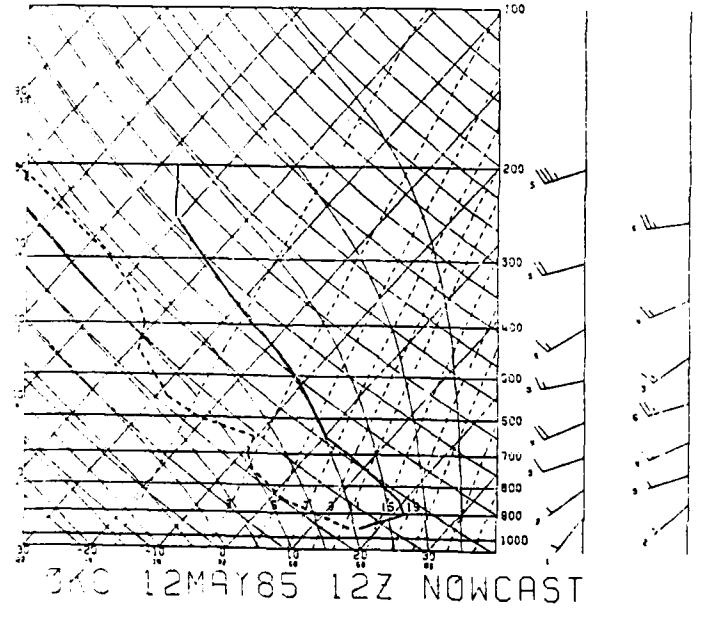

Figure 4.49. Skew T, log p diagram with 1200 GMT 12 May 1985 model-produced data for Oklahoma City, OK. Full wind barb represents 10 ms^{-1}.

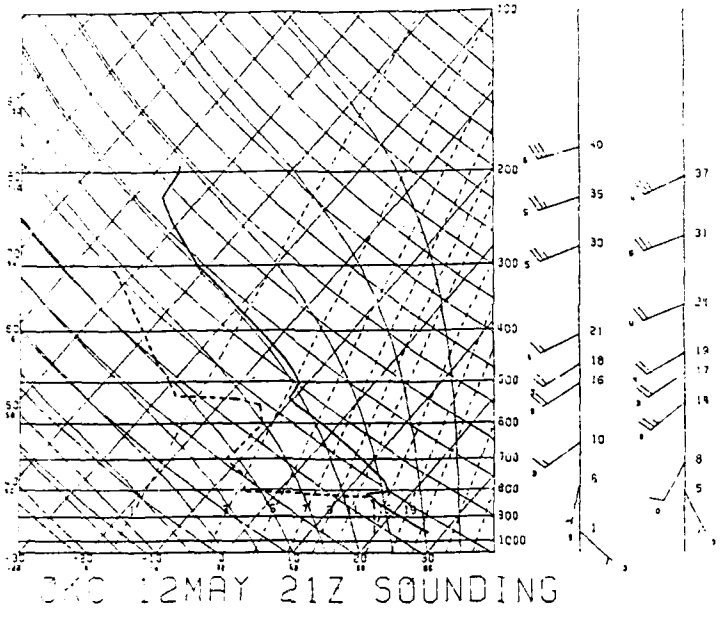

Figure 4.50. Same as in Figure 4.48 except for 2100 GMT 12 May 1985.

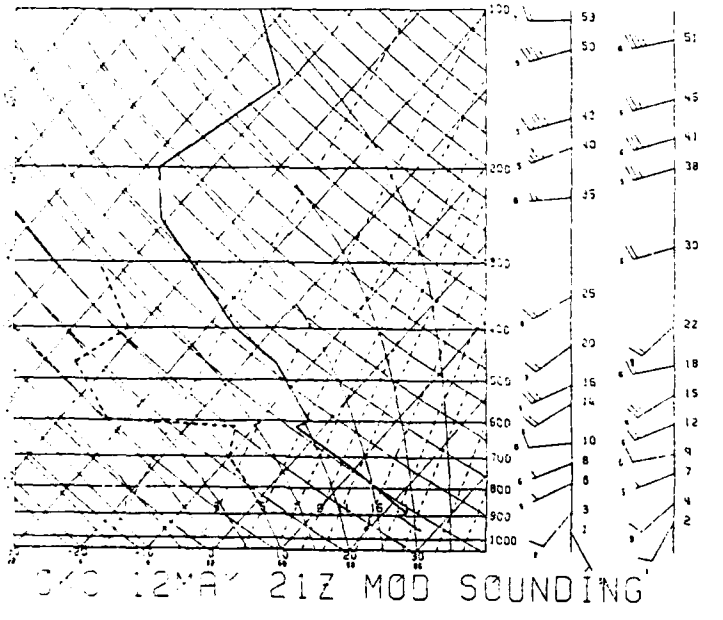

Figure 4.51. Skew T, log p diagram with 1200 GMT 12 May 1985 sounding data for Oklahoma City, OK modified with the surface temperature and dewpoint temperature from the 2100 GMT 12 May 1985 Oklahoma City sounding. Full wind barb represents 10 ms^{-1}.

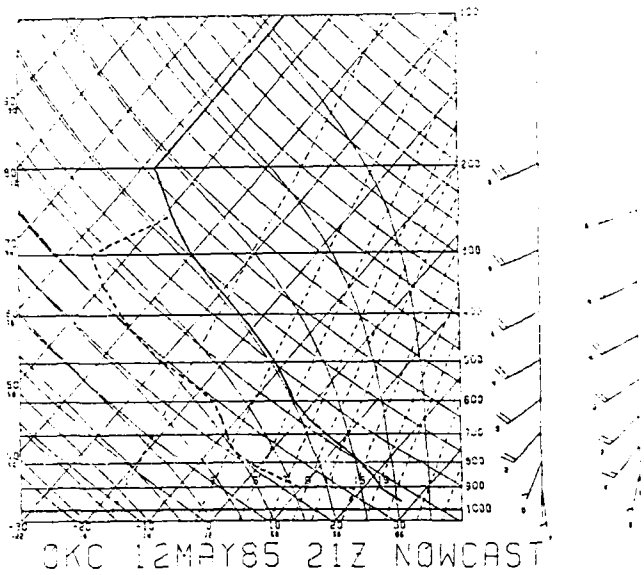

Figure 4.52. Same as in Figure 4.49 except for 2100 GMT 12 May 1985.

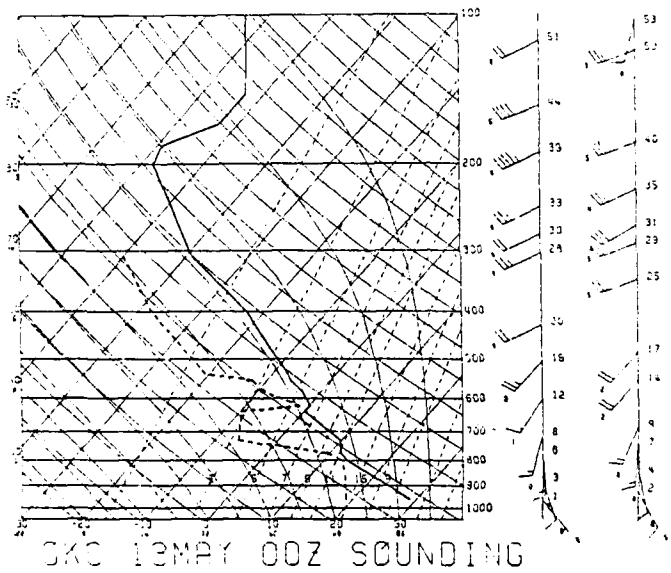

Figure 4.53. Same as in Figure 4.48 except for 0000 GMT 13 May 1985.

in the 850-500 mb, 1°C of warming has occurred between 600 and 500 mb and the low-level winds have continued to back. Again, the modified sounding at 0000 GMT (Fig. 4.54) indicates only the warming near the surface. It does not show any changes in the wind profile, or in the temperature and moisture profiles above 900 mb. Conversely, the 0000 GMT nowcast wind and temperature profiles for Oklahoma City (Fig. 4.55) match very closely with the observed sounding. The only significant discrepancies are the 800 mb temperature which is approximately 3°C too warm and the 600 mb temperature which is 1°C too cool. The model shows some increase in moisture below 500 mb, but not nearly as much as what actually occurred. Nevertheless, the model-produced soundings provide a more accurate depiction of the observed profiles than do the modified soundings.

Case II Summary

The results from the May 12-13 case are quite favorable. Although the wind-updating model understandably has difficulty depicting the frontal zone below 750 mb, the advection model still successfully indicates the return of low-level moisture to central and eastern Oklahoma. The modeled 900 mb wind field at 0000 GMT matches closely with the verification data. Finally, and most importantly, the model-produced soundings at 2100 and 0000 GMT provide a better depiction of the wind and thermodynamic profiles than do the soundings which have been modified with just the 2100 and 0000 GMT surface data.

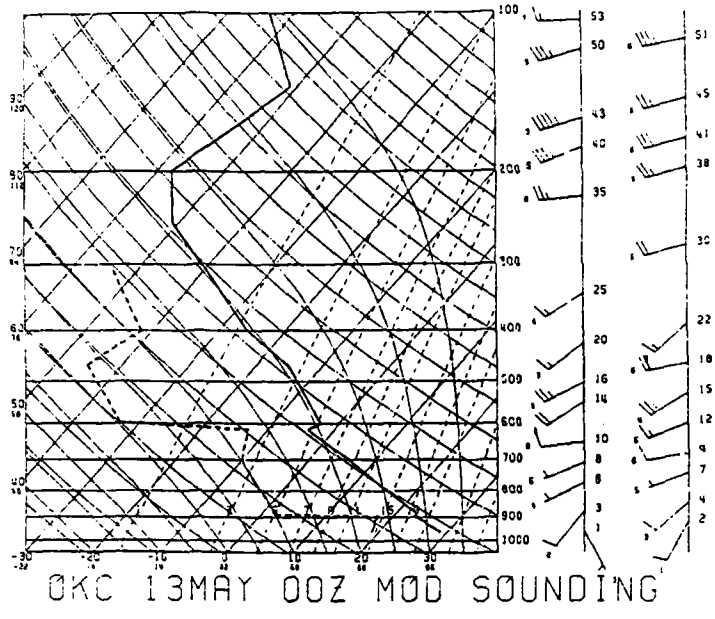

Figure 4.54. Same as in Figure 4.51 except modified with the surface temperature and dewpoint temperature from the 0000 GMT 13 May 1985 Oklahoma City sounding.

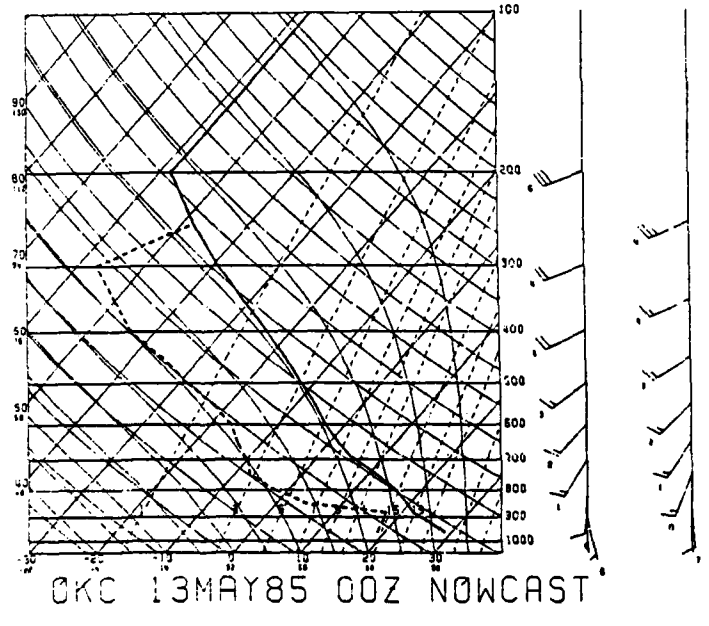

Figure 4.55. Same as in Figure 4.49 except for 0000 GMT 13 May 1985.

CHAPTER V

CONCLUSIONS AND FUTURE WORK

The triangular array of 50 MHz wind profilers established as part of the PRE-STORM project during May-June 1985 provides a unique opportunity to study the utility of wind profilers in the Central Plains. As a supplement to the twice-daily rawinsonde observation network, data from these profilers can enhance our knowledge of the atmospheric wind fields. One method of capitalizing on the higher temporal resolution provided by wind profilers is to use the data in a regional advection model. In this study, a model has been formulated to use hourly profiler winds to update the wind analysis used to compute changes in the temperature and moisture fields.

Two fundamentally different cases from the PRE-STORM program are studied with similar results. Both cases indicate that when and where profiler data are available, the horizontal and vertical motion fields produced by the wind-updating model are quite realistic for subsynoptic-scale motions near the profiler triangle The advection model successfully uses these winds to show general changes in the temperature and moisture fields. The soundings produced by the model present a better depiction of the observed soundings than do the modified soundings or persistence. In addition, the fact that the model can

produce a reasonable sounding at locations and times which rawinsonde data are normally not available is a valuable accomplishment.

There are, however, several shortfalls in the model results. The success of the model is restricted by a lack of profiler data below 1-2 km AGL and by having only three wind profilers in the 1530 km square domain. This often results in either an overestimation or underestimation of changes in the low-level temperature and moisture fields. The June 11th case demonstrates the model's inability to depict the correct position and speed of fronts and the vertical motions associated with thunderstorms. These deficiencies have a detrimental impact on the accuracy of the modeled thermodynamic fields. The May 12-13 case indicates that interpolating between the lowest available profiler wind and the surface wind observation helps to fill the data void left by the profilers, but the interpolation cannot accurately delineate the vertical structure of a frontal zone. Finally, although the nowcast soundings show improvement over persistence and modified soundings, they do not always compare well with the observed soundings.

The availability of more profiler data is the primary way in which the results of this research can be improved. This can come about through four means. The first is having the capability to sense boundary layer winds using wind profilers (or some other adjacent instrument). A 405 MHz profiler can provide 150 m vertical resolution from 0.5 to 5 km AGL and 300 m vertical resolution up to approximately 10 km AGL (Kaimal, Dec., 1985). By supplementing this data with the surface wind observation at the profiler site, a much more complete depiction of the tropospheric winds can be obtained. Knowledge of the

boundary layer winds allows one to relax the restriction which set 900 mb as the lowest pressure level in the model. The model could then be reformulated in a terrain-following coordinate system and include the boundary layer thermodynamic data in the initial temperature and moisture fields. Secondly, having more wind profilers will provide more profiler data. With a network of profilers scattered throughout the region, the wind-updating model used in this research could be replaced by a much simpler objective analysis scheme over the complete domain on just the new profiler winds. The additional data will eliminate the "constant wind field" problem which occurs outside the influence radius of the profiler data. This solution is expected to become a reality in 1989 when a network of thirty wind profilers across the central United States is scheduled for completion. The third method for obtaining additional profiler data is through the improved sensing capabilities of the profilers themselves. Presently, four similar wind measurements must be received during a thirty or sixty minute averaging period for a given height to be awarded a u and v component. Sometimes these values are in obvious error and must be removed from the data set prior to use. If fewer than four similar values are found, the wind value for the height is labeled as missing. By eliminating the outliers and the holes left by missing data, not only will the results of the model improve, but the time required to process the data will be significantly reduced. Assuming the availability of a network of wind profilers, the fourth way to improve the model results is through the use of a third, vertically-pointing antenna beam. Since a vertically-pointing beam can directly observe the vertical wind component, the need to kinematically

compute the vertical velocities could be eliminated. The vertical wind field can be updated as often as the data is available by a simple objective analysis scheme. This not only bypasses the possible error induced by the kinematic technique, but it also allows the vertical velocities within a thunderstorm which tracks directly over a profiler to be measured and entered into the advection model. Of course to do this, one must take into account the horizontal scale of the thunderstorm versus the grid resolution. Also, the direct measurement of vertical motion reduces the total computer time required for data processing.

In addition to obtaining better and more abundant profiler data, the model results can be improved through enhancement to the advection model itself. One technique is to include a more complete formulation of diabatic heating into the model. However, the computation of sensible heat and radiation terms is cumbersome and may impact upon the operational utility and timeliness of the model. A second and much more feasible enhancement is to integrate hourly surface data into the model. By applying a technique similar to that used when modifying a sounding, this enhancement can effectively incorporate the boundary layer heating and cooling terms into the thermodynamic fields. A third method through which the model results can be improved is to use observed rainfall rates at surface observation stations to compute latent heating rates. This requires the assumption of a reasonable vertical distribution profile for the evaporation and condensation terms. A recurring drawback in this procedure is that it is difficult to apply in an operational sense because hourly surface rainfall rates are not

generally available. Another possible enhancement would be to incorporate an elliptical weighting scheme in the objective analysis such as described by Barnes (1964). The principle advantages here are to reduce the tendency to smooth out small variations in the field and to have more control over the upstream and downstream influence of the profiler data on the updated wind fields. Finally, the model could be reformulated in the θ-coordinate system. This would greatly improve the model's ability to handle fronts, inversions and stable layers. Also, for adiabatic motions, under certain assumptions, the flow along a θ-surface yields the vertical wind component. This eliminates the need for kinematic ω's.

Finally, a few easily adaptable modifications can be made which will improve the model. The first is to use standard atmosphere data when initializing the potential temperature, specific humidity and geopotential height fields for the Cressman analysis. The second is to abandon the "station-of-interest" concept when formulating the model grid. Instead, a constant grid can be developed which uses bilinear interpolation to extract the nowcast sounding data for the verification point. This latter enhancement will make it much easier to compare data from additional PRE-STORM sounding sites and shorten the required model-setup tim

In conclusion, a wind-updating and advection model has been formulated which effectively uses hourly profiler winds to produce thermodynamic profiles between standard rawinsonde launch times. Despite being limited by the availability of profiler winds, the simple design of the model and the effects of deep convection, the model-

produced soundings are an improvement over both persistence and modifying the soundings with just surface data. Many enhancements are identified which will improve the quality and quantity of the profiler data as well as the advection model results. Our ability to produce a nowcast sounding for any time or location will progress with each modification.

REFERENCES

Balsley, B.B., and K.S. Gage, 1982: On the use of radars for operational wind profiling. Bull. Amer. Meteor. Soc., 63, 1009-1018.

Barnes, S.L., 1964: A technique for maximizing details in numerical weather map analysis. J. Appl. Meteor., 3, 396-409.

Bellamy, J.C., 1949: Objective calculations of divergence, vertical velocity and vorticity. Bull. Amer. Meteor. Soc., 30, 45-49.

Belt, C.L., and H.E. Fuelberg, 1982: The effects of random errors in rawinsonde data on derived kinematic quantities. Mon. Wea. Rev., 110, 91-101.

Browning, K.A., ed., 1982: Nowcasting. New York: Academic Press, Inc., 256 pp.

Brumer, R., R. Bleck, and M.A. Shapiro, 1984: The potential use of atmospheric profilers in short-range prediction. Proceedings of the Second International Symposium on Nowcasting, Norrkiping, Sweden, ESA SP-208, European Space Agency, Paris, 3-7 September, 209-212.

Ceselski, B.F. and L.L. Sapp, 1975: Objective wind field analysis using line integrals. Mon. Wea. Rev., 103, 89-100.

Chadwich, R.B., A.S. Frisch, and F.G. Strauch, 1984: A feasibility study on the use of wind profilers to support space shuttle launches. NASA Contractor Report 3861, Washington, D.C., 109 pp.

Cressman, G.P., 1959: An operational objective analysis system. Mon. Wea. Rev., 87, 367-374.

Cunning, J.B., 1985: Design and Operations Plan for the Oklahoma-Kansas Preliminary Regional Experiment for Storm-Central, NOAA/ERL, 106 pp.

Ecklund, W.L., D.A. Carter and K.S. Gage, 1977: Sounding of the lower atmosphere with a portable 50 MHz coherent radar. J. Geophys. Res., 82, 4969-4971.

_____, D.A. Carter and B.B. Balsley, 1979: Continuous measurement of upper atmospheric winds and turbulence using a VHF radar: Preliminary results. J. Atmos. Terr. Phys., 41, 983-994.

Eilts, M., 1986: Correcting for the slope of the 50 MHz GPA wind profiling system. Memo for the Record, National Severe Storms Laboratory, 18 Feb 1986. 6 pp.

Fischler, M.A., and R.C. Bolles, 1981: Random sample consensus: A paradigm for model fitting with applications to image analysis and automated cartography. Commun. Assoc. Comput. Mach., 24, 381-395.

Gage, K.S., and B.B. Balsley, 1978: Doppler radar probing of the clear atmosphere. Bull. Amer. Meteor. Soc., 59, 1074-1093.

_____ and T.W. Schlatter, 1984: VHF/UHF radar and its application in nowcasting. Proceedings of the Second International Symposium on Nowcasting, Norrkiping, Sweden, ESA SP-208, European Space Agency, Paris, 3-7 September, 193-200.

_____ and G. D. Nastrom, 1985: Relationship of precipitation to vertical motion observed directly by a VHF wind profiler during a spring upslope storm near Denver, Colorado. Bull. Amer. Meteor. Soc., 66, 394-397.

Hogg, D.C., M.T. Decker, F.O. Guiraud, K.B. Earnshaw, D.A. Merritt, K.P. Moran, W.B. Sweezy, R.G. Strauch, E.R. Westwater and C.G. Little, 1983: An automatic profiler of the temperature, wind and humidity in the atmosphere. J. Climate. Appl. Meteor., 22, 807-831.

Iribarne, J.V. and W.L. Godson, 1973: Atmospheric Thermodynamics. Boston: D. Reidel Publishing Company, 259 pp.

Kaimal, L., ed., Sep 1985: Profiler Forum. Boulder, Colorado: NOAA/ERL Wave Propagation Laboratory, 6 pp.

_____, ed., Dec 1985: Profiler Forum. Boulder, Colorado: NOAA/ERL Wave Propagation Laboratory, 8 pp.

Kessler, E., ed., 1982: Thunderstorms: A Social, Scientific and Technological Documentary; Vol. 2: Thunderstorm Morphology and Dynamics. Washington, D.C., 603 pp.

_____, M. Eilts, and K. Thomas, 1985: Submitted to the 1985 workshop on technical and scientific aspects of MST radar session on weather analysis and forecasting applications: A look at profiler performance, 21 pp.

Koscielny, A.J., R.J. Doviak, and D.S. Zrnic', 1984: An evaluation of the accuracy of some radar wind profiling techniques. J. Atmos. and Oceanic Tech., 1, 309-320.

Lowe, P.R., 1977: An approximating polynomial for the computation of saturation vapor pressure. J. Appl. Meteor., 16, 100-103.

O'Brien, J., 1970: Alternative solutions to the classical vertical velocity problem. J. Appl. Meteor., 9, 197-203.

Peterson, R.E., Jr., 1984: A triple-doppler radar analysis of a discretely propagating multicell convective storm. J. Atmos. Sci., 41, 2973-2990.

Rusk, D.J., 1985: Examination of a static initialization procedure for a regional primative equation model: A comparative study. M.S. Thesis, School of Meteorology, University of Oklahoma, Norman, 101 pp.

Sasaki, Y.K., P.S. Ray, J.S. Goerss and P. Soliz, 1979: Inconsistent finite differencing errors in the variational adjustment of horizontal wind components. J. Meteor. Soc. Japan, 57, 88-92.

Schaefer, J.T., and C.A. Doswell III, 1979: On the interpolation of a vector field. Mon. Wea. Rev., 107, 458-476.

Schlatter, T.W., 1985: Use of ground-based wind profilers in mesoscale forecasting. Proceedings from Symposium and Workshop on Global Wind Measurements, Columbia, MO, NASA, 29 Jul - 1 Aug, 7 pp.

Steyaert, L.T. and G.L. Darkow, 1973: Diurnal variations in the ability to infer spatial variability in the thermodynamic properties of the lowest kilometer from surface data. Preprints, 8th Conference on Severe Local Storms, Denver, CO, American Meteorological Society, 238-243.

Strauch, R.G., M.T. Decker and D.C. Hogg, 1983: Automated profiling of the troposphere. J. Aircraft, 20, 359-362.

_____, D.A. Merritt, K.P. Moran, K.B. Earnshaw and D. Van de Kamp, 1984: The Colorado wind profiling network. J. Atmos. and Oceanic Tech., 1, 37-49.

_____, 1985: Oklahoma antenna pointing. NOAA/ERL 8 May 1985 ltr. 2 pp.

Zamora, R.J., and M.A. Shapiro, 1984: Diagnostic divergence and vorticity calculations using a network of mesoscale wind profilers. Preprints, 10th Conference on Weather Forecasting and Analysis, Clearwater Beach, Florida, American Meteorological Society, Boston, MA, 25-29 June, 386-391.

APPENDIX

CORRECTION FOR NORMAN PROFILER

ANTENNA POINTING ERROR

Correcting the Azimuth and Elevation Angles

The 50 MHz wind profiler located near Norman, OK has two beams which are mechanically aligned as

N/S = 11.3°/191.3°

E/W = 101.3°/281.3°

The electronic phasing introduces a beam pointing that steers the beam 14.5° relative to the normal of the plane of the antenna. Therefore the elevation angle relative to the plane of the dipoles is 75.5° (Strauch, 1985). The azimuth (AZ) and elevation (EL) angles for the two beams are

$AZ'_S = 191.3^\circ$ $\quad AZ'_E = 101.3^\circ$

$EL'_S = 75.5^\circ$ $\quad EL'_E = 75.5^\circ$

where "'" denotes uncorrected angles

s denotes "south" pointing beam, and

E denotes "east" pointing beam.

However, the plane of the antenna slopes 2.1° towards the south beam pointing direction (191.3°). The corrected azimuth and elevation angles are given by Strauch, 1985 and Eilts, 1986 to be

$AZ_S = 191.3^o$ $\quad AZE = 109.4^o$

$EL_S = 73.4^o$ $\quad EL_E = 75.4^o$

Solving for the Correct Values of u and v

The raw PRE-STORM data from the Norman, OK profiler was processed and archived using the uncorrected azimuth and elevation angles for the south and east pointing beams. Using the exact angles given above for the two pointing beams, the u (positive to the east) and v (positive to the south) components can be computed (Eilts, 1986). The relationship between the radial velocity and the u and v wind components (assuming no vertical velocity) is

$$V_R = (u \sin AZ + v \cos AZ) \cos EL \qquad (A.1)$$

where V_R is the radial velocity which is positive away from the radar

AZ is the azimuth from north with clockwise rotation positive, and

EL is the elevation angle with horizontal pointing equal to 0o.

Since there are two unknowns, u and v, and two radial velocities, V_{Re} (east) and V_{Rs} (south), there are two equations

$$V_{Re} = (u \sin AZE + v \cos AZE) \cos EL_E \qquad (A.2)$$

$$V_{Rs} = (u \sin AZ_S + v \cos AZ_S) \cos EL_S \qquad (A.3)$$

Inserting the values AZ'_E = 101.3°, EL'_E = 75.5°, AZ'_S = 191.3°, EL'_S = 75.5° and the uncorrected u and v from the raw profiler data into Equations (A.2) and (A.3) yield the uncorrected radial velocities V'_{Re} and V'_{Rs}. Solving (A.2) and (A.3) for u and v yields

$$u = \frac{\frac{V_{Re} \cos AZ_S}{\cos EL_E} - \frac{V_{Rs} \cos AZ_E}{\cos EL_S}}{\sin AZ_E \cos AZ_S - \sin AZ_S \cos AZ_E} \qquad (A.4)$$

$$v = \frac{\frac{V_{Re} \sin AZ_S}{\cos EL_E} - \frac{V_{Rs} \sin AZ_E}{\cos EL_S}}{\sin AZ_S \cos AZ_E - \sin AZ_E \cos AZ_E} \qquad (A.5)$$

Finally, plugging in the corrected azimuth and elevation angle values AZ_E = 109.4°, EL_E = 75.4°, AZ_S = 191.3°, and EL_S = 73.4°, Equations (A.1) and (A.2) reduce to

$$u = 3.9292\ V'_{Re} - 1.1744\ V'_{Rs} \qquad (A.6)$$

$$v = -\ 0.7852\ V'_{Re} - 3.3349\ V'_{Rs} \qquad (A.7)$$

where u and v are the corrected horizontal wind components and V'_{Re} and V'_{Rs} are the uncorrected radial velocities obtained above.

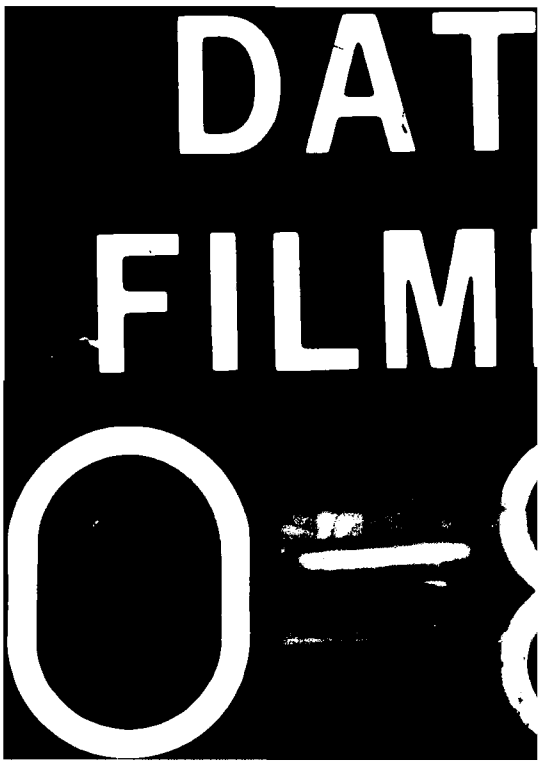
DAT
FILM